Temporal and spatial coral-algae dynamics with larval dispersal

by

Xiaotian Hua

A thesis submitted in partial fulfillment of the requirements for the degree of

Master of Science

in

Applied Mathematics

Department of Mathematical and Statistical Sciences

University of Alberta

Abstract

Coral reefs are essential to the marine ecosystem, and provide some of the most diverse habitats in the world. Coral reef fisheries contribute 6.8 billion to the economy a year globally. However, coral reefs are under significant threat because of human activities such as overfishing, ocean pollution, and habitat destruction. Overfishing leads to shrinkage of the herbivorous fish population, and ocean pollution results in the rapid growth of nutrients in the water. These activities give rise to macroalgae, since herbivorous fish eat many algae and excessive nutrients provide macroalgae with abundant necessities to grow. Macroalgae constantly compete with coral for living space. Adult coral and algae can grow by overgrowing other functional groups or available space. Coral larvae and algae propagules can recruit into adult coral and algae by dispersal and settlement onto available space. Existing literature mainly treats the whole coral reefs as one big patch and focused on one functional group overgrowing other functional groups. However, that is rarely the case in nature. Coral reefs are composed of hundreds of coral skeleton patches and between each patch are sand and rocks. Living coral, macroalgae, and turf algae grow on the coral skeletons. The mechanism of how coral, macroalgae, and turf algae occupy available space while competing; and how macroalgae invade coral and turf algae spatially through larval or propagules dispersal and settlement is still poorly understood. We develop several differential equation models from the first principles and a solid biological background to answer those two questions in chapters 2 and 3. We also give conditions under which

coral will retreat or expand. The interactions between macroalgae and coral were widely studied, but how turf algae interact with other benthic groups is still poorly understood. We also generate some insights into the role of turf algae from the analysis from chapters 2 and 3.

In chapter 2, we develop a one-patch ordinary differential equation model by introducing available space explicitly and incorporating larval dispersal. We undertake bifurcation analysis to understand the effect of grazing on the coral-algae dynamics. We show coral persist under high grazing pressure. We show reasonable fishing helps maintain the herbivorous fish population, and a healthier herbivorous fish population can support a higher level of coral cover. We find coral are more resistant to the decline of larval recruitment when the rate of turf algae occupying available space is high.

In the chapter 3, we consider multiple patches and derive a weakly-coupled network of ordinary differential equations and a reaction-diffusion equation model for the continuous space case from the first principles for modelling brooding coral dynamics. We use the spatially explicit reaction-diffusion equation model to understand the spatial dynamics of the coral-algae ecosystem, and we simulate travelling waves to explain how the macroalgae invade coral spatially through larval dispersal at different grazing levels.

Keywords: coral, algae, larval dispersal, patches, reaction-diffusion equation, persistence, bifurcation, travelling wave.

Preface

This thesis is an original work by Xiaotian Hua. No part of this thesis has been previously published.

Acknowledgements

Foremost, I would like to express my sincere gratitude to my supervisors, Dr. Mark Lewis and Dr. Hao Wang, for the continuous support of my Master's study and research. Their guidance helps me in all the time of research and writing of this thesis. I could not have imagined having better supervisors for my Master's study. Sometimes I struggled with time management issues and did not meet the goals I planned and let them down, but they are always there for me when I need help. I can not be more grateful.

Besides my supervisors, I would like to thank my thesis committee: Dr. Thomas Hillen, for his encouragement, insightful comments, and challenging questions.

I want to thank my fellow lab members in Interdisciplinary Lab for Mathematical Ecology & Epidemiology and Lewis Research Group: Christopher Heggerud, Jingjing Xu, Yurij Salmaniw, Pablo Venegas Garcia, Zhenkun Wang, Kai Wang, Juping Ji, Peter Harrington, Peter Thompson, Emma Atkinson, Micah Brush, and many others for giving me constructive feedback, latex templates, software support and a lot more.

Table of Contents

List of Tables

List of Figures

Glossary

Available space (S)

Available space, not occupied by any functional groups.

Coral (C)

Adult coral.

Delay differential equation (DDE)

Differential equations that involve both time derivatives and delay, which can be represented as the trajectory of the solution in the past.

Macroalgae (M)

Adult macroalgae.

Macroalgae, coral, turf algae, and parrotfish model (MCTP model)

A differential equation model with macroalgae, coral, turf algae, and parrotfish as dependent variables.

Macroalgae, coral, and turf algae model (MCT model)

A differential equation model with macroalgae, coral, and turf algae as dependent variables.

Ordinary differential equation (ODE)

Differential equations that only involve time derivative.

Partial differential equation (PDE)

Differential equations that involve both time and space derivatives.

Travelling wave (TW)

A special form of solution to reaction-diffusion equations, that keeps the same shape of time profile.

Turf algae (T)

Adult turf algae.

Chapter 1

Introduction

In this chapter, we summarize the challenges that coral reefs face and list the efforts other researchers have made to understand coral-algae phase shift. We narrow down the broad question of how we can help prevent coral reefs from degrading to specific coral-algae related problems. Coral reefs are degrading due to anthropogenic influences, such as ocean polluting, overfishing herbivorous fish, destructive fishing methods, and global warming. Phase shift from coral-dominant state to macroalgae-dominant state is one of the critical signals of coral reef degradation, where macroalgae replace abundant coral (Bellwood et al., 2004; Hughes, 1994). There has been extensive work to understand the phase shift and give management suggestions. The goal has been to find anthropogenic and climatic causes of phase shift and provide management measures on how to prevent or reverse the unwanted phase shift (McManus and Polsenberg, 2004; Mumby et al., 2007; Blackwood et al., 2010; Hughes et al., 2007, 2010; Fung et al., 2011, 2013; Brown et al., 2018; Briggs et al., 2018; Tekwa et al., 2021). There have been various methods to study phase shift and interactions between coral and algae. There are both exogenous and endogenous factors that drive coral algae phase shift. These include runoff, upwelling, storms, direct impact from human activities, fishing, macroalgae, herbivores, urchins, and predators. See McManus and Polsenberg (2004) for a conceptual diagram. Controlled experiments on the Great Barrier Reef to test the influence of herbivorous fish on the resilience of coral after a regional coral bleaching found population density of herbivorous fish was a critical compo-

nent in understanding the phase shift (Hughes et al., 2007). Experiments and statistical results suggested the need for new methods for monitoring coral reefs to understand the signals of degrading reefs and innovative designs for marine reserves to reverse the unwanted phase shift (Hughes et al., 2010). Surveys conducted at the Great Barrier Reef found seasonal changes in environmental conditions promoted predictable seasonal cycles in the coral-algae interaction (Brown et al., 2018). In addition to statistical tools, mathematical models, predominantly deterministic ordinary differential equation models, have been used to understand the phase shift (Mumby et al., 2007; Blackwood et al., 2010; Fung et al., 2011, 2013; Briggs et al., 2018; Tekwa et al., 2021).

It is easy to distinguish macroalgae cover from coral cover, so it is common to observe coral cover replaced by macroalgae cover. However, turf algae are also an essential part of the benthic coral reefs ecosystem, and their effects on other benthic groups are poorly explored (Vermeij et al., 2012). We aim to 1) understand how coral, macroalgae, and turf algae occupy available space while competing; 2) understand how macroalgae invade coral and turf algae spatially through larval or propagules dispersal and settlement; 3) generate insights into the role of turf algae in the coral-algae ecosystem.

1.1 Biological background

In this section, we introduce our three main functional groups of focus in this thesis, macroalgae (M), coral (C), and turf algae (T).

1.1.1 Macroalgae

Macroalgae are a common term used for seaweeds and other benthic algae. They are visible to the eyes, and most macroalgae reproduce sexually by producing gametes or propagules and asexually by vegetative propagation or fragmentation. Macroalgae may replace coral because overfishing and ocean pollution. In the context of coral reefs, macroalgae are unwanted, and a large number of macroalgae is one sign of coral reef degradation (Diaz-Pulido and McCook, 2008).

1.1.2 Coral

In this thesis, we refer to ***living coral*** as the marine invertebrates coral, ***dead coral*** as coral skeletons, and the colony formed by both living and dead coral as ***coral reefs*** or ***patches***. Coral can reproduce both asexually and sexually, as summarized in figure 1.1. The asexual reproduction of coral involves budding or fragmentation. Budding happens when new coral polyps bud off from parent polyps, and together with the parent polyps, form an immense colony. Fragmentation happens when parent coral break into smaller fragments because of natural disturbances and, if the fragmented pieces land in suitable places, the fragmented pieces can grow and form a new colony (Richmond and Hunter, 1990). The location of fertilization can classify sexual reproduction. External fertilization happens when adult coral releases both sperm and eggs into water and spermatozoid meets eggs in the water. Internal fertilization happens when adult coral release only sperm into the water, and spermatozoid meets the eggs in the coral polyps. Spawning coral adapt the external fertilization strategy, and spawning coral larvae can survive and drift along with the current for days before settling in a suitable spot. As a result, the spawning coral larvae can disperse over a long distance. Brooding coral adapt the internal fertilization strategy.

In this thesis, we focus on coral sexual reproduction and the brooding coral situation. There are several steps involved for brooding coral sexual reproduction with internal fertilization. The first step is coral spawning; adult coral produce only sperm into the water column above the patch of coral reefs. The second step is coral brooding; the spawned sperm fertilizes the eggs inside coral polyps. The fertilized eggs become little larvae, and the larvae develop in the coral polyps for some time before they are released into the current. The final step is larval settling; the polyps release the well developed larvae and, if they attach to the suitable substrata, they can grow to new coral polyps by division. Since the brooding coral larvae are relatively well developed and ready to settle when they are released, the brooding coral larvae travel and disperse over a significantly shorter distance than the spawning coral larvae

(James Gilmour and Pincock, 2013).

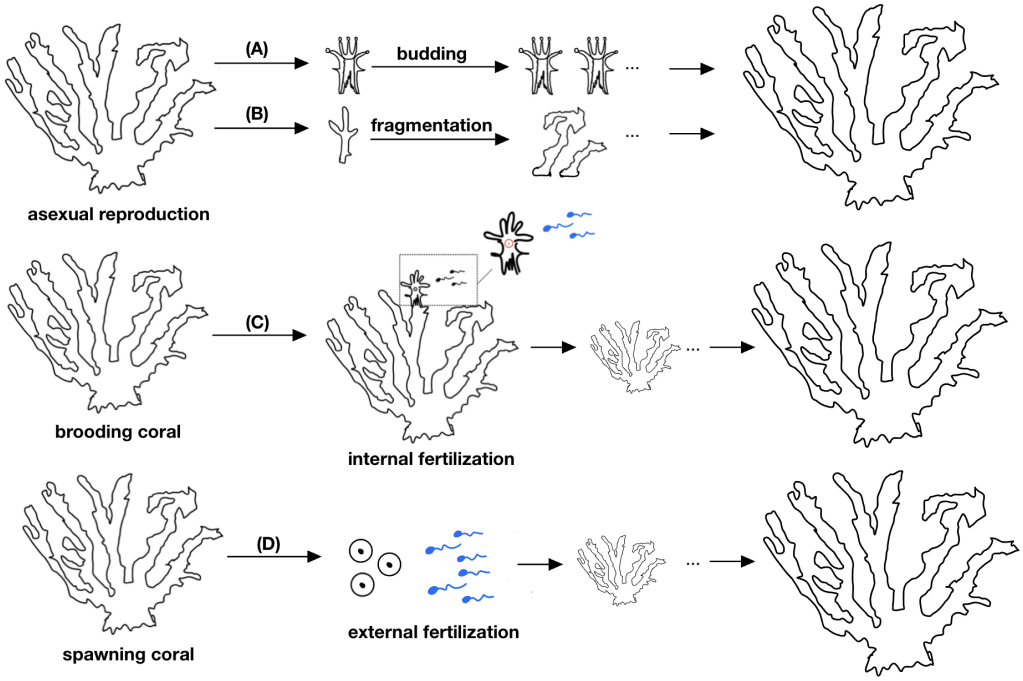

Fig. 1.1 Reproduction of coral. (A) Asexual reproduction of coral through budding. (B) Asexual reproduction of coral through fragmentation. (C) Sexual reproduction of brooding coral through internal fertilization. (D) Sexual reproduction of spawning coral through external fertilization.

1.1.3 Turf algae

Turf algae are a combination of filamentous algae, microalgae, zooxanthellae, and other types of benthic algae (Connell et al., 2014). The interaction between coral and turf algae largely depends on what specific species to include as a collective term for turf algae. With different compositions of species, turf algae may have a minor effect on coral, kill coral, or even help coral (Jompa and McCook, 2003). In this thesis, we consider the case when turf algae help coral. Turf algae are the fastest colonizer compared to macroalgae and coral and can fill up available space in a short time. Coral usually win in the competition against turf algae (Swierts and Vermeij, 2016).

1.2 Historical approaches

In this section, we specifically focus on the historical efforts of modelling coral-algae dynamics using ordinary differential equations (ODE).

Mumby et al. (2007) developed a macroalgae-coral-turf algae (MCT) model that includes three functional groups: macroalgae, coral, and turf algae. One of the primary assumption was that any particular location was occupied by a certain proportion of each of the three groups. In their model, the variables represented the proportion of space occupied by either macroalgae, coral, or turf algae in that given region and the proportions added up to one, in other words, $T = 1 - M - C$. Mumby et al. (2007)'s MCT model model showed bistability behaviour with either macroalgae-dominance or coral-dominance, when the grazing effect was high. A detailed global ODE analysis of the MCT model was undertaken by Li et al. (2014). They also developed a delay differential equation (DDE) model with inherent time delay for the system and undertook local stability analysis for the model, with a focus on assessing the impact of grazing on the population dynamics. The MCT model was extended to a MCTP model by explicitly incorporating the population dynamics of herbivorous parrotfish, and management options were considered based on the analysis of grazer dynamics (Blackwood et al., 2010). A comprehensive stability, bifurcation, and persistence analysis of a slightly modified version of the MCTP model was undertaken by Fattahpour et al. (2018). They also used a DDE model to provide biologically important coexistence state attracting region and management suggestions. A stage-structured model with the assumption that available free space was covered by turf algae immediately was promoted by Briggs et al. (2018) to study the effect of the vulnerability of macroalgae to grazing on coral-algae phase shift. Available space and larval recruitment were introduced into the ODE models by Fung et al. (2011) and Fung et al. (2013). However, the detailed mechanism of how coral and algae occupy available space and how larvae or propagules recruit into adults is still poorly understood. The idea of intraguild competition between coral and algae has been commonly used to formulate the deterministic models. Intraguild

predation involves both competition and predation. Species in intraguild predation kills and eats other potential competitive species that use the same limited resources (Polis, 1989). Algae and coral compete for living space by overgrowing each other rather than actually killing or eating, so here we avoid using the word predation directly. Instead, we use intraguild competition to show the difference.

One drawback of the existing methods is that ODE models cannot capture the spatial structures that are commonly seen in coral reefs. There are many patches of coral skeletons of a certain size in coral reefs, and macroalgae, coral, and turf algae grow on the surface of coral skeletons. These patches of coral skeletons become larger and even connect to other patches to form a bigger reef. Coral larvae and algae propagules travel from one patch to another, and the coral skeletons also expand through the metabolism of living coral (James Gilmour and Pincock, 2013).

In this thesis, we will develop ODE models based on Mumby et al. (2007)'s MCT model with explicit consideration of available space to emphasize the fact that it takes time for the dead coral and algae to form available space, and different groups take available at vastly different speeds. We will also develop a network of patches model and reaction-diffusion equation model to explicitly consider the spatial invasion of coral by macroalgae through larval dispersal.

1.3 Model assumptions

In this section, we state our main model assumptions.

We include four components in our model: macroalgae (M), coral (C), turf algae (T), and available space (S). Each variable is measured by the surface area of coral skeletons it occupied. The first three components interact through intraguild competition, and available space serves as a buffer between them, as illustrated by figure 1.2. Macroalgae are the most competitive component and can take the space occupied by coral and turf algae during competition. Coral are the second most competitive component. Coral overgrow turf algae

during the sub-competition between coral and turf algae (Barott et al., 2012). Space freed by the death of coral and algae becomes available space. We assume that although this space is available to both types of algae and coral, turf algae are the fastest colonizer and rapidly take up available space, as opposed to most literature that has been treating turf algae as a synonym of available space. In chapter 2, we consider the whole reefs as one big patch, as illustrated in figure 1.3(a), and we assume that the macroalgae, coral, and turf algae spread spatially within the big patch by larvae, in the case of coral, and propagules, in the cases of macroalgae and turf algae. In chapter 3, we assume there are multiple patches, and they are connected by larval dispersal, as illustrated in figure 1.3(b). We assume that the macroalgae, coral, and turf algae spread spatially between patches by larvae, in the case of coral, and propagules, in the cases of macroalgae and turf algae (James Gilmour and Pincock, 2013). More specifically, we focus on the brooding coral. Since the dispersal range of brooding coral larvae is relatively short, we can apply the nearest neighbour principle to simplify the larval dispersal process. This, in turn, gives rise to a partial differential equation (PDE) approximation, which can be analyzed for the spatial spread of macroalgae, coral, and turf algae using methods of travelling wave (TW) theory. PDE models, especially reaction-diffusion equation and TW analysis, can be instrumental in dealing with spatial spread and invasion problems.

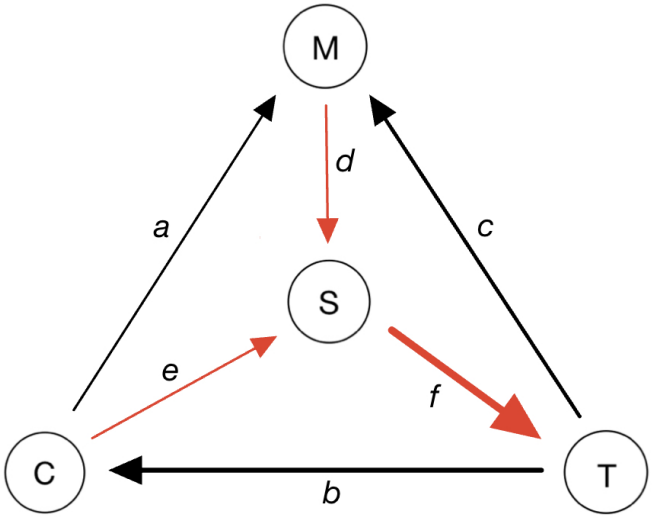

Fig. 1.2 Intraguild competition dynamics for macroalgae, coral, and turf algae. The arrow from X to Y means X is good for Y. (a) Macroalgae overgrow coral. (b) Coral overgrow turf algae. (c) Macroalgae overgrow turf algae. (d) Space freed by the death of macroalgae due to grazing becomes available space. (e) Space freed by the natural death of coral becomes available space. (f) Turf algae quickly take up available space. We neglect the processes of macroalgae and coral taking up available space in this figure because the rates are much lower than turf algae. We neglect the contribution from the natural death of macroalgae and turf algae to available space in this figure because grazing is the main death factor for algae. We neglect the contribution from the death of turf algae due to grazing to available space because turf algae occupy available space much faster than contribute to it.

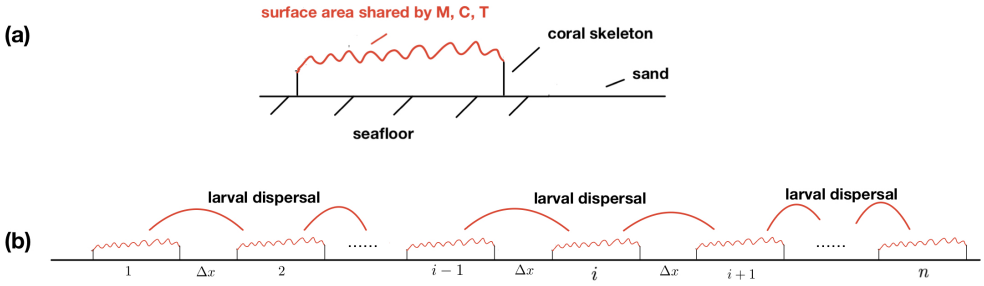

Fig. 1.3 One patch and multiple patches visualizations. (a) Illustration of one coral patch. The seafloor is covered by sand outside of the coral patch, and macroalgae, coral, and turf algae can not survive on the sand. Macroalgae, coral, and turf algae compete for living space within one patch, and living space is measured by the surface area of coral skeletons. (b) Illustration of multiple coral patches. For simplicity, we assume patches are on the same line. Multiple coral patches are connected by larval or propagules dispersal through current.

1.4 Mathematical tools

In this section, we introduce the mathematical tools that we will use.

We mainly use stability analysis, persistence theory, bifurcation analysis in chapter 2 and asymptotic expansion, diffusion approximation, and travelling wave analysis in chapter 3 as mathematical tools to derive the models and study the coral-algae dynamics. We use local stability analysis to figure out the behaviour of solutions near equilibria analytically for our ODE models in chapter 2; however global stability analysis usually is challenging to conduct for a non-linear ODE system of more than two variables. Persistence theory gives us a way to show some global properties of the solution without proving global stability for an equilibrium. We will use persistence theory to give conditions for the persistence of coral in the long run. Bifurcation analysis can help us study the qualitative change in solution behaviour concerning specific parameters. Although analytically bifurcation analysis is difficult to conduct for our ODE models in chapter 2, numerical bifurcation analysis is greatly helpful in understanding the equilibrium behaviour of solutions by varying the parameter of interest within a proper range and fixing all other parameters at appropriate values. We will use numerical bifurcation analysis to understand the coral-algae dynamics of our ODE models in chapter 2 by varying the grazing effect.

We will use PDE models, more specifically reaction-diffusion equation models, to investigate the population dynamics for continuous time and space. Spatially structured models, such as reaction-diffusion equation models, can account for environmental heterogeneity, heterogeneity in initial population distribution, and species dispersal (Kot, 2001). A typical routine is first to use ODE models to understand the multi-species intraguild competition without spatial dynamics and then develop the reaction-diffusion equation models based on the ODE models. Asymptotic expansion gives us a way to reduce the non-linear terms by ignoring the higher order terms and only focusing on the linear terms. We will use asymptotic expansion extensively to formulate the network of weakly-coupled patches model in chapter 3. We apply dif-

fusion approximation to transit from the network of weakly-coupled patches model in the discrete space case to the reaction-diffusion equation model in the continuous space case. Travelling wave analysis is excellent for investigating the spread of species and how certain species spatially invades other species (Bampfylde and Lewis, 2007).

We state the mathematical definition of weak persistence, strong persistence, uniform weak persistence, and uniform strong persistence adapted from Definition 3.1 on page 61 of Smith and Thieme (2011). These definitions will be helpful in the proof of persistence in chapter 2.

Let $\mathbb{X}$ be the nonempty state space, $\mathbb{J}$ be the time set, and function $\rho : \mathbb{X} \to \mathbb{R}^+$.

Definition 1.4.1 (**Persistence**). *A semiflow $\phi : \mathbb{J} \times \mathbb{X} \to \mathbb{X}$ is called weakly ρ-persistent, if*

$$\limsup_{t\to\infty} \rho\left(\phi_t(x)\right) > 0 \text{ for arbitrary } x \in \mathbb{X} \text{ such that } \rho(x) > 0.$$

ϕ is called strongly ρ-persistent, if

$$\liminf_{t\to\infty} \rho\left(\phi_t(x)\right) > 0 \text{ for arbitrary } x \in \mathbb{X} \text{ such that } \rho(x) > 0.$$

Definition 1.4.2 (**Uniform persistence**). *A semiflow $\phi : \mathbb{J} \times \mathbb{X} \to \mathbb{X}$ is called uniformly weakly ρ-persistent, if there exist $\epsilon > 0$ such that*

$$\limsup_{t\to\infty} \rho\left(\phi_t(x)\right) > \epsilon \text{ for arbitrary } x \in \mathbb{X} \text{ such that } \rho(x) > 0.$$

ϕ is called uniformly strongly ρ-persistent, if there exist $\epsilon > 0$ such that

$$\liminf_{t\to\infty} \rho\left(\phi_t(x)\right) > \epsilon \text{ for arbitrary } x \in \mathbb{X} \text{ such that } \rho(x) > 0.$$

Remark. *For uniform persistence, the choice of ϵ is independent of the initial conditions.*

Chapter 2

Temporal dynamics

In this chapter, we develop a one-patch ODE model, and undertake local stability analysis and bifurcation analysis to show how coral and algae occupy available space while competing. We show the conditions under which coral will persist. We investigate the effect of a decline in larval recruitment on coral persistence.

2.1 ODE model derivation and assumptions

In this section, we develop a six dimensional ODE model in subsection 2.1.1, which includes both adults and larvae. We reduce the six dimensional model to a three dimensional model using non-dimensionalization and quasi-steady-state approximation in subsection 2.1.2.

2.1.1 Dimensional one-patch model

One of the primary assumption in the MCT model from Mumby et al. (2007) was that any particular location was occupied by a certain proportion of each of the three groups, which implied there was no empty space left at any given time. One justification for their assumption was that turf algae were good at occupying empty space, so any empty space became turf algae immediately. This assumption is an oversimplification of reality. Although turf algae are faster in occupying available space, macroalgae and coral can still take available space at a lower rate. Explicit consideration of available space also allows us to study the process of larvae settlement and larval dispersal, which paves

the way for studying spatial dynamics in chapter 3. We modify the MCT model from Mumby et al. (2007) with explicit consideration of available space and larvae or propagules settling. Larvae or propagules are in the water, and adults are on the bottom. Since larvae are microscopic, we assume that larvae or propagules can settle anywhere in the reef. However, larvae or propagules can only grow if they land on available space S. If they land elsewhere, they settle and die immediately. Once settled on available space, we assume larvae or propagules grow into adults instantly, which is a simplifying assumption so as to keep the model analytically tractable.

$$
\begin{cases}
\dfrac{dM}{dt} = \underbrace{\alpha MC}_{\substack{\text{macroalgae}\\ \text{overgrow coral}}} \underbrace{+\beta MT}_{\substack{\text{macroalgae}\\ \text{overgrow turf}}} \underbrace{+\rho_M MS}_{\substack{\text{macroalgae}\\ \text{take space}}} \underbrace{-\delta_M M}_{\substack{\text{death}\\ \text{no grazing}}} \underbrace{-gM}_{\substack{\text{death}\\ \text{grazing}}} \underbrace{+\phi_M \kappa_M l_M S}_{\substack{\text{propagules}\\ \text{settling}}} & (2.1a)\\
\dfrac{dl_M}{dt} = \underbrace{b_M \dfrac{\psi_M M}{NL}}_{\substack{\text{macroalgae}\\ \text{produce propagules}}} \underbrace{-\mu_M l_M}_{\substack{\text{propagules}\\ \text{natural death}}} \underbrace{-\kappa_M l_M}_{\substack{\text{propagules}\\ \text{settling}}} & (2.1b)\\
\dfrac{dC}{dt} = \underbrace{\gamma CT}_{\substack{\text{coral}\\ \text{overgrow turf}}} \underbrace{+\rho_C CS}_{\substack{\text{coral}\\ \text{take space}}} - \alpha MC \underbrace{-\delta_C C}_{\substack{\text{coral}\\ \text{natural death}}} \underbrace{+\phi_C \kappa_C l_C S}_{\substack{\text{larvae}\\ \text{settling}}} & (2.1c)\\
\dfrac{dl_C}{dt} = \underbrace{b_C \dfrac{\psi_C C}{NL}}_{\substack{\text{coral}\\ \text{produce larvae}}} \underbrace{-\mu_C l_C}_{\substack{\text{larvae}\\ \text{natural death}}} \underbrace{-\kappa_C l_C}_{\substack{\text{larvae}\\ \text{settling}}} & (2.1d)\\
\dfrac{dT}{dt} = \underbrace{\rho_T TS}_{\substack{\text{turf}\\ \text{take space}}} - \beta MT - \gamma CT - \delta_T T - gT + \phi_T \kappa_T l_T S & (2.1e)\\
\dfrac{dl_T}{dt} = \underbrace{b_T \dfrac{\psi_T T}{NL}}_{\substack{\text{turf}\\ \text{produce propagules}}} - \mu_T l_T - \kappa_T l_T & (2.1f)\\
S = \underbrace{N - M - C - T}_{\text{available space is total space minus space occupied by three functional groups}} & (2.1g)
\end{cases}
$$

Variables are listed in table A.1 and parameters are listed in table A.2. We assume all the parameters are positive throughout our analysis. Larvae or propagules can only grow if they settle on available space S.

2.1.2 Non-dimensional one-patch model with larvae incorporated

We non-dimensionalize the dimensional one-patch model (2.1) and use tilde ˜ to denote the dimensionless values. R is a variable representing any of the three population groups: macroalgae, coral, and turf algae.

$$\begin{cases} \dfrac{d\tilde{M}}{d\tilde{t}} = \tilde{\alpha}\tilde{M}\tilde{C} + \tilde{\beta}\tilde{M}\tilde{T} + \tilde{\rho}_M\tilde{M}\tilde{S} - \tilde{\delta}_M\tilde{M} - \tilde{g}\tilde{M} + \tilde{\kappa}_M\tilde{l}_M\tilde{S} & \text{(2.2a)} \\ \epsilon_M\dfrac{d\tilde{l}_M}{d\tilde{t}} = \tilde{\psi}_M\tilde{b}_M\tilde{M} - \tilde{l}_M - \tilde{\kappa}_M\tilde{l}_M & \text{(2.2b)} \\ \dfrac{d\tilde{C}}{d\tilde{t}} = \tilde{\gamma}\tilde{C}\tilde{T} + \tilde{\rho}_C\tilde{C}\tilde{S} - \tilde{\alpha}\tilde{M}\tilde{C} - \tilde{C} + \tilde{\kappa}_C\tilde{l}_C\tilde{S} & \text{(2.2c)} \\ \epsilon_C\dfrac{d\tilde{l}_C}{d\tilde{t}} = \tilde{\psi}_C\tilde{b}_C\tilde{C} - \tilde{l}_C - \tilde{\kappa}_C\tilde{l}_C & \text{(2.2d)} \\ \dfrac{d\tilde{T}}{d\tilde{t}} = \tilde{\rho}_T\tilde{T}\tilde{S} - \tilde{\beta}\tilde{M}\tilde{T} - \tilde{\gamma}\tilde{C}\tilde{T} - \tilde{\delta}_T\tilde{T} - \tilde{g}\tilde{T} + \tilde{\kappa}_T\tilde{l}_T\tilde{S} & \text{(2.2e)} \\ \epsilon_T\dfrac{d\tilde{l}_T}{d\tilde{t}} = \tilde{\psi}_T\tilde{b}_T\tilde{T} - \tilde{l}_T - \tilde{\kappa}_T\tilde{l}_T & \text{(2.2f)} \\ \tilde{S} = 1 - \tilde{M} - \tilde{C} - \tilde{T} & \text{(2.2g)} \end{cases}$$

$\epsilon_R = \dfrac{\delta_C}{\mu_R}$ is a very small parameter, for $R = M$, C, or T. Non-dimensionalized variables and parameters are listed in table A.3. Larval equations (2.2b), (2.2d), and (2.2f) are assumed to have fast dynamics compared to adult dynamics described by equations (2.2a), (2.2c), and (2.2e). The mortality rate of coral is much smaller than the death rate of larvae or propagules. By using a quasi-steady-state approximation, we assume $\epsilon_R \to 0$, and then equations (2.2b), (2.2d), and (2.2f) can be summarized as the following equation (2.3):

$$\Rightarrow \tilde{\psi}_R\tilde{b}_R\tilde{R} - \tilde{l}_R - \tilde{\kappa}_R\tilde{l}_R = 0, \tag{2.3}$$

$$\Rightarrow \tilde{l}_R = \frac{\tilde{\psi}_R\tilde{b}_R}{\tilde{\kappa}_R + 1}\tilde{R}. \tag{2.4}$$

We substitute equation (2.4) into equations (2.2a), (2.2c), and (2.2e). We drop superscript tilde ˜ in the future for notational convenience.

$$\begin{cases} \dfrac{dM}{dt} = \alpha MC + \beta MT + \rho_M MS - \delta_M M - gM + \theta_M \psi_M b_M MS & (2.5a) \\ \dfrac{dC}{dt} = \gamma CT + \rho_C CS - \alpha MC - C + \theta_C \psi_C b_C CS & (2.5b) \\ \dfrac{dT}{dt} = \rho_T TS - \beta MT - \gamma CT - \delta_T T - gT + \theta_T \psi_T b_T TS & (2.5c) \\ S = 1 - M - C - T & (2.5d) \end{cases}$$

$\theta_R = \dfrac{\kappa_R}{\kappa_R + 1}$, $R = M$, C, or T. θ_R is the probability of settling before dying and $\dfrac{\kappa_R}{\kappa_R + 1} + \dfrac{1}{\kappa_R + 1} = 1$. We regroup $\theta_R \psi_R b_R$ into the parameter Θ_R. Θ_R denotes the total contribution rate from larvae or propagules settling to adult abundance. We obtain the following reduced non-dimensional one-patch model (2.6):

$$\begin{cases} \dfrac{dM}{dt} = \alpha MC + \beta MT + \rho_M MS - \delta_M M - gM + \Theta_M MS & (2.6a) \\ \dfrac{dC}{dt} = \gamma CT + \rho_C CS - \alpha MC - C + \Theta_C CS & (2.6b) \\ \dfrac{dT}{dt} = \rho_T TS - \beta MT - \gamma CT - \delta_T T - gT + \Theta_T TS & (2.6c) \\ S = 1 - M - C - T. & (2.6d) \end{cases}$$

We undertake analysis of the above reduced non-dimensional one-patch model (2.6) in section 2.2.

2.1.3 Assumptions on parameters

We assume all the parameters are positive throughout our analysis, and we introduce two additional classes of assumptions and conditions. Assumptions labelled with a A tag are based on biological mechanisms and A1 to A4 are assumed to always hold throughout the analysis of the reduced non-dimensional one-patch model (2.6). Conditions labelled with a CD tag may not always hold. Thus, different combinations of CD conditions lead to different equilibrium dynamics, which are discussed in section 2.2.

Assumption A1.

$$\rho_T \gg \rho_M, \rho_T \gg \rho_C, \rho_M > \alpha, \rho_M > \beta, \textit{and } \rho_C > \gamma$$

A1 is about the rate of taking available and overgrowing other functional groups. We assume turf algae are the fastest colonizer, so the rate of taking available space for turf algae is much larger than the rate for macroalgae and coral. We assume occupying empty space is much easier than overgrowing other functional groups.

Assumption A2.

$$\gamma > 2, 2 > \beta > 1, \textit{and } 1 > \alpha > 0$$

A2 is made based on the choice of parameter values listed in table A.3.

Assumption A3.

$$\delta_M < g \textit{ and } \delta_T < g$$

A3 states the death rate of macroalgae and turf algae if not grazed is less than the grazing effect from herbivorous fish because, in literature, the grazing effect from herbivorous fish is considered the main death factor for algae.

Assumption A4.

$$\frac{\rho_T}{\Theta_T} > \frac{\rho_M}{\Theta_M} \textit{ and } \frac{\rho_T}{\Theta_T} > \frac{\rho_C}{\Theta_C}$$

A4 states the ratio of growth from occupying available space and larvae or propagules settling for turf algae is larger than the ratio for macroalgae and coral. We further assume turf algae mainly expand from vegetative growth or lateral growth over available space rather than propagules settling.

It makes biological sense if we only consider the case when all functional groups are non-negative and available space is non-negative. We prove the reduced non-dimensional one-patch model (2.6) has dynamics such that the region $\mathbb{D}$ is positively invariant in Theorem 2.1.1.

Theorem 2.1.1 (**Positive invariance**). *If all parameters are positive, then the region,*

$$\mathbb{D} = \left\{(M, C, T, S) \mid 0 \leq M, C, T, S \leq 1\right\},$$

is positively invariant for the solution semiflow generated by the system (2.6)*, i.e.* $\phi_t(\mathbb{D}) \subseteq \mathbb{D}, t \geq 0$.

Proof.

$$\left.\frac{dM}{dt}\right|_{M=0} = \left(\alpha MC + \beta MT + \rho_M MS - \delta_M M - gM + \Theta_M MS\right)\big|_{M=0} = 0$$

$$\left.\frac{dC}{dt}\right|_{C=0} = \left(\gamma CT + \rho_C CS - \alpha MC - C + \Theta_C CS\right)\big|_{C=0} = 0$$

$$\left.\frac{dT}{dt}\right|_{T=0} = \left(\rho_T TS - \beta MT - \gamma CT - \delta_T T - gT + \Theta_T T\right)\big|_{T=0} = 0$$

$\Rightarrow \phi_t(\mathbb{D}) \subseteq \left\{(M, C, T, S) \mid M, C, T \geq 0\right\}$, and $M + C + T = 1$ when $S = 0$, i.e. $\phi_t(\mathbb{D}) \subseteq \mathbb{D}, t \geq 0$.

$$\begin{aligned}
\Rightarrow \left.\frac{dS}{dt}\right|_{S=0} &= \left(\delta_M M + gM + C + \delta_T T + gT\right)\big|_{S=0} \\
&= \left[\left(\delta_M + g\right) M + C + \left(\delta_T + g\right) T\right]\Big|_{S=0} \\
&\geq \min\left\{\delta_M + g, 1, \delta_T + g\right\}\left(M + C + T\right)\big|_{S=0} \\
&= \min\left\{\delta_M + g, 1, \delta_T + g\right\}\big|_{S=0} \\
&> 0
\end{aligned}$$

$\Rightarrow \phi_t(\mathbb{D}) \subseteq \left\{(M, C, T, S) \mid M, C, T, S \geq 0\right\}$, and since M + C + T + S = 1, $\phi_t(\mathbb{D}) \subseteq \left\{(M, C, T, S) \mid 0 \leq M, C, T, S \leq 1\right\} = \mathbb{D}$. ■

Remark. *Theorem 2.1.1 implies the proportion of surface area occupied by each functional group and the proportion of available space are always non-negative and bounded by one, given the initial conditions are between zero and one.*

2.2 Local stability, persistence, and bifurcation results

In this section, we undertake local stability analysis and numerical bifurcation analysis to determine the stability of equilibria and the qualitative nature of the flow connecting the equilibria. We calculate one trivial equilibrium, three axial equilibria, and three boundary equilibria symbolically, and we give the linear system that the interior equilibrium should satisfy. We sort out the conditions of existence and the linear stability of trivial, axial, and boundary

equilibria. Those conditions are theoretical backup for the bifurcation analysis in subsection 2.2.4. Based on the bifurcation results, we show reasonable fishing helps maintain the herbivorous fish population, and a healthier herbivorous fish population can support a higher level of coral cover. Using time simulations, we find coral are more resistant to the decline in larvae recruitment when turf algae occupy available space fast. We undertake persistence analysis to determine the conditions under which coral will survive in the long run.

2.2.1 Equilibria

In this subsection, we calculate explicit formula for the equilibria of one-patch model (2.6).

We assume A1 to A4 always hold in the following equilibrium analysis, ensuring our model is reasonable. We use "CD number" to label conditions in subsection 2.2.1. We use "CD number$^-$" to denote the same condition but with the opposite sign. For example, if CD0 is "parameter $> x$", then CD0$^-$ would be "parameter $< x$". We regroup the reduced one-patch model (2.6) in the following way:

$$\begin{cases} \dfrac{dM}{dt} = M \underbrace{\left[\alpha C + \beta T + (\rho_M + \Theta_M) S - (\delta_M + g)\right]}_{= \text{function } F(M,C,T)} \coloneqq MF(M,C,T) & \text{(2.7a)} \\ \dfrac{dC}{dt} = C \underbrace{\left[\gamma T + (\rho_C + \Theta_C) S - \alpha M - 1\right]}_{= \text{function } G(M,C,T)} \coloneqq CG(M,C,T) & \text{(2.7b)} \\ \dfrac{dT}{dt} = T \underbrace{\left[(\rho_T + \Theta_T) S - \beta M - \gamma C - (\delta_T + g)\right]}_{= \text{function } H(M,C,T)} \coloneqq TH(M,C,T) & \text{(2.7c)} \\ S = 1 - M - C - T. & \text{(2.7d)} \end{cases}$$

Trivial equilibrium

1. Trivial equilibrium: $E_1 = (0, 0, 0)$. $E_1 \in \mathbb{D}$.

Axial equilibrium

1. M axis: We solve the macroalgae-only equilibrium from the following equation:

$$F(M,0,0) = \left[\alpha C + \beta T + (\rho_M + \Theta_M) S - (\delta_M + g)\right]\Big|_{C,T=0} = 0,$$

$$\Rightarrow E_2 = (M_2^*, 0, 0) = \left(1 - \frac{\delta_M + g}{\rho_M + \Theta_M}, 0, 0\right).$$

Condition CD1.

$$\delta_M + g < \rho_M + \Theta_M$$

The total death rate of macroalgae is less than macroalgae growth rate from occupying available space and propagules settling. $M_2^* > 0$ *iff CD1 holds.*

$M_2^* < 1$ because we assume all parameters are positive. $E_2 \in \mathbb{D}$ iff CD1 holds. Macroalgae-only equilibrium is in the positive invariant feasible region $\mathbb{D}$ when the total death rate of macroalgae is less than macroalgae growth rate from occupying available space and propagules settling.

2. C axis: We solve the coral-only equilibrium from the following equation:

$$G(0,C,0) = \left[\gamma T + (\rho_C + \Theta_C) S - \alpha M - 1\right]\Big|_{M,T=0} = 0,$$

$$\Rightarrow E_3 = (0, C_3^*, 0) = \left(0, 1 - \frac{1}{\rho_C + \Theta_C}, 0\right).$$

$C_3^* < 1$ because we assume all parameters are positive. $E_3 \in \mathbb{D}$. $\rho_C > \gamma > 2$ by A1 and A2, so $\rho_C + \Theta_C > 1$, implying $C_3^* > 0$. Coral-only equilibrium is always in the positive invariant feasible region $\mathbb{D}$. The total coral growth from occupying available space and larvae settling is always larger than the natural mortality of coral, guaranteed by A1 and A2.

3. T axis: We solve the turf algae-only equilibrium from the following equation:

$$H(0,0,T) = \left[(\rho_T + \Theta_T) S - \beta M - \gamma C - (\delta_T + g)\right]\Big|_{M,C=0} = 0,$$

$$\Rightarrow E_4 = (0, 0, T_4^*) = \left(0, 0, 1 - \frac{\delta_T + g}{\rho_T + \Theta_T}\right).$$

Condition CD2.

$$\delta_T + g < \rho_T + \Theta_T$$

The total death rate of turf algae is less than turf algae growth rate from occupying available space and propagules settling. $T_2^* > 0$ iff CD2 holds.

$T_4^* < 1$ because we assume all parameters are positive. $E_4 \in \mathbb{D}$ iff CD2 holds. Turf algae-only equilibrium is in the positive invariant feasible region $\mathbb{D}$ when the total death rate of turf algae is less than turf algae growth rate from occupying available space and propagules settling.

Boundary equilibrium

1. M C plane: We solve the macroalgae and coral coexistence equilibrium from the following equations:

$$\begin{cases} F(M, C, 0) = \left[\alpha C + \beta T + (\rho_M + \Theta_M) S - (\delta_M + g)\right]\Big|_{T=0} = 0 \\ G(M, C, 0) = \left[\gamma T + (\rho_C + \Theta_C) S - \alpha M - 1\right]\Big|_{T=0} = 0, \end{cases}$$

$$\Rightarrow E_5 = (M_5^*, C_5^*, 0),$$

with

$$M_5^* = \frac{(\rho_M + \Theta_M - \alpha) + (\rho_C + \Theta_C)(\alpha - \delta_M - g)}{\alpha(\alpha + \rho_C + \Theta_C - \rho_M - \Theta_M)} \tag{2.8}$$

$$C_5^* = \frac{(\delta_M + g)(\alpha + \rho_C + \Theta_C) - (\rho_M + \Theta_M)(\alpha + 1)}{\alpha(\alpha + \rho_C + \Theta_C - \rho_M - \Theta_M)}. \tag{2.9}$$

Assumption A5. *We assume*

$$\rho_C > \rho_M + \Theta_M - \alpha - \Theta_C$$

to eliminate cases and better focus on the grazing effect g. Denominator of M_5^* and C_5^* is positive under A5.

Condition CD3.

$$g > \frac{(\alpha + 1)(\rho_M + \Theta_M)}{\alpha + \rho_C + \Theta_C} - \delta_M$$

The grazing effect is larger than some threshold value. Numerator of C_5^* is positive iff CD3 holds.

Condition CD4.

$$g < \alpha + \frac{\rho_M + \Theta_M - \alpha}{\rho_C + \Theta_C} - \delta_M$$

The grazing effect is less than some threshold value. Numerator of M_5^* is positive iff CD4 holds.

$M_5^* + C_5^* < 1$ is equivalent to $g < \alpha + 1$, which is guaranteed by CD4 under A5. $E_5 \in \mathbb{D}$ iff CD3 and CD4 hold under A5. CD3 and CD4 combine to be:

$$\frac{(\alpha+1)(\rho_M + \Theta_M)}{\alpha + \rho_C + \Theta_C} - \delta_M < g < \alpha + \frac{\rho_M + \Theta_M - \alpha}{\rho_C + \Theta_C} - \delta_M.$$

This means macroalgae and coral coexistence equilibrium is in the positive invariant feasible region $\mathbb{D}$ when the grazing effect is between two threshold values.

2. M T plane: We solve the macroalgae and turf coexistence equilibrium from the following equations:

$$\begin{cases} F(M,0,T) = \left[\alpha C + \beta T + (\rho_M + \Theta_M) S - (\delta_M + g)\right]\Big|_{C=0} = 0 \\ H(M,0,T) = \left[(\rho_T + \Theta_T) S - \beta M - \gamma C - (\delta_T + g)\right]\Big|_{C=0} = 0, \end{cases}$$

$$\Rightarrow E_6 = (M_6^*, 0, T_6^*),$$

with

$$M_6^* = \frac{(\delta_T + g)(\rho_M + \Theta_M - \beta) + (\rho_T + \Theta_T)(\beta - \delta_M - g)}{\beta(\beta + \rho_T + \Theta_T - \rho_M - \Theta_M)} \tag{2.10}$$

$$T_6^* = \frac{(\delta_M + g)(\beta + \rho_T + \Theta_T) + (\rho_M + \Theta_M)(-\beta - \delta_T - g)}{\beta(\beta + \rho_T + \Theta_T - \rho_M - \Theta_M)}. \tag{2.11}$$

Assumption A6. *We further assume*

$$\rho_T > \rho_M + \Theta_M - \beta - \Theta_T$$

to eliminate cases and better focus on the grazing effect g. This assumption is more concrete than $\rho_T >> \rho_M$ in A1. Denominator of M_6^* and T_6^* is positive under A6.

Condition CD5.

$$g > \frac{(\beta + \delta_T - \delta_M)(\rho_M + \Theta_M)}{\beta + \rho_T + \Theta_T - \rho_M - \Theta_M} - \delta_M$$

The grazing effect is larger than some threshold value. Numerator of T_6^* *is positive iff CD5 holds.*

Condition CD6.

$$g < \frac{(\beta + \delta_T - \delta_M)(\rho_T + \Theta_T)}{\beta + \rho_T + \Theta_T - \rho_M - \Theta_M} - \delta_T$$

The grazing effect is less than some threshold. Numerator of M_6^* *is positive iff CD6 holds.*

Condition CD7.

$$\delta_M < \beta + \delta_T$$

Macroalgae growth from overgrowing turf algae plus mortality of turf algae if not grazed is larger than mortality of macroalgae if not grazed. $M_6^* + C_6^* < 1$ *iff CD7 holds.*

$M_6^* + C_6^* < 1$ is equivalent to $\delta_M < \beta + \delta_T$, which is guaranteed by CD7. $E_6 \in \mathbb{D}$ iff CD5, CD6, and CD7 hold under A6. CD5 and CD6 combine to be:

$$\frac{(\beta + \delta_T - \delta_M)(\rho_M + \Theta_M)}{\beta + \rho_T + \Theta_T - \rho_M - \Theta_M} - \delta_M < g < \frac{(\beta + \delta_T - \delta_M)(\rho_T + \Theta_T)}{\beta + \rho_T + \Theta_T - \rho_M - \Theta_M} - \delta_T.$$

This means macroalgae and turf algae coexistence equilibrium is in the positive invariant feasible region $\mathbb{D}$ when the grazing effect is between two threshold values.

3. C T plane: We solve the coral and turf algae coexistence equilibrium from the following equations:

$$\begin{cases} G(0, C, T) = \left[\gamma T + (\rho_C + \Theta_C) S - \alpha M - 1\right]\Big|_{M=0} = 0 \\ H(0, C, T) = \left[(\rho_T + \Theta_T) S - \beta M - \gamma C - (\delta_T + g)\right]\Big|_{M=0} = 0, \end{cases}$$

$$\Rightarrow E_7 = (0, C_7^*, T_7^*),$$

with

$$C_7^* = \frac{(\delta_T + g)(\rho_C + \Theta_C - \gamma) + (\rho_T + \Theta_T)(\gamma - 1)}{\gamma(\gamma + \rho_T + \Theta_T - \rho_C - \Theta_C)} \tag{2.12}$$

$$T_7^* = \frac{(\rho_T + \Theta_T + \gamma) + (\rho_C + \Theta_C)(-\gamma - \delta_T - g)}{\gamma(\gamma + \rho_T + \Theta_T - \rho_C - \Theta_C)}. \tag{2.13}$$

Assumption A7. *We further assume*

$$\rho_T > \rho_C + \Theta_C - \gamma - \Theta_T$$

to eliminate cases and better focus on the grazing effect g. This assumption is more concrete than $\rho_T >> \rho_C$ in A1. Denominator of C_7^* and T_7^* is positive under A7.

Condition CD8.

$$g < \frac{\gamma + \rho_T + \Theta_T}{\rho_C + \Theta_C} - \gamma - \delta_T$$

The grazing effect is less than some threshold value. The numerator of T_7^* is positive iff CD8 holds.

Numerator of $C_7^* > 0$ is equivalent to $g > -\frac{(\rho_T + \Theta_T)(\gamma - 1)}{\rho_C + \Theta_C - \gamma} - \delta_T$, which is always true under A1 and A2. Numerator of C_7^* is always positive. $C_7^* + T_7^* < 1$ is equivalent to $g > 1 - \gamma - \delta_T$, which is always true under A2 because $1 - \gamma - \delta_T < 0$. $E_7 \in \mathbb{D}$ iff CD8 holds under A7. CD8 and condition for numerator of $C_7^* > 0$ combine to be:

$$-\frac{(\rho_T + \Theta_T)(\gamma - 1)}{\rho_C + \Theta_C - \gamma} - \delta_T < g < \frac{\gamma + \rho_T + \Theta_T}{\rho_C + \Theta_C} - \gamma - \delta_T.$$

This means coral and turf algae coexistence equilibrium is in the positive invariant feasible region $\mathbb{D}$ when the grazing effect is between two threshold values.

Interior equilibrium

1. We solve the macroalgae, coral, and turf algae coexistence equilibrium from the following linear system:

$$\begin{cases} F(M, C, T) = \alpha C + \beta T + (\rho_M + \Theta_M) S - (\delta_M + g) = 0 \\ G(M, C, T) = \gamma T + (\rho_C + \Theta_C) S - \alpha M - 1 = 0 \\ H(M, C, T) = (\rho_T + \Theta_T) S - \beta M - \gamma C - (\delta_T + g) = 0. \end{cases} \tag{2.14}$$

The unique macroalgae, coral, and turf algae coexistence equilibrium $E_8 = (M_8^*, C_8^*, T_8^*)$ can be solved from the linear system (2.14), provided the matrix A is invertible.

$$\Rightarrow \begin{pmatrix} M_8^* \\ C_8^* \\ T_8^* \end{pmatrix} = A^{-1} \begin{pmatrix} \rho_M + \Theta_M - \delta_M - g \\ \rho_C + \Theta_C - 1 \\ \rho_T + \Theta_T - \delta_T - g \end{pmatrix} \tag{2.15}$$

$$\text{with } A = \begin{pmatrix} \rho_M + \Theta_M & \rho_M + \Theta_M - \alpha & \rho_M + \Theta_M - \beta \\ \alpha + \rho_C + \Theta_C & \rho_C + \Theta_C & \rho_C + \Theta_C - \gamma \\ \beta + \rho_T + \Theta_T & \gamma + \rho_T + \Theta_T & \rho_T + \Theta_T \end{pmatrix}$$

We calculate explicit formula for equilibria E_1 to E_7. The interior coexistence equilibrium, E_8, is implicitly described as the solution of a linear system. We give conditions for the equilibria E_1 to E_7 to be in the positive invariant region $\mathbb{D}$.

2.2.2 Local stability of equilibrium

In this subsection, we give conditions for the local stability of equilibria E_1 to E_7. The local stability of equilibria tells us whether the solution will approach the equilibrium or move away from it in the long run if the initial condition is near the equilibrium. The local stability analysis also helps us to prove persistence theorems.

We calculate the Jacobian matrix of ODE system (2.7) to determine the local stability of the equilibrium.

$$J(M,C,T) = \begin{pmatrix} F + MF_M & MF_C & MF_T \\ CG_M & G + CG_C & CG_T \\ TH_M & TH_C & H + TH_T \end{pmatrix}$$

$$= \begin{pmatrix} F - (\rho_M + \Theta_M)\, M & -(\rho_M + \Theta_M - \alpha)\, M & -(\rho_M + \Theta_M - \beta)\, M \\ -(\alpha + \rho_C + \Theta_C)\, C & G - (\rho_C + \Theta_C)\, C & -(\rho_C + \Theta_C - \gamma)\, C \\ -(\beta + \rho_T + \Theta_T)\, T & -(\gamma + \rho_T + \Theta_T)\, T & H - (\rho_T + \Theta_T)\, T \end{pmatrix} \tag{2.16}$$

Trivial equilibrium

1. We consider the trivial equilibrium. From subsection 2.2.1, we know $E_1 \in \mathbb{D}$. We evaluate the Jacobian matrix at equilibrium E_1:

$$J(0,0,0) = \begin{pmatrix} \rho_M + \Theta_M - \delta_M - g & 0 & 0 \\ 0 & \rho_C + \Theta_C - 1 & 0 \\ 0 & 0 & \rho_T + \Theta_T - \delta_T - g \end{pmatrix}. \tag{2.17}$$

$J(0,0,0)$ is a diagonal matrix. Eigenvalues are the diagonal elements: $\rho_M + \Theta_M - \delta_M - g$, $\rho_C + \Theta_C - 1$, and $\rho_T + \Theta_T - \delta_T - g$. We analyze the sign of the eigenvalues.

   (a) $\rho_M + \Theta_M - \delta_M - g = (\rho_M + \Theta_M) M_2^*$. $\rho_M + \Theta_M - \delta_M - g < 0$ is equivalent to $M_2^* < 0$, equivalent to CD1$^-$.

   (b) $\rho_C + \Theta_C - 1 = (\rho_C + \Theta_C) C_3^*$. $\rho_C + \Theta_C - 1 < 0$ is equivalent to $C_3^* < 0$, which is impossible under A1 and A2.

   (c) $\rho_T + \Theta_T - \delta_T - g = (\rho_T + \Theta_T) T_4^*$. $\rho_T + \Theta_T - \delta_T - g < 0$ is equivalent to $T_4^* < 0$, equivalent to CD2$^-$.

   In summary, trivial equilibrium E_1 is in the positive invariant feasible region $\mathbb{D}$ and is always unstable under A1 and A2. Biologically, three functional groups will not all go extinct.

Axial equilibrium

1. We consider the macroalgae-only equilibrium E_2. From subsection 2.2.1, we know $E_2 \in \mathbb{D}$ iff CD1 holds. We evaluate the Jacobian matrix at equilibrium E_2:

$$J(M_2^*,0,0) = \begin{pmatrix} -(\rho_M + \Theta_M) M_2^* & -(\rho_M + \Theta_M - \alpha) M_2^* & -(\rho_M + \Theta_M - \beta) M_2^* \\ 0 & G_2^* & 0 \\ 0 & 0 & H_2^* \end{pmatrix}, \tag{2.18}$$

   with $G_2^* = G(M_2^*,0,0)$ and $H_2^* = H(M_2^*,0,0)$. $J(M_2^*,0,0)$ is an upper triangular matrix. Eigenvalues are the diagonal elements: $-(\rho_M + \Theta_M) M_2^*$, G_2^*, and H_2^*. We analyze the sign of the eigenvalues.

(a) $-(\rho_M + \Theta_M) M_2^* < 0$ if $M_2^* > 0$, which is equivalent to CD1.

(b) $G_2^* = \dfrac{\alpha(\alpha + \rho_C + \Theta_C - \rho_M - \Theta_M)}{\rho_M + \Theta_M} C_5^*$. $G_2^* < 0$ is equivalent to $C_5^* < 0$, equivalent to CD3^-.

(c) $H_2^* = \dfrac{\beta(\beta + \rho_T + \Theta_T - \rho_M - \Theta_M)}{\rho_M + \Theta_M} T_6^*$. $H_2^* < 0$ is equivalent to $T_6^* < 0$, equivalent to CD5^-.

In summary, macroalgae-only equilibrium E_2 is in the positive invariant feasible region $\mathbb{D}$ and locally stable if CD1, CD3^-, and CD5^- hold. Those local stability conditions also imply that the local stability of macroalgae-only equilibrium E_2 and the existence of macroalgae and coral coexistence equilibrium E_5, as well as macroalgae and turf algae coexistence equilibrium E_6, are mutually exclusive. Biologically, if no coral and turf algae exist, then macroalgae will remain dominant when the grazing pressure is low.

2. We consider the coral-only equilibrium E_3. From subsection 2.2.1, we know $E_3 \in \mathbb{D}$. We evaluate the Jacobian matrix at equilibrium E_3:

$$J(0, C_3^*, 0) = \begin{pmatrix} F_3^* & 0 & 0 \\ -(\alpha + \rho_C + \Theta_C) C_3^* & -(\rho_C + \Theta_C) C_3^* & -(\rho_C + \Theta_C - \gamma) C_3^* \\ 0 & 0 & H_3^* \end{pmatrix}, \tag{2.19}$$

with $F_3^* = F(0, C_3^*, 0)$ and $H_3^* = H(0, C_3^*, 0)$. We can view $J(0, C_3^*, 0)$ as a lower triangular block matrix. Eigenvalues are the diagonal elements: F_3^*, $-(\rho_C + \Theta_C) C_3^*$, and H_3^*. We analysis the sign of the eigenvalues.

(a) $F_3^* = \dfrac{\alpha(\alpha + \rho_C + \Theta_C - \rho_M - \Theta_M)}{\rho_C + \Theta_C} M_5^*$. $F_3^* < 0$ is equivalent to $M_5^* < 0$, equivalent to CD4^-.

(b) $-(\rho_C + \Theta_C) C_3^* < 0$ if $C_3^* > 0$, which is guaranteed by A1 and A2 in subsection 2.2.1.

(c) $H_3^* = \dfrac{\gamma(\gamma + \rho_T + \Theta_T - \rho_C - \Theta_C)}{\rho_C + \Theta_C} T_7^*$. $H_3^* < 0$ is equivalent to $T_7^* < 0$, equivalent to CD8^-.

In summary, coral-only equilibrium E_3 is in the positive invariant feasible region $\mathbb{D}$ and locally stable if CD4$^-$ and CD8$^-$ hold. Those local stability conditions also imply that the local stability of coral-only equilibrium E_3 and the existence of macroalgae and coral coexistence equilibrium E_5, as well as coral and turf algae coexistence equilibrium E_7, are mutually exclusive. Biologically, if no macroalgae and turf algae exist, then coral will remain dominant when the grazing pressure is high.

3. We consider the turf algae-only equilibrium E_4. From subsection 2.2.1, we know $E_4 \in \mathbb{D}$ iff CD2 holds. We evaluate the Jacobian matrix at equilibrium E_4:

$$J\left(0,0,T_4^*\right) = \begin{pmatrix} F_4^* & 0 & 0 \\ 0 & G_4^* & 0 \\ -\left(\beta+\rho_T+\Theta_T\right)T_4^* & -\left(\gamma+\rho_T+\Theta_T\right)T_4^* & -\left(\rho_T+\Theta_T\right)T_4^* \end{pmatrix}, \tag{2.20}$$

with $F_4^* = F\left(0,0,T_4^*\right)$ and $G_4^* = G\left(0,0,T_4^*\right)$. $J\left(0,0,T_4^*\right)$ is a lower triangular matrix. Eigenvalues are the diagonal elements: F_4^*, G_4^*, and $-\left(\rho_T+\Theta_T\right)T_4^*$. We analysis the sign of the eigenvalues.

   (a) $F_4^* = \dfrac{\beta\left(\beta+\rho_T+\Theta_T-\rho_M-\Theta_M\right)}{\rho_T+\Theta_T}M_6^*$. $F_4^* < 0$ is equivalent to $M_6^* < 0$, equivalent to CD6$^-$.

   (b) $G_4^* = \dfrac{\gamma\left(\gamma+\rho_T+\Theta_T-\rho_C-\Theta_C\right)}{\rho_T+\Theta_T}C_7^*$. $G_4^* < 0$ is equivalent to $C_7^* < 0$, which is not possible under A1 and A2.

   (c) $-\left(\rho_T+\Theta_T\right)T_4^* < 0$ if $T_4^* > 0$, which is equivalent to CD2.

In summary, turf algae-only equilibrium E_4 is in the positive invariant region feasible region $\mathbb{D}$ if CD2 holds but is always unstable under A1 and A2. Those local stability conditions also imply that the local stability of turf algae-only equilibrium E_4 and the existence of macroalgae and turf algae coexistence equilibrium E_6, as well as coral and turf algae coexistence equilibrium E_7, are mutually exclusive. Biologically, if no macroalgae and coral exist, then turf algae can not remain dominant alone.

Boundary equilibrium

1. We consider the macroalgae and coral coexistence equilibrium E_5. From subsection 2.2.1, we know $E_5 \in \mathbb{D}$ if A5, CD3, and CD4 hold. We evaluate the Jacobian matrix at equilibrium E_5:

$$J\left(M_5^*, C_5^*, 0\right) = \begin{pmatrix} -\left(\rho_M + \Theta_M\right) M_5^* & -\left(\rho_M + \Theta_M - \alpha\right) M_5^* & -\left(\rho_M + \Theta_M - \beta\right) M_5^* \\ -\left(\alpha + \rho_C + \Theta_C\right) C_5^* & -\left(\rho_C + \Theta_C\right) C_5^* & -\left(\rho_C + \Theta_C - \gamma\right) C_5^* \\ 0 & 0 & H_5^* \end{pmatrix}, \tag{2.21}$$

with $H_5^* = H\left(M_5^*, C_5^*, 0\right)$. When $T = 0$, $\dfrac{dT}{dt} = 0$, so the M-C plane is invariant. We decompose the 3×3 Jacobian matrix (2.21) in the M-C plane. In the M-C plane, $J\left(M_5^*, C_5^*, 0\right)$ reduces to the minor matrix:

$$J\left(M_5^*, C_5^*, 0\right)_{3,3} = \begin{pmatrix} -\left(\rho_M + \Theta_M\right) M_5^* & -\left(\rho_M + \Theta_M - \alpha\right) M_5^* \\ -\left(\alpha + \rho_C + \Theta_C\right) C_5^* & -\left(\rho_C + \Theta_C\right) C_5^* \end{pmatrix}, \tag{2.22}$$

$$\Rightarrow \operatorname{tr}\left(J\left(M_5^*, C_5^*, 0\right)_{3,3}\right) = -\left(\rho_M + \Theta_M\right) M_5^* - \left(\rho_C + \Theta_C\right) C_5^*,$$

$$\Rightarrow \det\left(J\left(M_5^*, C_5^*, 0\right)_{3,3}\right) = \underbrace{\left[\alpha\left(\alpha + \rho_C + \Theta_C - \rho_M - \Theta_M\right)\right]}_{\text{denominator of } M_5^* \text{ and } C_5^*} M_5^* C_5^*.$$

When $E_5 \in \mathbb{D}$, $\operatorname{tr}\left(J\left(M_5^*, C_5^*, 0\right)_{3,3}\right) < 0$, and $\det\left(J\left(M_5^*, C_5^*, 0\right)_{3,3}\right) > 0$. Macroalgae and coral coexistence equilibrium E_5 is always locally stable in the M-C plane if $E_5 \in \mathbb{D}$. The local stability of E_5 in the full three dimensional space is determined by the sign of $\dfrac{dT}{dt}$ evaluated at E_5, which is equivalent to the sign of the third eigenvalue H_5^* in matrix (2.21). H_5^* is positive proportional to T_8^* from the interior equilibrium. $H_5^* \propto T_8^*$, so $H_5^* < 0$ is equivalent to $T_8^* < 0$.

In summary, macroalgae and coral coexistence equilibrium E_5 is in the positive invariant region feasible region $\mathbb{D}$ and locally stable if CD3 and CD4 hold, and $H_5^* < 0$ under A5. Those local stability conditions also imply that the local stability of macroalgae and coral coexistence equilibrium E_5 and the existence of interior equilibrium E_8 are mutually

exclusive. Biologically, if no turf algae exist, then macroalgae and coral can coexist when the grazing effect is between two threshold values.

2. We consider the macroalgae and turf algae coexistence equilibrium E_6. From subsection 2.2.1, we know $E_6 \in \mathbb{D}$ if A6, CD5, CD6, and CD7 hold. We evaluate the Jacobian matrix at equilibrium E_6:

$$J\left(M_6^*, 0, T_6^*\right) = \begin{pmatrix} -\left(\rho_M + \Theta_M\right) M_6^* & -\left(\rho_M + \Theta_M - \alpha\right) M_6^* & -\left(\rho_M + \Theta_M - \beta\right) M_6^* \\ 0 & G_6^* & 0 \\ -\left(\beta + \rho_T + \Theta_T\right) T_6^* & -\left(\gamma + \rho_T + \Theta_T\right) T_6^* & -\left(\rho_T + \Theta_T\right) T_6^* \end{pmatrix}, \tag{2.23}$$

with $G_6^* = G\left(M_6^*, 0, T_6^*\right)$. When $C = 0$, $\dfrac{dC}{dt} = 0$, so the M-T plane is invariant. We can decompose the 3×3 Jacobian matrix (2.23) in the M-T plane. In the M-T plane, $J\left(M_6^*, 0, T_6^*\right)$ reduces to the minor matrix:

$$J\left(M_6^*, 0, T_6^*\right)_{2,2} = \begin{pmatrix} -\left(\rho_M + \Theta_M\right) M_6^* & -\left(\rho_M + \Theta_M - \beta\right) M_6^* \\ -\left(\beta + \rho_T + \Theta_T\right) T_6^* & -\left(\rho_T + \Theta_T\right) T_6^* \end{pmatrix}, \tag{2.24}$$

$$\Rightarrow \operatorname{tr}\left(J\left(M_6^*, 0, T_6^*\right)_{2,2}\right) = -\left(\rho_M + \Theta_M\right) M_6^* - \left(\rho_T + \Theta_T\right) T_6^*,$$

$$\Rightarrow \det\left(J\left(M_6^*, 0, T_6^*\right)_{2,2}\right) = \underbrace{\left[\beta\left(\beta + \rho_T + \Theta_T - \rho_M - \Theta_M\right)\right]}_{\text{denominator of } M_6^* \text{ and } T_6^*} M_6^* T_6^*.$$

When $E_6 \in \mathbb{D}$, $\operatorname{tr}\left(J\left(M_6^*, 0, T_6^*\right)_{2,2}\right) < 0$, and $\det\left(J\left(M_6^*, 0, T_6^*\right)_{2,2}\right) > 0$. Macroalgae and turf algae coexistence equilibrium E_6 is always locally stable in the M-T plane if $E_6 \in \mathbb{D}$. The local stability of E_6 in the full three dimensional space is determined by the sign of $\dfrac{dC}{dt}$ evaluated at E_6, which is equivalent to the sign of the second eigenvalue G_6^* in matrix (2.23). G_6^* is positive proportional to C_8^* from the interior equilibrium. $G_6^* \propto C_8^*$, so $G_6^* < 0$ is equivalent to $C_8^* < 0$.

In summary, macroalgae and turf algae coexistence equilibrium E_6 is in the positive invariant region feasible region $\mathbb{D}$ and locally stable if CD5, CD6, and CD7 hold, and $G_6^* < 0$ under A6. Those local stability conditions also imply that the local stability of macroalgae and turf algae coexistence equilibrium E_6 and the existence of interior equilibrium

E_8 are mutually exclusive. Biologically, if no coral exist, then macroalgae and turf algae can coexist when the grazing effect is between two threshold values.

3. We consider the coral and turf algae coexistence equilibrium E_7. From subsection 2.2.1, we know $E_7 \in \mathbb{D}$ if A7 and CD8 hold. We evaluate the Jacobian matrix at equilibrium E_7:

$$J\left(0, C_7^*, T_7^*\right) = \begin{pmatrix} F_7^* & 0 & 0 \\ -\left(\alpha + \rho_C + \Theta_C\right) C_7^* & -\left(\rho_C + \Theta_C\right) C_7^* & -\left(\rho_C + \Theta_C - \gamma\right) C_7^* \\ -\left(\beta + \rho_T + \Theta_T\right) T_7^* & -\left(\gamma + \rho_T + \Theta_T\right) T_7^* & -\left(\rho_T + \Theta_T\right) T_7^* \end{pmatrix}, \tag{2.25}$$

with $F_7^* = F\left(0, C_7^*, T_7^*\right)$. When $M = 0$, $\dfrac{dM}{dt} = 0$, so the C-T plane is invariant. We can decompose the 3×3 Jacobian matrix (2.25) in the C-T plane. In the C-T plane, $J\left(0, C_7^*, T_7^*\right)$ reduces to the minor matrix:

$$J\left(0, C_7^*, T_7^*\right)_{1,1} = \begin{pmatrix} -\left(\rho_C + \Theta_C\right) C_7^* & -\left(\rho_C + \Theta_C - \gamma\right) C_7^* \\ -\left(\gamma + \rho_T + \Theta_T\right) T_7^* & -\rho_T T_7^* \end{pmatrix}, \tag{2.26}$$

$$\Rightarrow \operatorname{tr}\left(J\left(0, C_7^*, T_7^*\right)_{1,1}\right) = -\left(\rho_C + \Theta_C\right) C_7^* - \left(\rho_T + \Theta_T\right) T_7^*,$$

$$\Rightarrow \det\left(J\left(0, C_7^*, T_7^*\right)_{1,1}\right) = \underbrace{\left[\gamma\left(\gamma + \rho_T + \Theta_T - \rho_C - \Theta_C\right)\right]}_{\text{denominator of } C_7^* \text{ and } T_7^*} C_7^* T_7^*.$$

When $E_7 \in \mathbb{D}$, $\operatorname{tr}\left(J\left(0, C_7^*, T_7^*\right)_{1,1}\right) < 0$, and $\det\left(J\left(0, C_7^*, T_7^*\right)_{1,1}\right) > 0$. Coral and turf algae coexistence equilibrium E_7 is always locally stable in the C-T plane if $E_7 \in \mathbb{D}$. The local stability of E_7 in the full three dimensional space is determined by the sign of $\dfrac{dM}{dt}$ evaluated at E_7, which is equivalent to the sign of the first eigenvalue F_7^* in matrix (2.25). F_7^* is positive proportional to M_8^* from the interior equilibrium. $F_7^* \propto M_8^*$, so $F_7^* < 0$ is equivalent to $M_8^* < 0$.

In summary, coral and turf algae coexistence equilibrium E_7 is in the positive invariant region feasible region $\mathbb{D}$ and locally stable if CD8 holds and $F_7^* < 0$ under A7. Those local stability conditions also imply that the

local stability of coral and turf algae coexistence equilibrium E_7 and the existence of interior equilibrium E_8 are mutually exclusive. Biologically, if no macroalgae exist, then coral and turf algae can coexist when the grazing effect is between two threshold values.

We summarize the equilibrium and local stability discussion in the following theorem 2.2.1 and table 2.1.

Theorem 2.2.1 (**Coral equilibria**). *If all parameters are positive and A1 to A7 hold, then the trivial equilibrium E_1 and turf algae-only equilibrium E_4 of the system* (2.6) *are unstable. Moreover,*

(a) Coral-only equilibrium E_3 is locally stable if CD4$^-$ and CD8$^-$ hold,

(b) Coral and macroalgae coexistence equilibrium E_5 is locally stable if CD3 and CD4 hold, and $H_5^* < 0$,

(c) Coral and turf algae coexistence equilibrium E_7 is locally stable if CD8 holds, and $F_5^* < 0$.

Table 2.1 Summary of the existence and stability conditions of equilibrium

Equilibrium	Existence	Local stability conditions
E_1 (0)	always in $\mathbb{D}$	always unstable
E_2 (M)	CD1	CD1, CD3$^-$, and CD5$^-$
E_3 (C)	always in $\mathbb{D}$	CD4$^-$ and CD8$^-$
E_4 (T)	CD2	always unstable
E_5 (M,C)	CD3 and CD4	CD3, CD4, and $H_5^* < 0$
E_6 (M,T)	CD5, CD6, and CD7	CD5, CD6, CD7, and $G_6^* < 0$
E_7 (C,T)	CD8	CD8 and $F_7^* < 0$

This table summarizes the existence and local stability results of equilibria in subsections 2.1.1 and 2.1.2, one trivial equilibrium, three axial equilibria, and three boundary equilibria. We assume A1 through A4 always hold, and we further assume A5 through A7 hold to eliminate uninteresting cases. We do not give conditions for the unique interior equilibrium E_8.

2.2.3 Persistence results

It is challenging to derive the global stability conditions for the one-patch model (2.2). In this subsection, we use the persistence theory as a rigorous mathematical tool to determine whether coral will survive or go extinct in the long run. Under certain conditions, we can ensure coral will not go extinct by formulating a positive lower bound for the long-term value of the coral population. We show that there is always some available space left under all conditions, and coral persist under high grazing pressure by proving persistence theorems for available space and coral.

Theorem 2.2.2 (**Space-persistence**). *If all parameters are positive, then the solution semiflow generated by the system* (2.6) *is uniformly strongly space-persistent on the state space* $\mathbb{X} = \mathbb{D}$.

Proof. We use the contradiction to show uniform weak space-persistence first. If all parameters are positive and the solution semiflow ϕ is not uniformly weakly space-persistent, then for arbitrary $\epsilon > 0$, there exists a solution with $S(0) > 0$ and $\limsup_{t\to\infty} S(t) \leq \epsilon$. Furthermore, there exists some $t_0 > 0$ such that $S(t) < \epsilon$ for $t \geq t_0$. For $t \geq t_0$, we have the following:

$$\begin{aligned}
\frac{dS}{dt} &= -\frac{dM}{dt} - \frac{dC}{dt} - \frac{dT}{dt} \\
&= -\left(\rho_M M + \rho_C C + \rho_T T\right) S - \left(\Theta_M M + \Theta_C C + \Theta_T T\right) S \\
&\quad + \left(\delta_M + g\right) M + C + \left(\delta_T + g\right) T \\
&= -\left[\left(\rho_M + \Theta_M\right) M + \left(\rho_C + \Theta_C\right) C + \left(\rho_T + \Theta_T\right) T\right] S \\
&\quad + \left(\delta_M + g\right) M + C + \left(\delta_T + g\right) T \\
&\geq -\max\left\{\rho_M + \Theta_M, \rho_C + \Theta_C, \rho_T + \Theta_T\right\} \left(M + C + T\right) S \\
&\quad + \min\left\{\delta_M + g, 1, \delta_T + g\right\} \left(M + C + T\right) \\
&= -\max\left\{\rho_M + \Theta_M, \rho_C + \Theta_C, \rho_T + \Theta_T\right\} \left(1 - S\right) S \\
&\quad + \min\left\{\delta_M + g, 1, \delta_T + g\right\} \left(1 - S\right) \\
&= \left[-\max\left\{\rho_M + \Theta_M, \rho_C + \Theta_C, \rho_T + \Theta_T\right\} S \right. \\
&\quad \left. + \min\left\{\delta_M + g, 1, \delta_T + g\right\}\right] \left(1 - S\right).
\end{aligned} \tag{2.27}$$

We choose $\epsilon < \dfrac{\min\{\delta_M + g, 1, \delta_T + g\}}{\max\{\rho_M + \Theta_M, \rho_C + \Theta_C, \rho_T + \Theta_T\}}$ such that the right hand side of (2.27) > 0. $S(t)$ is monotone increasing $\Rightarrow S(t) \to 1$ as $t \to \infty$, a contradiction. We check a few conditions, which lead to uniform strong space-persistence based on uniform weak space-persistence. We choose the time set $\mathbb{J} = \mathbb{R}^+$ and the state space $\mathbb{X} = \mathbb{D}$. We choose the nonempty subset $\mathbb{B} = \mathbb{X}$. $\rho(M, C, T, S) = S$ and $\sigma = \rho(\phi_t)$ are continuous. For every $(M, C, T, S) \in \mathbb{X}$ such that $\rho(M, C, T, S) > 0$, $\phi_t(\mathbb{X}) \to \mathbb{B}$ as $t \to \infty$. If $0 < d_1 < d_2 < \infty$, then $\mathbb{B} \cap \{d_1 \leq S \leq d_2\}$ is compact. If $S(0) > 0$, then $S(t) > 0$ for all $t > 0$. The conditions in Theorem 4.13 on page 99 of Smith and Thieme (2011) are satisfied. The uniform weak space-persistence and Theorem 4.13 on page 99 of Smith and Thieme (2011) together imply uniform strong persistence of available space. ■

Theorem 2.2.3 (**Coral-persistence**). *If all parameters are positive, A1 to A7 hold, and $g > c^*$, where $c^* = \max\{\rho_M + \Theta_M - \delta_M, \rho_T + \Theta_T - \delta_T\}$, then the solution semiflow generated by the system* (2.6) *is uniformly strongly coral-persistent on the state space $\mathbb{X} = \mathbb{D}$.*

Proof. We use the contradiction to show uniform weak coral-persistence first. If all parameters are positive, A1 to A7 hold, $g > c^*$, and the solution semiflow ϕ is not uniformly weakly coral-persistent, then for arbitrary $\epsilon > 0$, there exists a solution with $C(0) > 0$ and $\limsup_{t\to\infty} C(t) \leq \epsilon$. $M(t), C(t)$, and $T(t) > 0$ for $t \geq 0$. Furthermore, there exists some $t_0 > 0$ such that $C(t) < \epsilon$ for $t \geq t_0$.

For $t \geq t_0$, we have the following:

$$\begin{aligned}
\frac{d\,(M+T)}{dt} &= \alpha MC + \rho_M MS - \delta_M M - gM + \Theta_M MS \\
&\quad + \rho_T TS - \gamma CT - \delta_T T - gT + \Theta_T TS \\
&= \alpha MC + (\rho_M + \Theta_M)\, MS - (\delta_M + g)\, M \\
&\quad + (\rho_T + \Theta_T)\, TS - \gamma CT - (\delta_T + g)\, T \\
&\leq \alpha MC + (\rho_M + \Theta_M)\, M - (\delta_M + g)\, M \\
&\quad + (\rho_T + \Theta_T)\, T - \gamma CT - (\delta_T + g)\, T \\
&= (\alpha C + \rho_M + \Theta_M - \delta_M - g)\, M \\
&\quad + (\rho_T + \Theta_T - \gamma C - \delta_T - g)\, T \\
&\leq (\alpha\epsilon + \rho_M + \Theta_M - \delta_M - g)\, M \\
&\quad + (\rho_T + \Theta_T - \delta_T - g)\, T.
\end{aligned} \tag{2.28}$$

Since $g > c^*$, $\rho_M + \Theta_M - \delta_M - g < 0$ and $\rho_T + \Theta_T - \delta_T - g < 0$. We choose $\epsilon < \dfrac{g - (\rho_M + \Theta_M - \delta_M)}{\alpha}$ such that the right hand side of (2.28) < 0. $M(t)+T(t)$ is monotone decreasing $\Rightarrow M(t)+T(t) \to 0$ as $t \to \infty \Rightarrow M(t) \to 0$ and $T(t) \to 0$ as $t \to \infty$. Furthermore, $\liminf_{t\to\infty} S(t) \geq 1 - \epsilon$.

$$\begin{aligned}
\liminf_{t\to\infty} \frac{dC}{dt} &= \rho_C CS - C + \Theta_C CS \\
&= \left[(\rho_C + \Theta_C)\, S - 1\right] C \\
&\geq \left[(\rho_C + \Theta_C)\,(1-\epsilon) - 1\right] C
\end{aligned} \tag{2.29}$$

We choose $\epsilon < \min\left\{\dfrac{g - (\rho_M + \Theta_M - \delta_M)}{\alpha}, 1 - \dfrac{1}{\rho_T + \Theta_C}\right\}$ such that the right hand side of (2.29) > 0. $1 - \dfrac{1}{\rho_T + \Theta_C} > 0$ because $\rho_C > 1$ by assumptions A1 and A2. $C(t)$ is monotone increasing $\Rightarrow C(t) \to 1$ as $t \to \infty$, a contradiction. We check a few conditions, which lead to uniform strong coral-persistence based on uniform weak coral-persistence. We choose the time set $\mathbb{J} = \mathbb{R}^+$ and the state space $\mathbb{X} = \mathbb{D}$. We choose the nonempty subset $\mathbb{B} = \mathbb{X}$. $\rho(M, C, T, S) = C$ and $\sigma = \rho\,(\phi_t)$ are continuous. For every $(M, C, T, S) \in \mathbb{X}$ such that $\rho(M, C, T, S) > 0$, $\phi_t(\mathbb{X}) \to \mathbb{B}$ as $t \to \infty$. If $0 < d_1 < d_2 < \infty$, then $\mathbb{B} \cap \{d_1 \leq C \leq d_2\}$ is compact. There is no $(M, C, T, S) \in \mathbb{B}, t_1, t_2 > 0$ such that $C(0) > 0, C(t_1) = 0$, and $C(t_2) > 0$ due to the format of coral equation

in the system (2.6). The conditions in Theorem 4.13 on page 99 of Smith and Thieme (2011) are satisfied. The uniform weak coral-persistence and Theorem 4.13 on page 99 of Smith and Thieme (2011) together imply uniform strong persistence of coral under high grazing pressure. ■

Theorem 2.2.2 implies there will always be some available space left at any given time for any initial conditions and any positive parameter values as long as $S(0) > 0$. Theorem 2.2.2 also suggests the three functional groups will never use up the available space in the long run. However, it is possible to have minimal empty space left in the long run because Theorem 2.2.2 only guarantees available space is bounded away from zero. Still, it does not ensure the amount of available space left is adequate. Theorem 2.2.3 implies coral will persist in the long run at high grazing pressure. Biologically, suppose the sum of the grazing effect and the natural death rate is larger than the total growth rate from occupying available space and propagules settling for both macroalgae and turf algae. In that case, coral will not go extinct in the long run. However, coral persist in what form is still unknown: it is possible that the reefs are dominated by coral, or coral coexist with algae, or even the coral population does not go extinct but eventually remains at a low level. Theorem 2.2.3 only guarantees coral are bounded away from zero at high grazing pressure. Still, it does not ensure the amount of coral left in the long run is adequate or that the coral population remains healthy.

2.2.4 Bifurcation results

In this subsection, we analyze the possible equilibrium states using bifurcation diagrams based on the grazing effect g for slow turf algae and fast turf algae scenarios. Both empirical observations and experiments indicate the density of herbivorous fish has a considerable influence on the phase shift of the coral-algae ecosystem. The absence of herbivorous fish leads to the boom of macroalgae, which weakens the larval recruitment and squeezes the living space of adult coral (Hughes et al., 2007). The abundance of herbivorous fish is positive related to the grazing effect. A decrease in grazing effect led to an

increase in algae biomass (Lirman, 2001). In the following numerical bifurcation analysis, we find four possible stable states in the slow turf algae scenario: macroalgae only or macroalgae and turf algae coexistence at low grazing pressure, macroalgae and coral coexistence at moderate grazing pressure, and coral only at high grazing pressure. We find five possible stable states in the fast turf algae scenario: macroalgae only or macroalgae and turf algae coexistence at low grazing pressure, three functional groups coexistence or coral and turf algae coexistence at moderate grazing pressure, and coral only at high grazing pressure. We show reasonable fishing helps support a higher level of coral cover.

Bifurcation at slow turf algae

In A1, we assume turf algae are the fastest colonizer. However, how much faster turf algae occupy available space than other functional groups is still unknown. As a result, we undertake bifurcation analysis in both slow and fast turf algae scenarios. In the first scenario, we undertake bifurcation when turf algae occupy available space relatively slowly. We choose parameter values based on A1 to A7 and table A.3: $\alpha = 0.23$, $\beta = 1.82$, $\gamma = 2.27$, $\Theta_M = 0.2$, $\Theta_C = 0.2$, $\Theta_T = 0.2$, $\delta_M = 0.05$, $\delta_T = 0.05$, $\rho_M = 3$, $\rho_C = 5$, and $\rho_T = 10$. ρ_T can range from 4.55 to 90.91, so $\rho_T = 10$ indicates turf algae occupy available space faster than macroalgae and coral. Still, the rate of turf algae occupying available space is relatively low in its own feasible range. We vary the value of grazing effect g to investigate how grazing effect affects the stability of equilibrium of interest in this scenario.

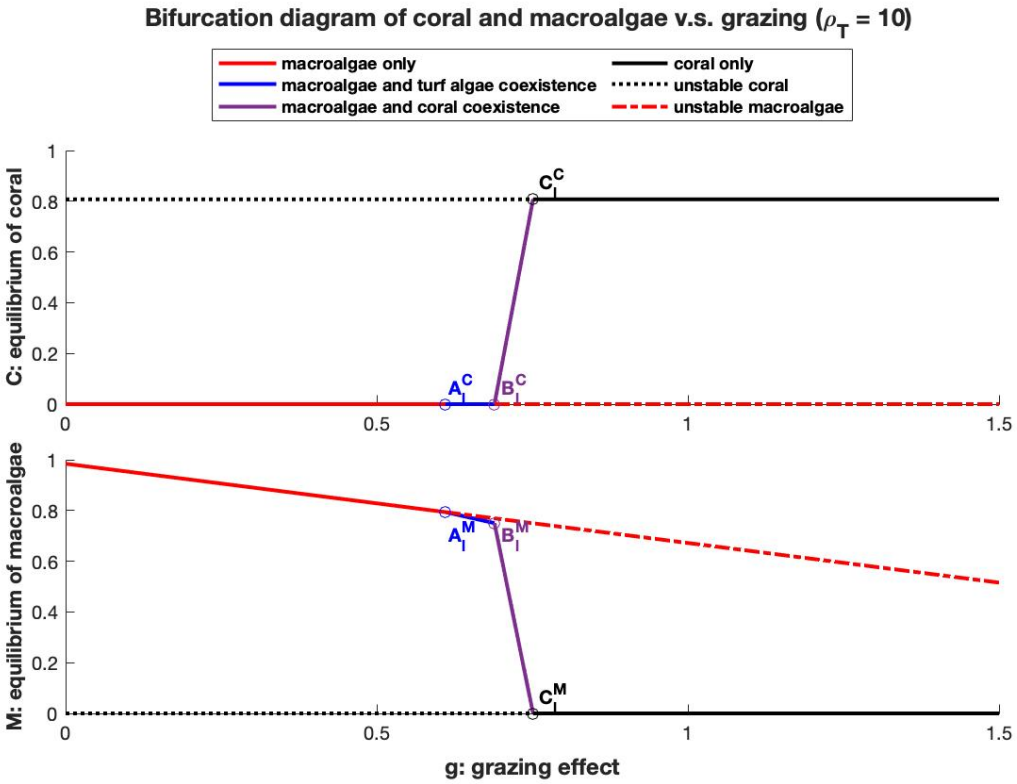

Fig. 2.1 Bifurcation diagram at low ρ_T. The upper panel shows the bifurcation result of the equilibrium level of coral and the lower panel for macroalgae. They share the same bifurcation values for grazing effect g. We summarize bifurcation points and values for low ρ_T case in table 2.2. All equilibria are linear with respect to g, based on the equilibrium calculation in section 2.2.1.

Table 2.2 Bifurcation points and values at low ρ_T

Bifurcation points (C)	Bifurcation points (M)	Bifurcation values
$A_l^C = (0.6103, 0)$	$A_l^M = (0.6103, 0.7937)$	$g_{low}^{CD5} = 0.6103$
$B_l^C = (0.6892, 0)$	$B_l^M = (0.6892, 0.7501)$	$g_{low}^{G_6^*} = 0.6892$
$C_l^C = (0.7512, 0.8077)$	$C_l^M = (0.7512, 0)$	$g^{CD4} = 0.7512$

This table summarizes the bifurcation points and values for the slow turf algae case. We find the bifurcation value $g_{low}^{G_6^*} = 0.6892$ using matcont package in MATLAB. We calculate other bifurcation values from the stability analysis of equilibrium.

Macroalgae-only equilibrium E_2, represented as the red line, is globally stable at grazing level $0 < g < g_{low}^{CD5}$, where $g_{low}^{CD5} = 0.6103$. When the grazing effect rises above g_{low}^{CD5}, E_2 loses stability and macroalgae and turf

algae coexistence equilibrium E_6, represented as the blue line, is globally stable for a short grazing effect range. Macroalgae and coral coexistence equilibrium E_5, represented as the purple line, emerges and is globally stable at grazing level $g_{low}^{G_6^*} < g < g^{CD4}$, where $g_{low}^{G_6^*} = 0.6892$, and $g^{CD4} = 0.7512$. When the grazing effect rises above g^{CD4}, E_5 loses stability and joins the globally stable coral-only equilibrium E_3, represented as the black line.

Biologically, for the slow turf algae scenario, the reefs will be dominated by macroalgae and turf algae in the long run when the grazing pressure is low. The reefs will be dominated by coral in the long run when the grazing pressure rises to a very high level. When the grazing pressure remains at a moderate level, macroalgae and coral can coexist in the long run.

Bifurcation at fast turf algae

In the second scenario, we undertake bifurcation when turf algae occupy available space relatively fast. We choose parameter values based on A1 to A7 and table A.3: $\alpha = 0.23$, $\beta = 1.82$, $\gamma = 2.27$, $\Theta_M = 0.2$, $\Theta_C = 0.2$, $\Theta_T = 0.2$, $\delta_M = 0.05$, $\delta_T = 0.05$, $\rho_M = 3$, $\rho_C = 5$, and $\rho_T = 70$. $\rho_T = 70$ indicates turf algae occupy available space faster than macroalgae and coral, and the rate is relatively high in its own feasible range. We vary the value of grazing effect g to investigate how grazing effect affects the stability of equilibrium of interest in this scenario.

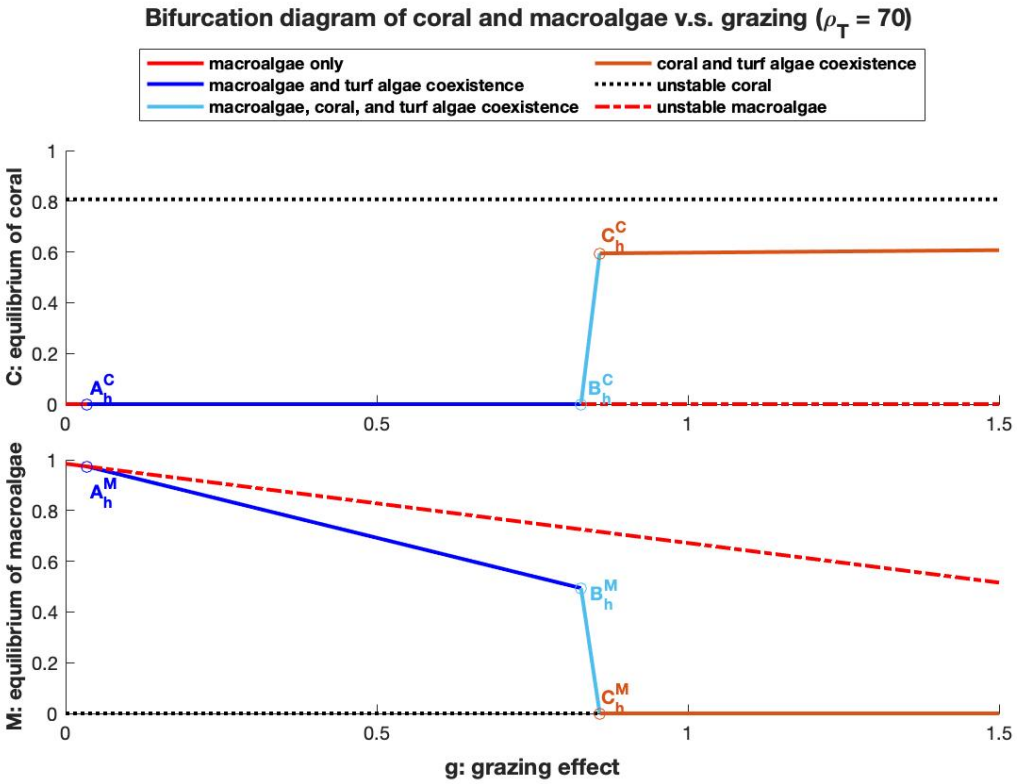

Fig. 2.2 Bifurcation diagram at high ρ_T. The upper panel shows the bifurcation result of equilibrium level of coral and the lower panel for macroalgae. They share the same bifurcation values for grazing effect g. The stable coral and turf algae coexistence equilibrium will join the stable coral-only equilibrium under extremely high grazing pressure, which is not shown in the figure range. We summarize bifurcation points and values for high ρ_T case in table 2.3. All equilibria are linear with respect to g, based on the equilibrium calculation in section 2.2.1.

Table 2.3 Bifurcation points and values at high ρ_T

Bifurcation points (C)	Bifurcation points (M)	Bifurcation values
$A_h^C = (0.0346, 0)$	$A_h^M = (0.0346, 0.9736)$	$g_{high}^{CD5} = 0.0346$
$B_h^C = (0.8283, 0)$	$B_h^M = (0.8283, 0.4939)$	$g_{high}^{G_6^*} = 0.8283$
$C_h^C = (0.8583, 0.5944)$	$C_h^M = (0.8583, 0)$	$g_{high}^{int} = 0.8583$

This table summarizes the bifurcation points and values for the fast turf algae case. We find the bifurcation values $g_{high}^{G_6^*} = 0.8283$ and $g_{high}^{int} = 0.8583$ using matcont package in MATLAB. We calculate other bifurcation values from the stability analysis of equilibrium.

Macroalgae-only equilibrium E_2, represented as the red line, is globally

stable at a very narrow range of low grazing level $0 < g < g_{high}^{CD5}$, where $g_{high}^{CD5} = 0.0346$. When the grazing effect rises above g_{high}^{CD5}, E_2 loses stability and macroalgae and turf algae coexistence equilibrium E_6, represented as the blue line, is globally stable at grazing level $g_{high}^{CD5} < g < g_{high}^{G_6^*}$, where $g_{high}^{G_6^*} = 0.8283$. Macroalgae, coral, and turf algae coexistence equilibrium E_8, represented as the cyan line, emerges and is globally stable at grazing level $g_{high}^{G_6^*} < g < g_{high}^{int}$, where $g_{high}^{int} = 0.8583$. When the grazing effect rises above g_{high}^{int}, E_8 loses stability and joins the globally stable coral and turf algae coexistence equilibrium E_7, represented as the orange line.

Biologically, for the fast turf algae scenario, the reefs will be dominated by macroalgae and turf algae in the long run when the grazing pressure is low. The reefs will be dominated by coral and turf algae in the long run when the grazing pressure rises to a very high level. When the grazing pressure remains at a moderate level, macroalgae, coral, and turf algae can coexist in the long run.

Overall, the equilibrium level of coral is positive related to the grazing effect g. The grazing effect is positive related to the population density of herbivorous fish, such as giant humphead parrot fish, and the fish population is inversely related to fishing effort. Overfishing dramatically decreases the population density of herbivorous fish around the reef, significantly decreasing the grazing effect g. As a result, reasonable fishing helps maintain the herbivorous fish population, and a healthier herbivorous fish population can support a higher level of coral cover. Most degrading reefs are moving from macroalgae and coral coexistence equilibrium to no coral equilibrium, point C_l^C to point B_l^C in figure 2.1 when turf algae are slow; from macroalgae, coral, and turf algae coexistence equilibrium to no coral equilibrium, point C_h^C to point B_h^C in figure 2.2 when turf algae are fast. If the the herbivorous fish population declines, there is less coral cover, replaced by more macroalgae and turf algae cover, as shown in figure 2.1 point C_l^C to point B_l^C and figure 2.2 point C_h^C to point B_h^C.

2.2.5 Effect of larval contribution

In this subsection, we investigate how coral larval contribution affects the persistence of adult coral in both slow turf algae and fast turf algae scenarios. Competition between coral and macroalgae causes a severe decline in the fecundity of coral larvae (Foster et al., 2008). A decrease in the birth rate of coral larvae leads to the decline of coral larval contribution. The presence of macroalgae dramatically decreases the survivorship of juvenile coral (Box and Mumby, 2007). The left panel of figure 2.3 shows that when ρ_T is low, coral shift gradually from stable macroalgae and coral coexistence equilibrium to no coral equilibrium as coral larval contribution Θ_C drops from 0.2 to a low level of 0.01. However, the structure is more robust when ρ_T is high. The equilibrium level of coral decreases as Θ_C drops. Still, it does not decrease to zero even for a deficient level of coral larval contribution, as shown in the right panel of figure 2.3. A high rate of turf algae occupying available space serves as a shield to help coral resist hostile environmental hazard. Coral persist even when coral larval contribution drops to zero if turf algae can occupy available space fast enough.

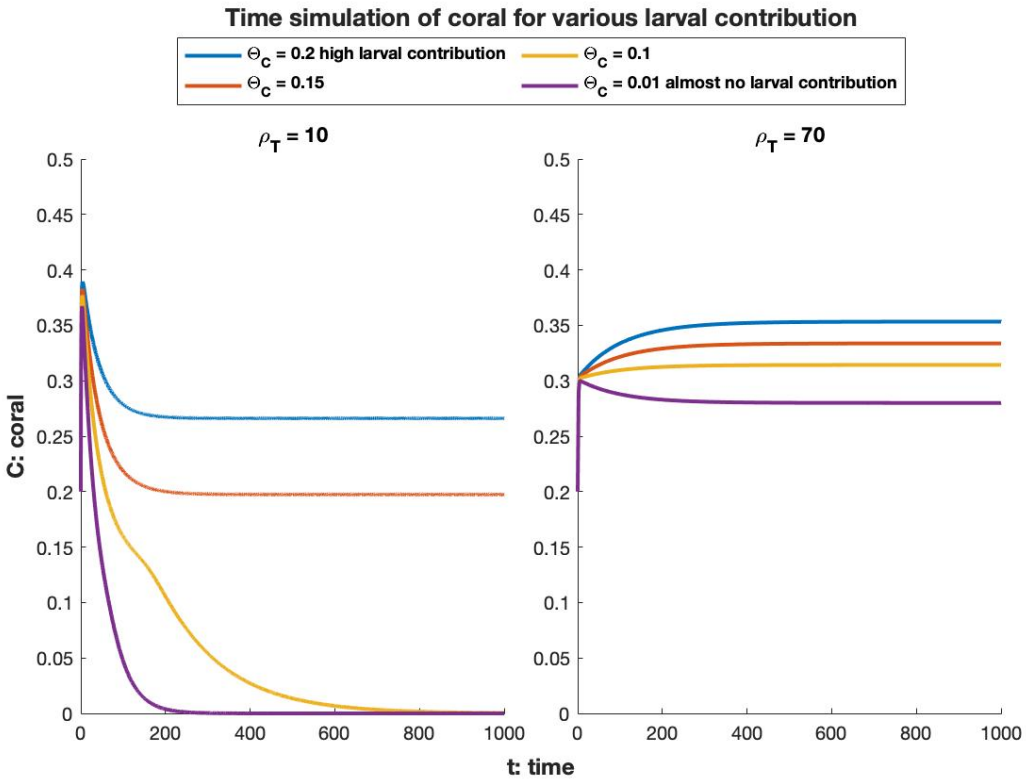

Fig. 2.3 Coral a with declining larval contribution. The left panel is the time simulation of coral when $\rho_T = 10$, $g = 0.7$, and larval contribution Θ_C declines from 0.2 to 0.01. The right panel is the time simulation of coral when $\rho_T = 70$, $g = 0.845$, and larval contribution Θ_C declines from 0.2 to 0.01.

2.3 Discussion

Throughout the analysis of the one-patch model (2.6), we get a pretty good understanding of coral-algae interactions within the patch. We calculate the explicit formula of equilibria, E_1 to E_7, and give conditions for their existence and stability, as summarized in table 2.1. We prove available space persists under all conditions, whereas coral persist under high grazing pressure. We illustrate a high rate of turf algae occupying available space helps coral persist during the decline of larval contribution. The numerical bifurcation analysis shows algae dominate in the long run at low grazing pressure, coral dominate in the long run at very high grazing pressure, and algae and coral can coexist at moderate grazing pressure. Based on the bifurcation results, we show reasonable fishing helps maintain the herbivorous fish population, and a healthier

herbivorous fish population can support a higher level of coral cover. The numerical bifurcation analysis also provides theoretical backup and paves the way for the travelling wave analysis in the chapter 3.

Chapter 3

Spatial dynamics

In chapter 2, we develop a reduced non-dimensional one-patch model (2.6) to answer how coral and algae occupy space while competing and what is the effect of a decline in larval recruitment on coral persistence. In this chapter, we relax the assumption of only one patch and consider multiple patches for the discrete space case. We develop a reaction-diffusion equation model for the continuous space case to investigate how macroalgae invade coral spatially through larval dispersal using TW analysis. We give conditions under which coral will retreat or expand based on the TW results.

3.1 PDE model derivation and assumptions

In this section, we derive a network of weakly-coupled multiple-patches model for the discrete space case and a reaction-diffusion equation model for the continuous space case. In subsection 3.1.1, we develop a multiple-patches model incorporating adult and larvae or propagules based on the one-patch ODE model in chapter 2. In subsection 3.1.2, we simplify the multiple-patches model by assuming patches are weakly coupled and solving larvae or propagules in terms of adults. Next step in subsection 3.1.3, we derive the network of weakly-coupled ODE system by combining the previous two steps. Lastly in subsection 3.1.4, we apply diffusion approximation to the network of weakly-coupled ODE system, and we derive a reaction-diffusion equation model to capture larval dispersal.

3.1.1 Weakly-coupled spatial patches

In this subsection, we specify assumptions and spatial setups for multiple patches. We write down the dimensional system of ODE with semipermeable boundary condition, and then we non-dimensionalize the system.

We consider several patches of coral skeletons located on the same line, as illustrated in figure 1.3(b) . We assume there are no significant differences between patches, so parameter values are the same for every patch. As a result, the patch size presented by N is homogeneous among patches. R is a variable representing any of the three population groups: macroalgae, coral, and turf algae. $d_{Ri,j}$ represents the immigration or emigration rate from patch j to patch i for functional group R. We specifically consider the spatial dynamics of brooding coral. Since the dispersal range of brooding coral larvae is much shorter than spawning coral larvae, we further assume that each brooding coral patch only interacts with its nearest two neighbours and the immigration or emigration rates are the same for every patch. We choose semipermeable boundary condition for patches $i = 1$ and $i = n$, and use hostile exterior $l_{R0} = l_{Rn+1} = 0$. We assume that larvae or propagates move out of the boundaries from patches $i = 1$ and $i = n$ at a fraction $0 \leq \xi \leq 1$ of the standard rate e_R. The immigration or emigration rate for functional group R takes the following form (3.1):

$$d_{Ri,j} = \begin{cases} \xi e_R & i = 1, j = 0 \text{ and } i = n, j = n + 1 \\ e_R & 2 \leq i \leq n - 1 \text{ and } |i - j| = 1 \\ 0 & \text{otherwise .} \end{cases} \tag{3.1}$$

We assume patches are weakly coupled, so e_R is very small such that the second order terms or higher order terms of e_R goes to zero and can be neglected.

Dimensional multiple-patches model

For $2 \leq i \leq n-1$, we have the following system of equations:

$$\frac{dM_i}{dt} = \underbrace{\alpha M_i C_i + \beta M_i T_i + \rho_M M_i S_i - \delta_M M_i - g M_i}_{\text{adult dynamics in patch } i} \quad \underbrace{+\phi_M \kappa_M l_{Mi} S_i}_{\text{juvenile settling to patch } i} \tag{3.2a}$$

$$\frac{dl_{Mi}}{dt} = \underbrace{b_M \frac{\psi_M M_i}{NL}}_{\text{birth}} \underbrace{-\mu_M l_{Mi}}_{\text{death}} \quad \underbrace{-\kappa_M l_{Mi}}_{\text{settling to patch } i} \underbrace{+ \left(\sum_{j \neq i}^{n} d_{Mi,j} l_{Mj} \right)}_{\text{flow into patch } i} \underbrace{- \left(\sum_{j \neq i}^{n} d_{Mj,i} l_{Mi} \right)}_{\text{flow out of patch } i} \tag{3.2b}$$

$$\frac{dC_i}{dt} = \gamma C_i T_i + \rho_C C_i S_i - \alpha M_i C_i - \delta_C C_i + \phi_C \kappa_C l_{Ci} S_i \tag{3.2c}$$

$$\frac{dl_{Ci}}{dt} = b_C \frac{\psi_C C_i}{NL} - \mu_C l_{Ci} - \kappa_C l_{Ci} + \left(\sum_{j \neq i}^{n} d_{Ci,j} l_{Cj} \right) - \left(\sum_{j \neq i}^{n} d_{Cj,i} l_{Ci} \right) \tag{3.2d}$$

$$\frac{dT_i}{dt} = \rho_T T_i S_i - \beta M_i T_i - \gamma C_i T_i - \delta_T T_i - g T_i + \phi_T \kappa_T l_{Ti} S_i \tag{3.2e}$$

$$\frac{dl_{Ti}}{dt} = b_T \frac{\psi_T T_i}{NL} - \mu_T l_{Ti} - \kappa_T l_{Ti} + \left(\sum_{j \neq i}^{n} d_{Ti,j} l_{Tj} \right) - \left(\sum_{j \neq i}^{n} d_{Tj,i} l_{Ti} \right) \tag{3.2f}$$

$$S_i = N - M_i - C_i - T_i, \tag{3.2g}$$

with semipermeable boundary condition with hostile exterior:

$$\frac{dM_1}{dt} = \alpha M_1 C_1 + \beta M_1 T_1 + \rho_M M_1 S_1 - \delta_M M_1 - g M_1 + \phi_M \kappa_M l_{M1} S_1 \tag{3.3a}$$

$$\frac{dl_{M1}}{dt} = b_M \frac{\psi_M M_1}{NL} - \mu_M l_{M1} - \kappa_M l_{M1} + e_R l_{M2} - (\xi e_R l_{M1} + e_R l_{M1}) \tag{3.3b}$$

$$\frac{dC_1}{dt} = \gamma C_1 T_1 + \rho_C C_1 S_1 - \alpha M_1 C_1 - \delta_C C_1 + \phi_C \kappa_C l_{C1} S_1 \tag{3.3c}$$

$$\frac{dl_{C1}}{dt} = b_C \frac{\psi_C C_1}{NL} - \mu_C l_{C1} - \kappa_C l_{C1} + e_R l_{C2} - (\xi e_R l_{C1} + e_R l_{C1}) \tag{3.3d}$$

$$\frac{dT_1}{dt} = \rho_T T_1 S_1 - \beta M_1 T_1 - \gamma C_1 T_1 - \delta_T T_1 - g T_1 + \phi_T \kappa_T l_{T1} S_1 \tag{3.3e}$$

$$\frac{dl_{T1}}{dt} = b_T \frac{\psi_T T_1}{NL} - \mu_T l_{T1} - \kappa_T l_{T1} + e_R l_{T2} - (\xi e_R l_{T1} + e_R l_{T1}) \tag{3.3f}$$

$$S_1 = N - M_1 - C_1 - T_1, \tag{3.3g}$$

$$\frac{dM_n}{dt} = \alpha M_n C_n + \beta M_n T_n + \rho_M M_n S_n - \delta_M M_n - g M_n + \phi_M \kappa_M l_{Mn} S_n \quad (3.4a)$$

$$\frac{dl_{Mn}}{dt} = b_M \frac{\psi_M M_n}{NL} - \mu_M l_{Mn} - \kappa_M l_{Mn} + e_R l_{Mn-1} - (\xi e_R l_{Mn} + e_R l_{Mn}) \quad (3.4b)$$

$$\frac{dC_n}{dt} = \gamma C_n T_n + \rho_C C_n S_n - \alpha M_n C_n - \delta_C C_n + \phi_C \kappa_C l_{Cn} S_n \quad (3.4c)$$

$$\frac{dl_{Cn}}{dt} = b_C \frac{\psi_C C_n}{NL} - \mu_C l_{Cn} - \kappa_C l_{Cn} + e_R l_{Cn-1} - (\xi e_R l_{Cn} + e_R l_{Cn}) \quad (3.4d)$$

$$\frac{dT_n}{dt} = \rho_T T_n S_n - \beta M_n T_n - \gamma C_n T_n - \delta_T T_n - g T_n + \phi_T \kappa_T l_{Tn} S_n \quad (3.4e)$$

$$\frac{dl_{Tn}}{dt} = b_T \frac{\psi_T T_n}{NL} - \mu_T l_{Tn} - \kappa_T l_{Tn} + e_R l_{Tn-1} - (\xi e_R l_{Tn} + e_R l_{Tn}) \quad (3.4f)$$

$$S_n = N - M_n - C_n - T_n. \quad (3.4g)$$

Variables are listed in table B.1, and parameters are listed in table B.2. If we focus on coral and patch i, the adult coral in patch i produce larvae and larvae produced in other patches $j \neq i$ can flow into patch i. These are the two primary incoming sources of larvae in patch i. Then, the larvae in patch i may die or settle to patch i. The idea is larvae from patch j will not directly settle on patch i but travel to patch i first and then become part of larvae in patch i, die or settle to patch i afterwards.

Non-dimensional multiple-patches model

We non-dimensionalize the dimensional multiple-patches model. For $2 \leq i \leq n-1$, we have the following system of equations:

$$\frac{d\tilde{M}_i}{d\tilde{t}} = \tilde{\alpha}\tilde{M}_i\tilde{C}_i + \tilde{\beta}\tilde{M}_i\tilde{T}_i + \tilde{\rho}_M\tilde{M}_i\tilde{S}_i - \tilde{\delta}_M\tilde{M}_i - \tilde{g}\tilde{M}_i + \tilde{\kappa}_M\tilde{l}_{Mi}\tilde{S}_i \tag{3.5a}$$

$$\epsilon_M\frac{d\tilde{l}_{Mi}}{d\tilde{t}} = \tilde{\psi}_M\tilde{b}_M\tilde{M}_i - \tilde{l}_{Mi} - \tilde{\kappa}_M\tilde{l}_{Mi} + \left(\sum_{j\neq i}^{n}\tilde{d}_{Mi,j}\tilde{l}_{Mj}\right) - \left(\sum_{j\neq i}^{n}\tilde{d}_{Mj,i}\tilde{l}_{Mi}\right) \tag{3.5b}$$

$$\frac{d\tilde{C}_i}{d\tilde{t}} = \tilde{\gamma}\tilde{C}_i\tilde{T}_i + \tilde{\rho}_C\tilde{C}_i\tilde{S}_i - \tilde{\alpha}\tilde{M}_i\tilde{C}_i - \tilde{C}_i + \tilde{\kappa}_C\tilde{l}_{Ci}\tilde{S}_i \tag{3.5c}$$

$$\epsilon_C\frac{d\tilde{l}_{Ci}}{d\tilde{t}} = \tilde{\psi}_C\tilde{b}_C\tilde{C}_i - \tilde{l}_{Ci} - \tilde{\kappa}_C\tilde{l}_{Ci} + \left(\sum_{j\neq i}^{n}\tilde{d}_{Ci,j}\tilde{l}_{Cj}\right) - \left(\sum_{j\neq i}^{n}\tilde{d}_{Cj,i}\tilde{l}_{Ci}\right) \tag{3.5d}$$

$$\frac{d\tilde{T}_i}{d\tilde{t}} = \tilde{\rho}_T\tilde{T}_i\tilde{S}_i - \tilde{\beta}\tilde{M}_i\tilde{T}_i - \tilde{\gamma}\tilde{C}_i\tilde{T}_i - \tilde{\delta}_T\tilde{T}_i - \tilde{g}\tilde{T}_i + \tilde{\kappa}_T\tilde{l}_{Ti}\tilde{S}_i \tag{3.5e}$$

$$\epsilon_T\frac{d\tilde{l}_{Ti}}{d\tilde{t}} = \tilde{\psi}_T\tilde{b}_T\tilde{T}_i - \tilde{l}_{Ti} - \tilde{\kappa}_T\tilde{l}_{Ti} + \left(\sum_{j\neq i}^{n}\tilde{d}_{Ti,j}\tilde{l}_{Tj}\right) - \left(\sum_{j\neq i}^{n}\tilde{d}_{Tj,i}\tilde{l}_{Ti}\right) \tag{3.5f}$$

$$\tilde{S}_i = 1 - \tilde{M}_i - \tilde{C}_i - \tilde{T}_i, \tag{3.5g}$$

with semipermeable boundary condition with hostile exterior:

$$\frac{d\tilde{M}_1}{d\tilde{t}} = \tilde{\alpha}\tilde{M}_1\tilde{C}_1 + \tilde{\beta}\tilde{M}_1\tilde{T}_1 + \tilde{\rho}_M\tilde{M}_1\tilde{S}_1 - \tilde{\delta}_M\tilde{M}_1 - \tilde{g}\tilde{M}_1 + \tilde{\kappa}_M\tilde{l}_{M1}\tilde{S}_1 \tag{3.6a}$$

$$\epsilon_M\frac{d\tilde{l}_{M1}}{d\tilde{t}} = \tilde{\psi}_M\tilde{b}_M\tilde{M}_1 - \tilde{l}_{M1} - \tilde{\kappa}_M\tilde{l}_{M1} + \tilde{e}_R\tilde{l}_{M2} - \left(\xi\tilde{e}_R + \tilde{e}_R\tilde{l}_{M1}\right) \tag{3.6b}$$

$$\frac{d\tilde{C}_1}{d\tilde{t}} = \tilde{\gamma}\tilde{C}_1\tilde{T}_1 + \tilde{\rho}_C\tilde{C}_1\tilde{S}_1 - \tilde{\alpha}\tilde{M}_1\tilde{C}_1 - \tilde{C}_1 + \tilde{\kappa}_C\tilde{l}_{C1}\tilde{S}_1 \tag{3.6c}$$

$$\epsilon_C\frac{d\tilde{l}_{C1}}{d\tilde{t}} = \tilde{\psi}_C\tilde{b}_C\tilde{C}_1 - \tilde{l}_{C1} - \tilde{\kappa}_C\tilde{l}_{C1} + \tilde{e}_R\tilde{l}_{C2} - \left(\xi\tilde{e}_R + \tilde{e}_R\tilde{l}_{C1}\right) \tag{3.6d}$$

$$\frac{d\tilde{T}_1}{d\tilde{t}} = \tilde{\rho}_T\tilde{T}_1\tilde{S}_1 - \tilde{\beta}\tilde{M}_1\tilde{T}_1 - \tilde{\gamma}\tilde{C}_1\tilde{T}_1 - \tilde{\delta}_T\tilde{T}_1 - \tilde{g}\tilde{T}_1 + \tilde{\kappa}_T\tilde{l}_{T1}\tilde{S}_1 \tag{3.6e}$$

$$\epsilon_T\frac{d\tilde{l}_{T1}}{d\tilde{t}} = \tilde{\psi}_T\tilde{b}_T\tilde{T}_1 - \tilde{l}_{T1} - \tilde{\kappa}_T\tilde{l}_{T1} + \tilde{e}_R\tilde{l}_{T2} - \left(\xi\tilde{e}_R + \tilde{e}_R\tilde{l}_{T1}\right) \tag{3.6f}$$

$$\tilde{S}_1 = 1 - \tilde{M}_1 - \tilde{C}_1 - \tilde{T}_1, \tag{3.6g}$$

$$\frac{d\tilde{M}_n}{d\tilde{t}} = \tilde{\alpha}\tilde{M}_n\tilde{C}_n + \tilde{\beta}\tilde{M}_n\tilde{T}_n + \tilde{\rho}_M\tilde{M}_n\tilde{S}_n - \tilde{\delta}_M\tilde{M}_n - \tilde{g}\tilde{M}_n + \tilde{\kappa}_M\tilde{l}_{Mn}\tilde{S}_n \tag{3.7a}$$

$$\epsilon_M\frac{d\tilde{l}_{Mn}}{d\tilde{t}} = \tilde{\psi}_M\tilde{b}_M\tilde{M}_n - \tilde{l}_{Mn} - \tilde{\kappa}_M\tilde{l}_{Mn} + \tilde{e}_R\tilde{l}_{Mn-1} - \left(\xi\tilde{e}_R + \tilde{e}_R\tilde{l}_{Mn}\right) \tag{3.7b}$$

$$\frac{d\tilde{C}_n}{d\tilde{t}} = \tilde{\gamma}\tilde{T}_n\tilde{C}_n + \tilde{\rho}_C\tilde{C}_n\tilde{S}_n - \tilde{\alpha}\tilde{M}_n\tilde{C}_n - \tilde{C}_n + \tilde{\kappa}_C\tilde{l}_{Cn}\tilde{S}_n \tag{3.7c}$$

$$\epsilon_C\frac{d\tilde{l}_{Cn}}{d\tilde{t}} = \tilde{\psi}_C\tilde{b}_C\tilde{C}_n - \tilde{l}_{Cn} - \tilde{\kappa}_C\tilde{l}_{Cn} + \tilde{e}_R\tilde{l}_{Cn-1} - \left(\xi\tilde{e}_R + \tilde{e}_R\tilde{l}_{Cn}\right) \tag{3.7d}$$

$$\frac{d\tilde{T}_n}{d\tilde{t}} = \tilde{\rho}_T\tilde{T}_n\tilde{S}_n - \tilde{\beta}\tilde{M}_n\tilde{T}_n - \tilde{\gamma}\tilde{C}_n\tilde{T}_n - \tilde{\delta}_T\tilde{T}_n - \tilde{g}\tilde{T}_n + \tilde{\kappa}_T\tilde{l}_{Tn}\tilde{S}_n \tag{3.7e}$$

$$\epsilon_T\frac{d\tilde{l}_{Tn}}{d\tilde{t}} = \tilde{\psi}_T\tilde{b}_T\tilde{T}_n - \tilde{l}_{Tn} - \tilde{\kappa}_T\tilde{l}_{Tn} + \tilde{e}_R\tilde{l}_{Tn-1} - \left(\xi\tilde{e}_R + \tilde{e}_R\tilde{l}_{Tn}\right) \tag{3.7f}$$

$$\tilde{S}_n = 1 - \tilde{M}_n - \tilde{C}_n - \tilde{T}_n, \tag{3.7g}$$

where $\epsilon_R = \dfrac{\delta_C}{\mu_R}$, a very small parameter, for $R = M$, C, or T. Non-dimensionalized variables and parameters are listed in table B.3.

3.1.2 Larvae in terms of adults

In this subsection, we undertake quasi-steady-state approximation to eliminate larval or propagules equations, and we solve larvae or propagules in terms of adults. We use the assumption of weakly-coupled patches in subsection 3.1.1 with two special cases of $n = 2$ and $n = 3$ to find the general patterns of solution to larvae or propagules in terms of adults. Finally, we summarize the patterns for the general n case as Theorem 3.1.1.

We drop superscript tilde ˜ for convenience and undertake quasi-steady-state approximation to solve l_{Ri} in terms of R_i. R is a variable representing any of the three population groups: macroalgae, coral, and turf algae. R_i represents the surface area occupied by functional group R in patch i. We let $\epsilon_R \to 0$, then equations (3.5b), (3.5d), and (3.5f) can be summarized as the following equation (3.8):

$$\Rightarrow \psi_R b_R R_i - l_{Ri} - \kappa_R l_{Ri} + \left(\sum_{j\neq i}^{n} d_{Ri,j}l_{Rj}\right) - \left(\sum_{j\neq i}^{n} d_{Rj,i}l_{Ri}\right) = 0. \tag{3.8}$$

We substitute $d_{Ri,j}$ (3.1) into equation (3.8):

$$\begin{cases} \psi_R b_R R_1 = (1+\kappa_R+\xi e_R+e_R)\, l_{R1} - e_R l_{R2} \\ \psi_R b_R R_i = p_R l_{Ri} - e_R l_{Ri-1} - e_R l_{Ri+1} \text{ for } 2 \le i \le n-1 \\ \psi_R b_R R_n = (1+\kappa_R+\xi e_R+e_R)\, l_{Rn} - e_R l_{Rn-1}, \end{cases} \tag{3.9}$$

where $p_R = 1+\kappa_R+2e_R$. p_R describes the removal rate of larvae or propagules in patch i for functional group R. We choose hostile boundary condition, i.e. $l_{R0} = l_{Rn+1} = 0$. We write the system (3.9) in matrix form:

$$\underbrace{\begin{pmatrix} p_R-(1-\xi)\,e_R & -e_R & 0 & \dots & 0 \\ -e_R & p_R & \ddots & \ddots & \vdots \\ 0 & \ddots & \ddots & \ddots & 0 \\ \vdots & \ddots & \ddots & p_R & -e_R \\ 0 & \dots & 0 & -e_R & p_R-(1-\xi)\,e_R \end{pmatrix}}_{P_R} \underbrace{\begin{pmatrix} l_{R1} \\ l_{R2} \\ \vdots \\ \vdots \\ l_{Rn} \end{pmatrix}}_{L_R} = \underbrace{\begin{pmatrix} \psi_R b_R R_1 \\ \psi_R b_R R_2 \\ \vdots \\ \psi_R b_R R_{n-1} \\ \psi_R b_R R_n \end{pmatrix}}_{B_R}. \tag{3.10}$$

We rewrite the linear system (3.10) as $P_R L_R = B_R$ with P_R being a symmetric tridiagonal banded matrix, L_R for the vector for larvae or propagules, and B_R for the right hand side of the linear system.

Special case n = 2

We consider a special case with only two patches, the left and right boundary. The linear system (3.10) becomes the following 2×2 system:

$$\begin{pmatrix} p_R-(1-\xi)\,e_R & -e_R \\ -e_R & p_R-(1-\xi)\,e_R \end{pmatrix} \begin{pmatrix} l_{R1} \\ l_{R2} \end{pmatrix} = \begin{pmatrix} \psi_R b_R R_1 \\ \psi_R b_R R_2 \end{pmatrix}, \tag{3.11}$$

$$\Rightarrow \begin{pmatrix} 1+\kappa_R+(1+\xi)\,e_R & -e_R \\ -e_R & 1+\kappa_R+(1+\xi)\,e_R \end{pmatrix} \begin{pmatrix} l_{R1} \\ l_{R2} \end{pmatrix} = \begin{pmatrix} \psi_R b_R R_1 \\ \psi_R b_R R_2 \end{pmatrix}, \tag{3.12}$$

$$\begin{aligned} \Rightarrow L_R &= P_R^{-1} B_R \\ &= \frac{\psi_R b_R}{\left(p_R-(1-\xi)\,e_R\right)^2 - e_R^2} \begin{pmatrix} \left(p_R-(1-\xi)\,e_R\right) R_1 + e_R R_2 \\ e_R R_1 + \left(p_R-(1-\xi)\,e_R\right) R_2 \end{pmatrix} \\ &= \psi_R b_R \begin{pmatrix} \frac{\left(p_R-(1-\xi)e_R\right)R_1+e_R R_2}{\left(p_R-(1-\xi)e_R\right)^2-e_R^2} \\ \frac{e_R R_1+\left(p_R-(1-\xi)e_R\right)R_2}{\left(p_R-(1-\xi)e_R\right)^2-e_R^2} \end{pmatrix}. \end{aligned} \tag{3.13}$$

We consider a weak-dispersal situation and assume that e_R is very small such that the second order terms or higher order terms of e_R go to zero and can be neglected. We undertake linear Taylor expansion to $\dfrac{1}{p_R-(1-\xi)\,e_R}$ in terms of e_R:

$$\begin{aligned}\frac{1}{p_R-(1-\xi)\,e_R} &= \frac{1}{1+\kappa+(1+\xi)\,e_R}\\ &= \frac{1}{1+\kappa_R}-\frac{1}{(1+\kappa_R)^2}\,(1+\xi)\,e_R+\mathcal{O}(e_R^2).\end{aligned} \tag{3.14}$$

We substitute $\dfrac{1}{p_R-(1-\xi)\,e_R}$ (3.14) into equation (3.13):

$$\begin{aligned}\Rightarrow L_R &= \psi_R b_R \begin{pmatrix} \frac{\left(p_R-(1-\xi)e_R\right)R_1+e_R R_2}{\left(p_R-(1-\xi)e_R\right)^2-e_R^2} \\ \frac{e_R R_1+\left(p_R-(1-\xi)e_R\right)R_2}{\left(p_R-(1-\xi)e_R\right)^2-e_R^2} \end{pmatrix}\\ &= \psi_R b_R \begin{pmatrix} \frac{1}{\left(p_R-(1-\xi)e_R\right)}R_1+\frac{e_R}{\left(p_R-(1-\xi)e_R\right)^2}R_2 \\ \frac{e_R}{\left(p_R-(1-\xi)e_R\right)^2}R_1+\frac{1}{\left(p_R-(1-\xi)e_R\right)}R_2 \end{pmatrix}+\mathcal{O}(e_R^2),\end{aligned} \tag{3.15}$$

$$\Rightarrow \begin{cases} l_{R1}=\dfrac{\psi_R b_R}{1+\kappa_R}\left(R_1+\dfrac{e_R}{1+\kappa_R}R_2-\dfrac{(1+\xi)\,e_R}{1+\kappa_R}R_1\right)+\mathcal{O}(e_R^2) & (3.16)\\ l_{R2}=\dfrac{\psi_R b_R}{1+\kappa_R}\left(R_2+\dfrac{e_R}{1+\kappa_R}R_1-\dfrac{(1+\xi)\,e_R}{1+\kappa_R}R_2\right)+\mathcal{O}(e_R^2). & (3.17)\end{cases}$$

Special case n = 3

We consider a special case with only three patches, the left and right boundary and one interior patch. The linear system (3.10) becomes the following 3×3 system:

$$\begin{pmatrix} p_R-(1-\xi)\,e_R & -e_R & 0 \\ -e_R & p_R & -e_R \\ 0 & -e_R & p_R-(1-\xi)\,e_R \end{pmatrix}\begin{pmatrix} l_{R1} \\ l_{R2} \\ l_{R3} \end{pmatrix}=\begin{pmatrix} \psi_R b_R R_1 \\ \psi_R b_R R_2 \\ \psi_R b_R R_3 \end{pmatrix}. \tag{3.18}$$

We solve the inverse matrix using the adjugate matrix $P_R^{-1}=\dfrac{1}{\det(P_R)}adj(P_R)$,

$$\det(P_R)=p_R\left(p_R-(1-\xi)\,e_R\right)^2-2\left(p_R-(1-\xi)\,e_R\right)e_R^2$$

and

$$adj(P_R)=\begin{pmatrix} p_R\left(p_R-(1-\xi)\,e_R\right)-e_R^2 & \left(p_R-(1-\xi)\,e_R\right)e_R & e_R^2 \\ \left(p_R-(1-\xi)\,e_R\right)e_R & \left(p_R-(1-\xi)\,e_R\right)^2 & \left(p_R-(1-\xi)\,e_R\right)e_R \\ e_R^2 & \left(p_R-(1-\xi)\,e_R\right)e_R & p_R\left(p_R-(1-\xi)\,e_R\right)-e_R^2 \end{pmatrix}.$$

We consider a weak-dispersal situation and assume that e_R is very small such that the second order terms or higher order terms of e_R go to zero and can be neglected:

$$\Rightarrow P_R^{-1} = \begin{pmatrix} \frac{1}{p_R-(1-\xi)e_R} & \frac{e_R}{p_R\left(p_R-(1-\xi)e_R\right)} & 0 \\ \frac{e_R}{p_R\left(p_R-(1-\xi)e_R\right)} & \frac{1}{p_R} & \frac{e_R}{p_R\left(p_R-(1-\xi)e_R\right)} \\ 0 & \frac{e_R}{p_R\left(p_R-(1-\xi)e_R\right)} & \frac{1}{p_R-(1-\xi)e_R} \end{pmatrix} + \mathcal{O}(e_R^2), \tag{3.19}$$

$$\begin{aligned} \Rightarrow L_R &= P_R^{-1} B_R \\ &= \psi_R b_R \begin{pmatrix} \frac{1}{p_R-(1-\xi)e_R} R_1 + \frac{e_R}{p_R\left(p_R-(1-\xi)e_R\right)} R_2 \\ \frac{e_R}{p_R\left(p_R-(1-\xi)e_R\right)} R_1 + \frac{1}{p_R} R_2 + \frac{e_R}{p_R\left(p_R-(1-\xi)e_R\right)} R_3 \\ \frac{e_R}{p_R\left(p_R-(1-\xi)e_R\right)} R_2 + \frac{1}{\left(p_R-(1-\xi)e_R\right)} R_3 \end{pmatrix} + \mathcal{O}(e_R^2). \end{aligned} \tag{3.20}$$

We undertake linear Taylor expansion to $\dfrac{1}{p_R}$ in terms of e_R:

$$\frac{1}{p_R} = \frac{1}{1+\kappa+2e_R} = \frac{1}{1+\kappa_R} - \frac{1}{(1+\kappa_R)^2} 2e_R + \mathcal{O}(e_R^2). \tag{3.21}$$

We substitute P_R (3.21) and $\dfrac{1}{p_R - (1-\xi)\, e_R}$ (3.14) into equation (3.20):

$$\begin{aligned} \Rightarrow L_R &= \psi_R b_R \begin{pmatrix} \frac{1}{p_R-(1-\xi)e_R} R_1 + \frac{e_R}{p_R\left(p_R-(1-\xi)e_R\right)} R_2 \\ \frac{e_R}{p_R\left(p_R-(1-\xi)e_R\right)} R_1 + \frac{1}{p_R} R_2 + \frac{e_R}{p_R\left(p_R-(1-\xi)e_R\right)} R_3 \\ \frac{e_R}{p_R\left(p_R-(1-\xi)e_R\right)} R_2 + \frac{1}{\left(p_R-(1-\xi)e_R\right)} R_3 \end{pmatrix} + \mathcal{O}(e_R^2) \\ &= \frac{\psi_R b_R}{1+\kappa_R} \begin{pmatrix} R_1 + \frac{e_R}{1+\kappa_R} R_2 - \frac{(1+\xi)e_R}{1+\kappa_R} R_1 \\ R_2 + \frac{e_R}{1+\kappa_R} R_1 + \frac{e_R}{1+\kappa_R} R_3 - \frac{2e_R}{1+\kappa_R} R_2 \\ R_3 + \frac{e_R}{1+\kappa_R} R_2 - \frac{(1+\xi)e_R}{1+\kappa_R} R_3 \end{pmatrix} + \mathcal{O}(e_R^2), \end{aligned} \tag{3.22}$$

$$\Rightarrow \begin{cases} l_{R1} = \dfrac{\psi_R b_R}{1+\kappa_R} \left(R_1 + \dfrac{e_R}{1+\kappa_R} R_2 - \dfrac{(1+\xi)\, e_R}{1+\kappa_R} R_1 \right) + \mathcal{O}(e_R^2) & (3.23) \\ l_{R2} = \dfrac{\psi_R b_R}{1+\kappa_R} \left(R_2 + \dfrac{e_R}{1+\kappa_R} R_1 + \dfrac{e_R}{1+\kappa_R} R_3 - \dfrac{2e_R}{1+\kappa_R} R_2 \right) + \mathcal{O}(e_R^2) & (3.24) \\ l_{R3} = \dfrac{\psi_R b_R}{1+\kappa_R} \left(R_3 + \dfrac{e_R}{1+\kappa_R} R_2 - \dfrac{(1+\xi)\, e_R}{1+\kappa_R} R_3 \right) + \mathcal{O}(e_R^2). & (3.25) \end{cases}$$

l_{R1} and l_{R3} correspond to the left and right boundary patches and are symmetric. l_{R2} is a representative of all the interior patches, including flow in from two adjacent patches and flow out to two adjacent patches.

Generalization

We summarize the patterns found in the special cases, $n = 2$ and $n = 3$. We use the following Theorem 3.1.1 to show the linear approximated solution to the larval equation (3.8) for the generalize n patches case.

Theorem 3.1.1 (**Linear approximated solution**). *If we assume the patches are weakly coupled, i.e.*

$$d_{Ri,j} = \begin{cases} \epsilon \hat{d}_{Ri,j} & i \neq j \\ 0 & otherwise, \end{cases} \tag{3.26}$$

and ϵ is a small parameter such that $0 < \epsilon << 1$, then equation (3.27)

$$l_{Ri} = \frac{\psi_R b_R}{1+\kappa_R} \left[R_i + \frac{1}{1+\kappa_R} \epsilon \left(\sum_{j \neq i}^{n} \hat{d}_{Ri,j} R_j \right) - \frac{1}{1+\kappa_R} \epsilon \left(\sum_{j \neq i}^{n} \hat{d}_{Rj,i} \right) R_i \right] \tag{3.27}$$

is the solution to the larval equation (3.8) *with hostile boundary condition up to the leading order of ϵ.*

Proof. We substitute $d_{Ri,j}$ (3.26) into the left hand side of the larval equation (3.8) and rewrite the left hand side:

$$\begin{aligned} &\psi_R b_R R_i - l_{Ri} - \kappa_R l_{Ri} + \left(\sum_{j \neq i}^{n} d_{Ri,j} l_{Rj} \right) - \left(\sum_{j \neq i}^{n} d_{Rj,i} l_{Ri} \right) \\ &= \psi_R b_R R_i - l_{Ri} - \kappa_R l_{Ri} + \epsilon \left(\sum_{j \neq i}^{n} \hat{d}_{Ri,j} l_{Rj} \right) - \epsilon \left(\sum_{j \neq i}^{n} \hat{d}_{Rj,i} l_{Ri} \right) \\ &= \psi_R b_R R_i - \left[1 + \kappa_R + \epsilon \left(\sum_{j \neq i}^{n} \hat{d}_{Rj,i} \right) \right] l_{Ri} + \epsilon \left(\sum_{j \neq i}^{n} \hat{d}_{Ri,j} l_{Rj} \right). \end{aligned} \tag{3.28}$$

We substitute the equation (3.27) into equation (3.28) to verify the theorem. We write expressions explicitly up to order of ϵ, and terms with order ϵ^2 or

higher are absorbed in $\mathcal{O}(\epsilon^2)$:

$$\begin{aligned}
&\psi_R b_R R_i - \left[1+\kappa_R+\epsilon\left(\sum_{j\neq i}^{n}\hat{d}_{Rj,i}\right)\right] l_{Ri} + \epsilon\left(\sum_{j\neq i}^{n}\hat{d}_{Ri,j}l_{Rj}\right)\\
&= \psi_R b_R R_i - \psi_R b_R\left[R_i + \frac{\epsilon}{1+\kappa_R}\left(\sum_{j\neq i}^{n}\hat{d}_{Ri,j}R_j\right) - \frac{\epsilon}{1+\kappa_R}\left(\sum_{j\neq i}^{n}\hat{d}_{Rj,i}\right)R_i\right]\\
&\quad - \epsilon\left(\sum_{j\neq i}^{n}\hat{d}_{Rj,i}\right)\frac{\psi_R b_R}{1+\kappa_R}R_i + \frac{\psi_R b_R}{1+\kappa_R}\epsilon\left(\sum_{j\neq i}^{n}\hat{d}_{Ri,j}R_j\right) + \mathcal{O}(\epsilon^2)\\
&= \psi_R b_R R_i - \psi_R b_R R_i - \frac{\psi_R b_R}{1+\kappa_R}\left(\sum_{j\neq i}^{n}\hat{d}_{Ri,j}R_j\right)\epsilon + \frac{\psi_R b_R}{1+\kappa_R}\left(\sum_{j\neq i}^{n}\hat{d}_{Rj,i}\right)R_i\epsilon\\
&\quad - \frac{\psi_R b_R}{1+\kappa_R}\left(\sum_{j\neq i}^{n}\hat{d}_{Rj,i}\right)R_i\epsilon + \frac{\psi_R b_R}{1+\kappa_R}\left(\sum_{j\neq i}^{n}\hat{d}_{Ri,j}R_j\right)\epsilon + \mathcal{O}(\epsilon^2)\\
&= \mathcal{O}(\epsilon^2).
\end{aligned}$$

■

Since ϵ is a small parameter such that $0 < \epsilon << 1$, we drop the $\mathcal{O}(\epsilon^2)$ term and incorporate l_{Ri} into the non-dimensional multiple-patches model (3.5):

$$l_{Ri} = \frac{\psi_R b_R}{1+\kappa_R}\left[R_i + \frac{1}{1+\kappa_R}\left(\sum_{j\neq i}^{n}d_{Ri,j}R_j\right) - \frac{1}{1+\kappa_R}\left(\sum_{j\neq i}^{n}d_{Rj,i}\right)R_i\right], \tag{3.29}$$

$$\begin{aligned}
\Rightarrow \kappa_R l_{Ri} &= \frac{\kappa_R\psi_R b_R}{1+\kappa_R}\left[R_i + \frac{1}{1+\kappa_R}\left(\sum_{j\neq i}^{n}d_{Ri,j}R_j\right) - \frac{1}{1+\kappa_R}\left(\sum_{j\neq i}^{n}d_{Rj,i}\right)R_i\right]\\
&= \theta_R\psi_R b_R\left[R_i + \frac{1}{1+\kappa_R}\left(\sum_{j\neq i}^{n}d_{Ri,j}R_j\right) - \frac{1}{1+\kappa_R}\left(\sum_{j\neq i}^{n}d_{Rj,i}\right)R_i\right]\\
&= \Theta_R\left[R_i + \frac{1}{1+\kappa_R}\left(\sum_{j\neq i}^{n}d_{Ri,j}R_j\right) - \frac{1}{1+\kappa_R}\left(\sum_{j\neq i}^{n}d_{Rj,i}\right)R_i\right].
\end{aligned} \tag{3.30}$$

3.1.3 Network of weakly-coupled ODE system

In this subsection, we combine the results from subsections 3.1.1 and 3.1.2 to derive the network of weakly-coupled ODE system.

We substitute equation (3.30) into equations (3.5a), (3.5c), and (3.5e). We obtain the following network of weakly-coupled ODE system (3.31):

$$\frac{dM_i}{dt} = \underbrace{\alpha M_i C_i + \beta M_i T_i + \rho_M M_i S_i - \delta_M M_i - g M_i}_{\text{within patch interactions}} + \Theta_M S_i \left[\underbrace{M_i}_{\substack{\text{production of} \\ \text{propagules}}} \underbrace{+ \frac{1}{1+\kappa_M} \left(\sum_{j \neq i}^{n} d_{Mi,j} M_j \right)}_{\text{flow into patch } i} \underbrace{- \frac{1}{1+\kappa_M} \left(\sum_{j \neq i}^{n} d_{Mj,i} \right) M_i}_{\text{flow out of patch } i} \right] \tag{3.31a}$$

$$\frac{dC_i}{dt} = \underbrace{\gamma C_i T_i + \rho_C C_i S_i - \alpha M_i C_i - C_i}_{\text{within patch interactions}} + \Theta_C S_i \left[\underbrace{C_i}_{\substack{\text{production of} \\ \text{larvae}}} \underbrace{+ \frac{1}{1+\kappa_C} \left(\sum_{j \neq i}^{n} d_{Ci,j} C_j \right)}_{\text{flow into patch } i} \underbrace{- \frac{1}{1+\kappa_C} \left(\sum_{j \neq i}^{n} d_{Cj,i} \right) C_i}_{\text{flow out of patch } i} \right] \tag{3.31b}$$

$$\frac{dT_i}{dt} = \underbrace{\rho_T T_i S_i - \beta M_i T_i - \gamma C_i T_i - \delta_T T_i - g T_i}_{\text{within patch interactions}} + \Theta_T S_i \left[\underbrace{T_i}_{\substack{\text{production of} \\ \text{propagules}}} \underbrace{+ \frac{1}{1+\kappa_T} \left(\sum_{j \neq i}^{n} d_{Ti,j} T_j \right)}_{\text{flow into patch } i} \underbrace{- \frac{1}{1+\kappa_T} \left(\sum_{j \neq i}^{n} d_{Tj,i} \right) T_i}_{\text{flow out of patch } i} \right] \tag{3.31c}$$

$$S_i = 1 - M_i - C_i - T_i. \tag{3.31d}$$

3.1.4 Diffusion approximation

In this subsection, we undertake diffusion approximation to transform the weakly-coupled ODE system (3.31) into a reaction-diffusion equation model

(3.38) with non-linear diffusion for the continuous space case.

We assume all patches are on the same line, and each patch only interacts with adjacent patches. We assume

$$d_{Ri,j} = \begin{cases} \frac{d_R}{(\Delta x)^2} & \text{if } |i-j| = 1 \\ 0 & \text{otherwise} \end{cases} \tag{3.32}$$

by the nearest neighbour principle, where Δx is the uniform distance between adjacent patches. $d_{Ri,j}$ is the immigration or emigration rate from patch j to patch i for functional group $R = M$, C, or T. d_R is the diffusion coefficient for functional group R. $R_i(t)$ represents the fraction of surface area occupied by functional group R at time t in patch i, and $i \leq n$. We introduce one dimensional spatial variable by assuming:

$$R_i(t) = \hat{R}\left(i\Delta x, t\right), \tag{3.33}$$

where $R_0(t) = \hat{R}(0,t)$ is the origin of the one dimensional spatial x axis. $R_i(t)$ is defined on the lattice $\mathbb{Z} \times \mathbb{R}^+$, and $\hat{R}(x,t)$ is defined for the continuous space $\mathbb{R} \times \mathbb{R}^+$. We substitute $R_i(t)$ (3.33) into the weakly-coupled ODE system

(3.31):

$$\begin{aligned}\frac{d\hat{M}\left(i\Delta x,t\right)}{dt} &= \alpha\hat{M}\left(i\Delta x,t\right)\hat{C}\left(i\Delta x,t\right)+\beta\hat{M}\left(i\Delta x,t\right)\hat{T}\left(i\Delta x,t\right)\\ &\quad+\rho_M\hat{M}\left(i\Delta x,t\right)\hat{S}\left(i\Delta x,t\right)-\delta_M\hat{M}\left(i\Delta x,t\right)-g\hat{M}\left(i\Delta x,t\right)\\ &\quad+\Theta_M\hat{S}\left(i\Delta x,t\right)\left[\hat{M}\left(i\Delta x,t\right)+\frac{1}{1+\kappa_M}\left(\sum_{j\neq i}^{n}d_{Mi,j}\hat{M}\left(j\Delta x,t\right)\right)\right.\\ &\quad\left.-\frac{1}{1+\kappa_M}\left(\sum_{j\neq i}^{n}d_{Mj,i}\right)\hat{M}\left(i\Delta x,t\right)\right],\end{aligned} \tag{3.34a}$$

$$\begin{aligned}\frac{d\hat{C}\left(i\Delta x,t\right)}{dt} &= \gamma\hat{C}\left(i\Delta x,t\right)\hat{T}\left(i\Delta x,t\right)+\rho_C\hat{C}\left(i\Delta x,t\right)\hat{S}\left(i\Delta x,t\right)\\ &\quad-\alpha\hat{M}\left(i\Delta x,t\right)\hat{C}\left(i\Delta x,t\right)-\hat{C}\left(i\Delta x,t\right)\\ &\quad+\Theta_C\hat{S}\left(i\Delta x,t\right)\left[\hat{C}\left(i\Delta x,t\right)+\frac{1}{1+\kappa_C}\left(\sum_{j\neq i}^{n}d_{Ci,j}\hat{C}\left(j\Delta x,t\right)\right)\right.\\ &\quad\left.-\frac{1}{1+\kappa_C}\left(\sum_{j\neq i}^{n}d_{Cj,i}\right)\hat{C}\left(i\Delta x,t\right)\right],\end{aligned} \tag{3.34b}$$

$$\begin{aligned}\frac{d\hat{T}\left(i\Delta x,t\right)}{dt} &= \rho_T\hat{T}\left(i\Delta x,t\right)\hat{S}\left(i\Delta x,t\right)-\beta\hat{M}\left(i\Delta x,t\right)\hat{T}\left(i\Delta x,t\right)\\ &\quad-\gamma\hat{C}\left(i\Delta x,t\right)\hat{T}\left(i\Delta x,t\right)-\delta_T\hat{T}\left(i\Delta x,t\right)-g\hat{T}\left(i\Delta x,t\right)\\ &\quad+\Theta_T\hat{S}\left(i\Delta x,t\right)\left[\hat{T}\left(i\Delta x,t\right)+\frac{1}{1+\kappa_T}\left(\sum_{j\neq i}^{n}d_{Ti,j}\hat{T}\left(j\Delta x,t\right)\right)\right.\\ &\quad\left.-\frac{1}{1+\kappa_T}\left(\sum_{j\neq i}^{n}d_{Tj,i}\right)\hat{T}\left(i\Delta x,t\right)\right],\end{aligned} \tag{3.34c}$$

$$\hat{S}\left(i\Delta x,t\right)=1-\hat{M}\left(i\Delta x,t\right)-\hat{C}\left(i\Delta x,t\right)-\hat{T}\left(i\Delta x,t\right). \tag{3.34d}$$

We further substitute the immigration or emigration rate $d_{Ri,j}$ (3.32) into part of the equations (3.34a), (3.34b), and (3.34c), and we use R to denote M, C,

or T for concision:

$$\begin{aligned}
&\hat{R}\left(i\Delta x,t\right)+\frac{1}{1+\kappa_R}\left(\sum_{j\neq i}^{n}d_{Ri,j}\hat{R}\left(j\Delta x,t\right)\right)-\frac{1}{1+\kappa_R}\left(\sum_{j\neq i}^{n}d_{Rj,i}\right)\hat{R}\left(i\Delta x,t\right)\\
&=\hat{R}\left(i\Delta x,t\right)+\frac{1}{1+\kappa_R}\left(\frac{d_R}{(\Delta x)^2}\hat{R}\left((i-1)\Delta x,t\right)+\frac{d_R}{(\Delta x)^2}\hat{R}\left((i+1)\Delta x,t\right)\right)\\
&\quad-\frac{1}{1+\kappa_R}\left(\frac{d_R}{(\Delta x)^2}+\frac{d_R}{(\Delta x)^2}\right)\hat{R}\left(i\Delta x,t\right)\\
&=\hat{R}\left(i\Delta x,t\right)+\frac{d_R}{1+\kappa_R}\left(\frac{\hat{R}\left((i-1)\Delta x,t\right)-2\hat{R}\left(i\Delta x,t\right)+\hat{R}\left((i+1)\Delta x,t\right)}{(\Delta x)^2}\right).
\end{aligned}\tag{3.35}$$

We assume patches are arbitrarily close to each other, so we can take the limit by letting $\Delta x\to 0$, $i\to\infty$, and we write $i\Delta x=x$:

$$\lim_{\Delta x\to 0}\left(\frac{\hat{R}\left((i-1)\Delta x,t\right)-2\hat{R}\left(i\Delta x,t\right)+\hat{R}\left((i+1)\Delta x,t\right)}{(\Delta x)^2}\right)=\frac{\partial^2}{\partial x^2}\hat{R}\left(x,t\right).\tag{3.36}$$

We combine equations (3.35) and (3.36), and

$$\begin{aligned}
&\hat{R}\left(i\Delta x,t\right)+\frac{1}{1+\kappa_R}\left(\sum_{j\neq i}^{n}d_{Ri,j}\hat{R}\left(j\Delta x,t\right)\right)-\frac{1}{1+\kappa_R}\left(\sum_{j\neq i}^{n}d_{Rj,i}\right)\hat{R}\left(i\Delta x,t\right)\\
&\to\hat{R}\left(x,t\right)+\frac{d_R}{1+\kappa_R}\frac{\partial^2}{\partial x^2}\hat{R}\left(x,t\right)\ \text{ as }\Delta x\to 0.
\end{aligned}\tag{3.37}$$

We substitute equation (3.37) into equations (3.34a) to (3.34d) and take the limit $\Delta x\to 0$. We obtain the following reaction-diffusion equation model

(3.38):

$$\frac{\partial \hat{M}}{\partial t} = \underbrace{\alpha \hat{M}\hat{C} + \beta \hat{M}\hat{T} + \rho_M \hat{M}\hat{S} - \delta_M \hat{M} - g\hat{M}}_{\text{dynamic for adult macroalgae}} + \Theta_M \hat{S} \underbrace{\left(\hat{M} + \frac{d_M}{1+\kappa_M} \frac{\partial^2 \hat{M}}{\partial x^2} \right)}_{\text{production + diffusion}} \tag{3.38a}$$

$$\frac{\partial \hat{C}}{\partial t} = \underbrace{\gamma \hat{C}\hat{T} + \rho_C \hat{C}\hat{S} - \alpha \hat{M}\hat{C} - \hat{C}}_{\text{dynamic for adult coral}} + \Theta_C \hat{S} \underbrace{\left(\hat{C} + \frac{d_C}{1+\kappa_C} \frac{\partial^2 \hat{C}}{\partial x^2} \right)}_{\text{production + diffusion}} \tag{3.38b}$$

$$\frac{\partial \hat{T}}{\partial t} = \underbrace{\rho_T \hat{T}\hat{S} - \beta \hat{M}\hat{T} - \gamma \hat{C}\hat{T} - \delta_T \hat{T} - g\hat{T}}_{\text{dynamic for adult turf algae}} + \Theta_T \hat{S} \underbrace{\left(\hat{T} + \frac{d_T}{1+\kappa_T} \frac{\partial^2 \hat{T}}{\partial x^2} \right)}_{\text{production + diffusion}} \tag{3.38c}$$

$$\hat{S} = 1 - \hat{M} - \hat{C} - \hat{T}. \tag{3.38d}$$

Variables and parameters are listed in tables B.3 and B.4. $\hat{R}(x,t)$ denotes the proportion of surface area occupied by functional group R at time t and location x. We study the reaction-diffusion equation model (3.38) using numerical TW analysis in section 3.2.

3.2 Numerical travelling wave results

In chapter 2, we discuss all possibilities of equilibria, which describe the long-term fate of the coral reef ecosystem. However, how those equilibria are connected or related remains unknown. In this section, we investigate how macroalgae invade coral and turf algae spatially and how one equilibrium state transforms into another using travelling waves. We exclude the cases where coral cover is zero for all space x since those cases are not biologically relevant. We simulate the reaction-diffusion equation model (3.38) with homogeneous Neumann boundary conditions to approximate TW conditions. We take diffusion coefficients d_R as 0.0001 for all functional groups.

3.2.1 Invasion under slow turf algae

In this subsection, we investigate the invasion of coral by macroalgae at high ρ_T. The interactions between macroalgae, coral, and turf algae are complex,

especially how turf algae affect the invasion of coral by macroalgae is rarely investigated. Here we consider two scenarios, the slow turf algae case and the fast turf algae case. The slow turf algae case is when turf algae occupy available space relatively slowly, $\rho_T = 10$, and the fast turf algae case is when turf algae occupy available space relatively fast, $\rho_T = 70$. In the slow turf algae scenario, turf algae are always invaded and driven to extinction, as shown in figure 3.4. ρ_T is not big enough to support the persistence of turf algae.

Consider a case where coral are dominant initially, described by coral-only equilibrium; however, the grazing effect is low due to overharvesting of herbivorous fish, and turf algae are slow, $\rho_T = 10$. Figure 3.1 shows macroalgae invade coral fast when grazing $g = 0.3$ is minimal. As a result, coral-dominant state shifts to macroalgae-dominant state in a short period. Figure 3.2 shows macroalgae invade coral slowly when grazing $g = 0.6$ is higher but still below the threshold bifurcation value $g_{low}^{CD5} = 0.6103$. As a result, it takes more time for coral-dominant state to shift to macroalgae-dominant state.

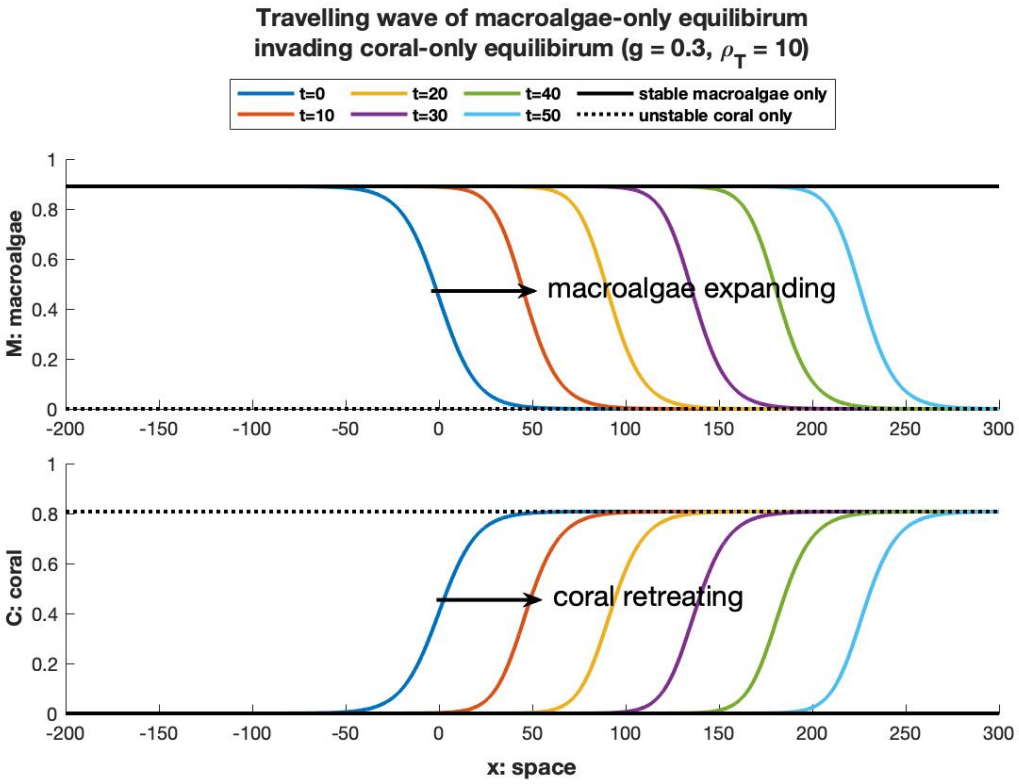

Fig. 3.1 TW of macroalgae invading coral fast at low ρ_T. Numerical TW simulation corresponds to the transition from point C_l to point A_l in figure 2.1. We apply homogeneous Neumann boundary conditions and take the grazing effect $g = 0.3$.

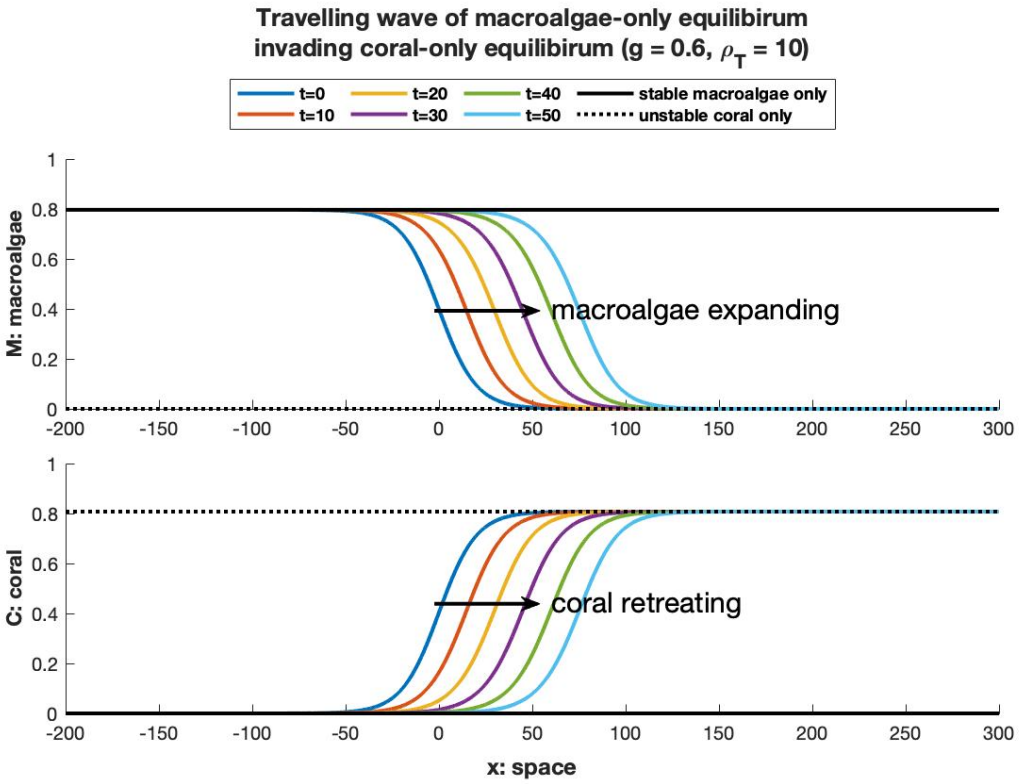

Fig. 3.2 TW of macroalgae invading coral slowly at low ρ_T. Numerical TW simulation corresponds to the transition from point C_l to point A_l in figure 2.1. We apply homogeneous Neumann boundary conditions and take the grazing effect $g = 0.6$.

Consider a case where herbivorous fish are not severely overharvested; thus, the grazing effect $g = 0.72$ remains at a moderate level, and turf algae is slow, $\rho_T = 10$. The invasion depends on the initial level of coral cover. Figure 3.3 shows macroalgae invade coral when the initial coral cover is above the macroalgae and coral coexistence level. As a result, coral-dominant state shifts to macroalgae and coral coexistence state. Figure 3.4 shows macroalgae fail to invade coral when the initial coral cover is below the coexistence level. As a result, macroalgae and turf algae coexistence state shifts to macroalgae and coral coexistence state.

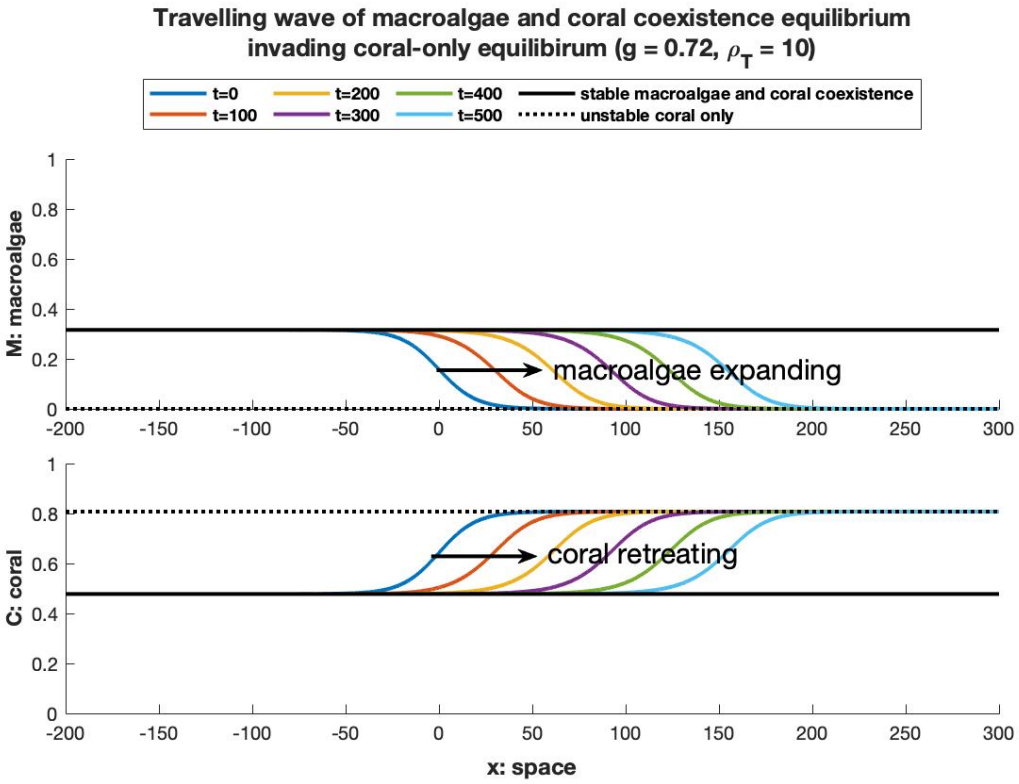

Fig. 3.3 TW of macroalgae invading coral and turf algae at low ρ_T. Numerical TW simulation corresponds to the transition at point C_l in figure 2.1. We apply homogeneous Neumann boundary conditions and take the grazing effect $g = 0.72$. We set the initial coral cover to coral-only equilibrium level 0.8077, which is above macroalgae and coral coexistence level.

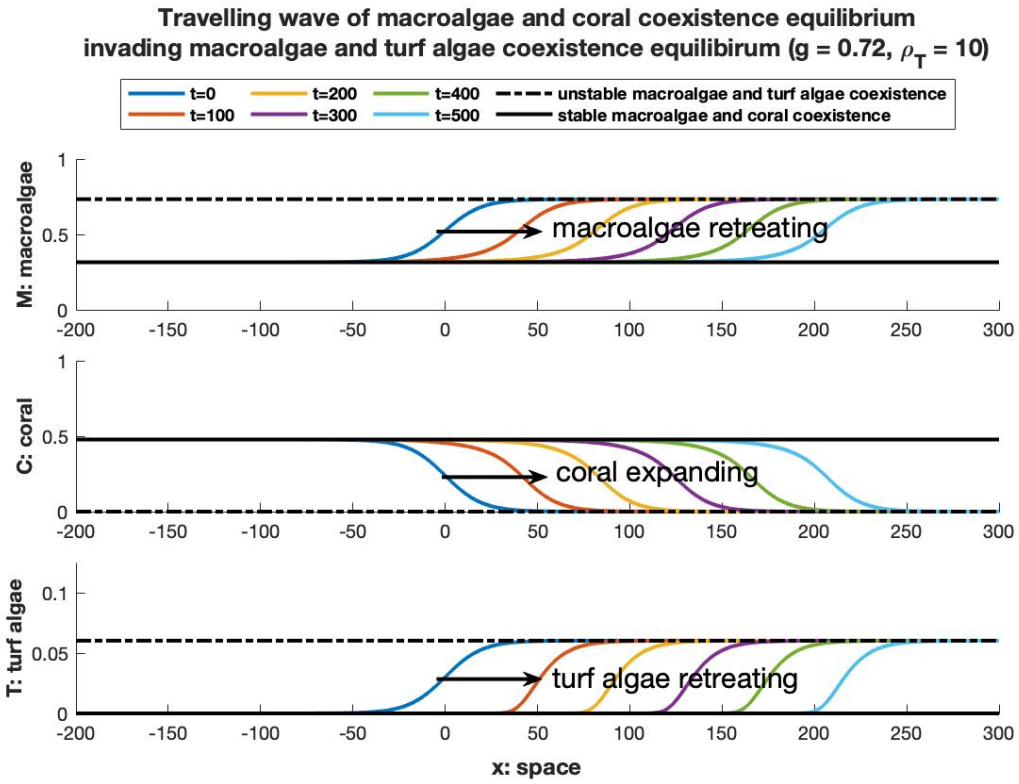

Fig. 3.4 TW of macroalgae failing to invade coral at low ρ_T. Numerical TW simulation corresponds to the transition at point B_l in figure 2.1. We apply homogeneous Neumann boundary conditions and take the grazing effect $g = 0.72$. We set the initial coral cover to 0, which is below macroalgae and coral coexistence level.

3.2.2 Invasion under fast turf algae

In this subsection, we investigate the invasion of coral by macroalgae at low ρ_T. In the fast turf algae scenario, turf algae always persist, as shown in figures 3.5, 3.6, 3.7, and 3.8. ρ_T is big enough to support the persistence of turf algae.

Consider a case where coral and turf algae are dominant initially, described by coral and turf algae coexistence equilibrium; however, the grazing effect is low due to overharvesting of herbivorous fish, and turf algae are fast, $\rho_T = 70$. Figure 3.5 shows macroalgae invade coral and turf algae fast when grazing $g = 0.3$ is minimal. As a result, coral and turf algae coexistence state shifts to macroalgae and turf algae coexistence state in a short period. Figure 3.6 shows macroalgae invade coral and turf algae slowly when grazing $g = 0.6$ is higher but still below the threshold bifurcation value $g_{high}^{G_6^*} = 0.8283$. As a

result, it takes more time for coral and turf algae coexistence state to shift to macroalgae and turf algae coexistence state.

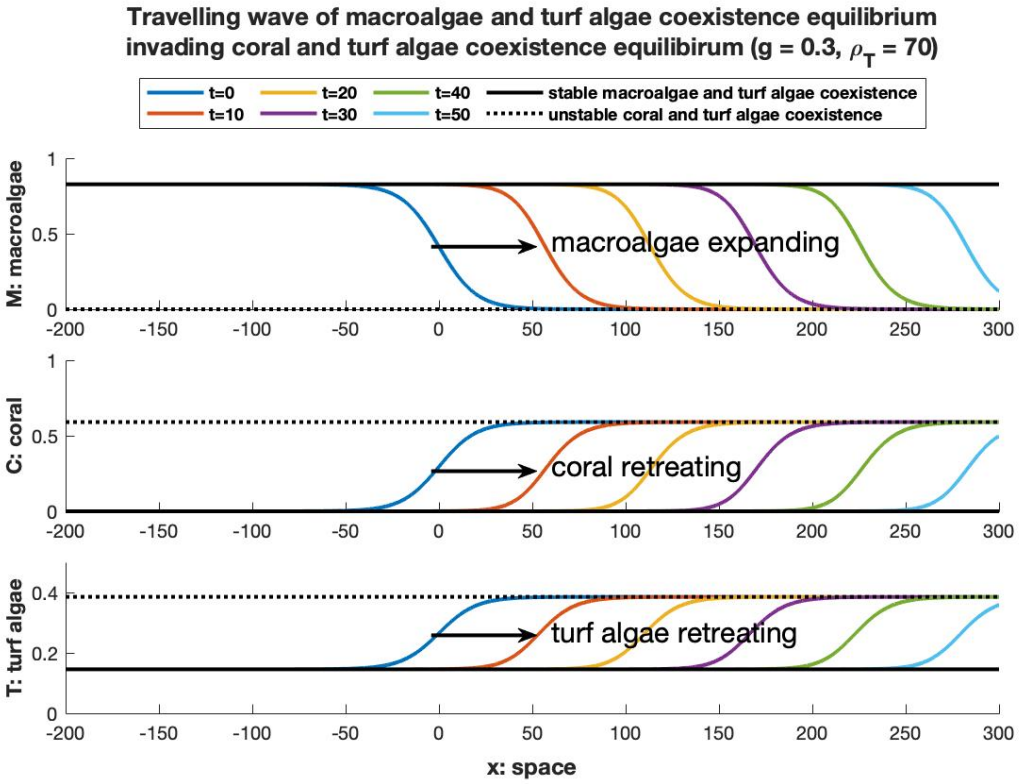

Fig. 3.5 TW of macroalgae invading coral and turf algae fast at high ρ_T. Numerical TW simulation corresponds to the transition from point C_h to point B_h in figure 2.2. We apply homogeneous Neumann boundary conditions and take the grazing effect $g = 0.3$.

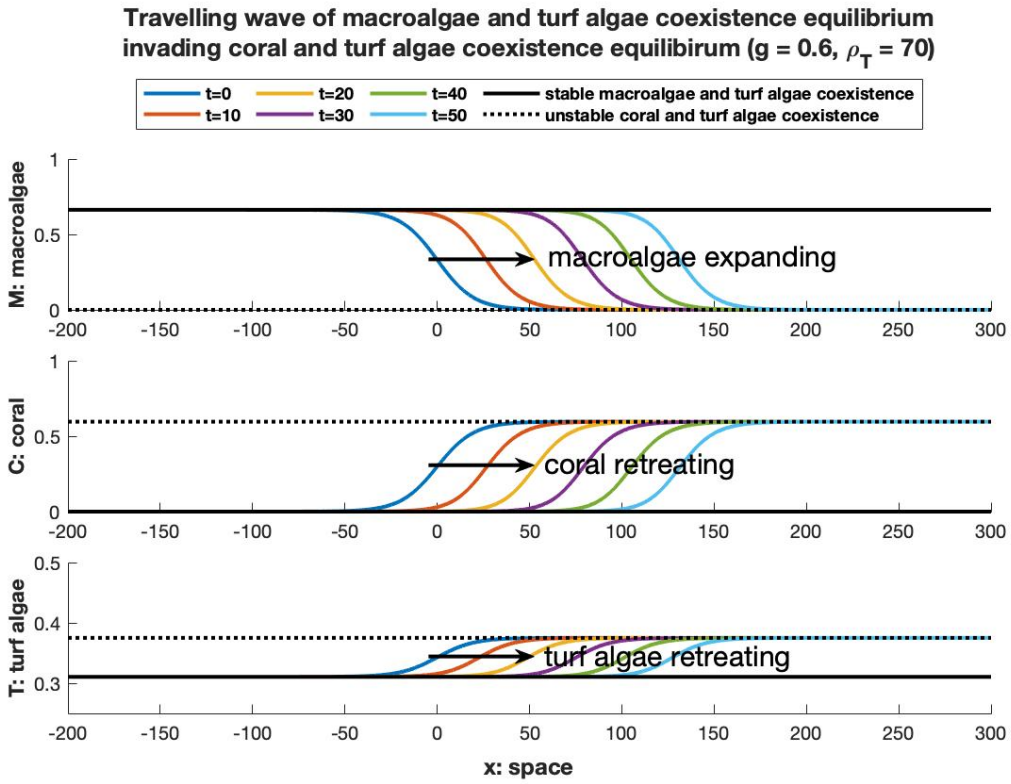

Fig. 3.6 TW of macroalgae invading coral and turf algae slowly at high ρ_T. Numerical TW simulation corresponds to the transition from point C_h to B_h in figure 2.2. We apply homogeneous Neumann boundary conditions and take the grazing effect $g = 0.6$.

Consider a case where herbivorous fish are not severely overharvested; thus, the grazing effect $g = 0.84$ remains at a moderate level, and turf algae are fast, $\rho_T = 70$. The invasion depends on the initial level of coral cover. Figure 3.7 shows macroalgae invade coral when the initial coral cover is above the three functional groups coexistence level. As a result, coral and turf algae coexistence state shifts to three functional groups coexistence state. Figure 3.8 shows macroalgae fail to invade coral when the initial coral cover is below the coexistence level. As a result, macroalgae and turf algae coexistence state shifts to three functional groups coexistence state.

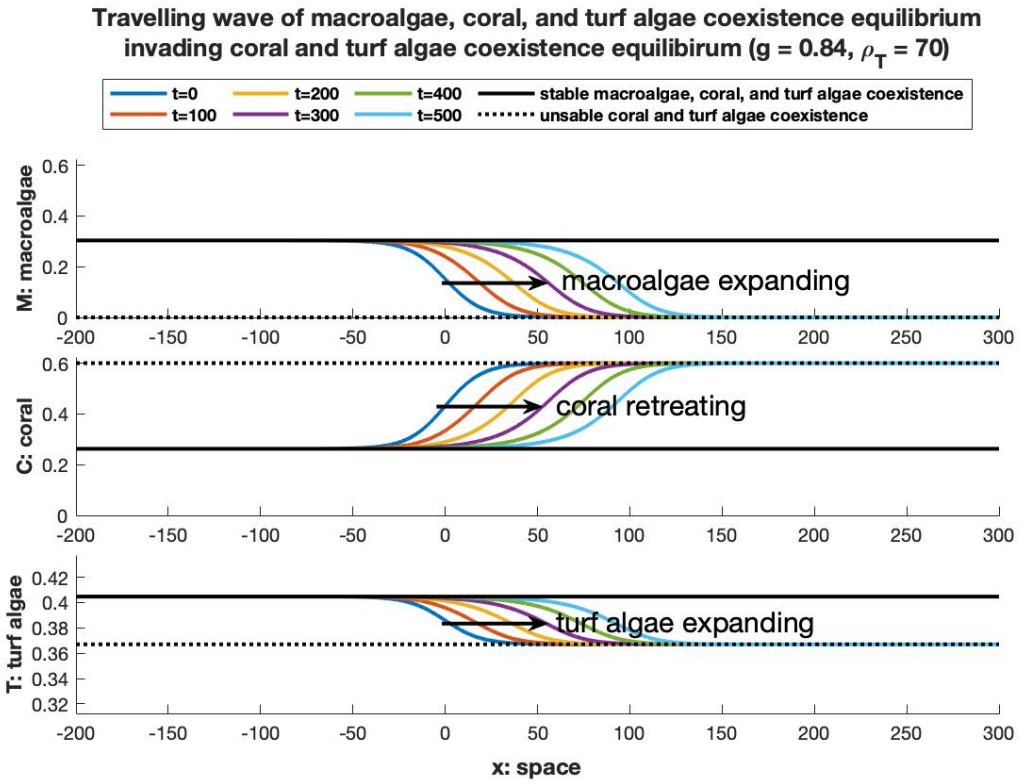

Fig. 3.7 TW of macroalgae invading coral at high ρ_T. Numerical TW simulation corresponds to the transition at point C_h in figure 2.2. We apply homogeneous Neumann boundary conditions and take the grazing effect $g = 0.84$. We set the initial coral cover to coral and turf algae coexistence equilibrium level 0.6009, which is above three functional groups coexistence level.

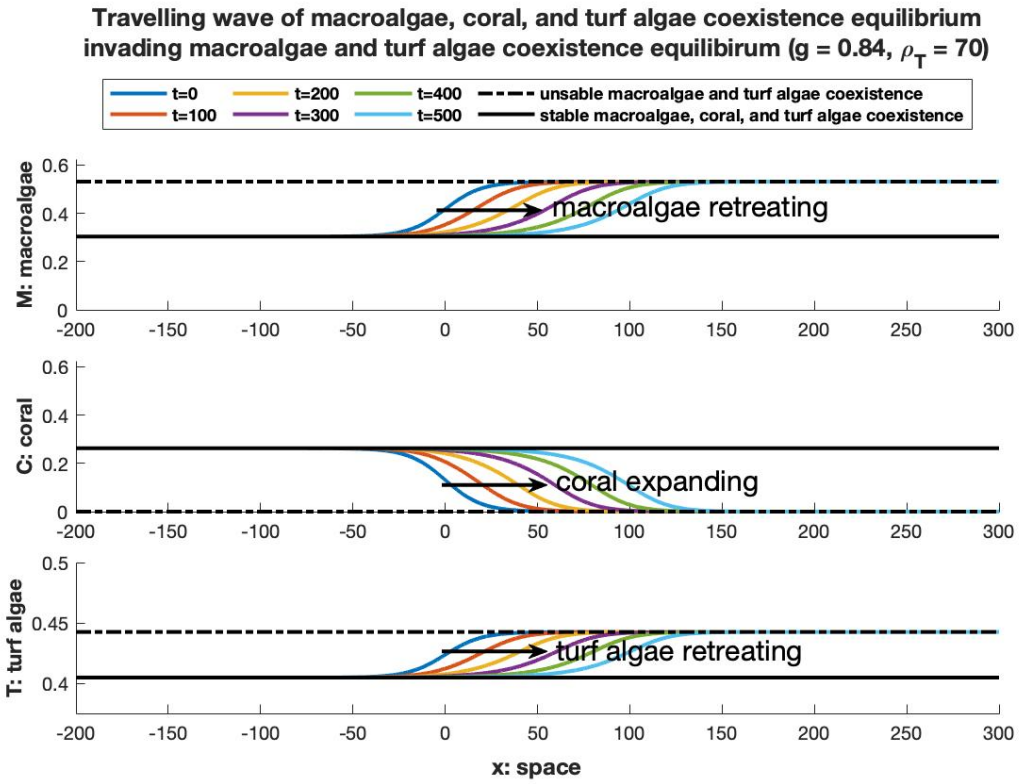

Fig. 3.8 TW of macroalgae failing to invade coral at high ρ_T. Numerical TW simulation corresponds to the transition at point B_h in figure 2.2. We apply homogeneous Neumann boundary conditions and take the grazing effect $g = 0.84$. We set the initial coral cover was set to 0, which is below three functional groups coexistence level.

If we do not harvest any herbivorous fish, the abundant herbivorous fish put high grazing pressure on both macroalgae and turf algae. Coral remain dominant in the slow turf algae case and drive macroalgae and turf algae to extinction. Coral only drive macroalgae to extinction and coexist with turf algae in the fast turf algae case. Maintaining such a high grazing pressure is unrealistic, so we do not discuss the transitions under high grazing pressure in detail.

3.3 Discussion

We derive a network of weakly-coupled ODE system to describe the dynamics of multiple patches in the discrete space case and a reaction-diffusion equation model to emphasize larval dispersal in the continuous space case. Using

numerical travelling wave analysis, we give conditions for coral to expand or retreat. In some cases, invasion depends not solely on the grazing effect but on the initial coral cover. If the grazing effect is low, macroalgae invade coral anyway; if the grazing effect is very high, macroalgae fail to invade coral anyway. The less extreme middle case with moderate grazing effect is more interesting. If the initial coral cover is high, macroalgae invade coral; if the initial coral cover is low, macroalgae fail to invade coral. Whether coral retreat or expand, multiple functional groups can eventually coexist at moderate grazing effect.

Table 3.1 summarizes the TW results for slow turf algae scenario. Macroalgae invade coral and drive coral to extinction if the grazing effect g is less than the bifurcation value $g_{low}^{G_6^*} = 0.6892$. The invasion speed is inversely related to the grazing effect, provided that the grazing effect is less than 0.6892. Macroalgae and coral can coexist if the grazing effect g is between two bifurcation values $g_{low}^{G_6^*} = 0.6892$ and $g^{CD4} = 0.7512$. Macroalgae fail to invade coral, and coral drive macroalgae and turf algae to extinction if the grazing effect g is larger than the bifurcation value $g^{CD4} = 0.7512$.

Table 3.1 Summary of TW results at low ρ_T

Grazing	Initial coral cover	Macroalgae (M)	Coral (C)
low	any	invade coral	extinct
moderate	high	invade coral	M and C coexist
	low	not invade coral	M and C coexist
high	any	not invade coral	dominant

This table summarizes the TW simulations at low ρ_T. The last column shows the equilibrium state of coral. Extinction corresponds to zero coral equilibrium, and dominance corresponds to coral-only equilibrium.

Table 3.2 summarizes the TW results for fast turf algae scenario. Macroalgae invade coral and turf algae and drive coral to extinction if the grazing effect g is less than the bifurcation value $g_{high}^{G_6^*} = 0.8283$. The invasion speed is inversely related to the grazing effect, provided that the grazing effect is less than 0.8283. Macroalgae, coral, and turf algae can coexist if the grazing

effect g is between two bifurcation values $g_{high}^{G_6^*} = 0.8283$ and $g_{high}^{int} = 0.8583$. Macroalgae fail to invade coral, and coral drive macroalgae to extinction if the grazing effect g is larger than the bifurcation value $g_{high}^{int} = 0.8583$.

Table 3.2 Summary of TW results at high ρ_T

Grazing	Initial coral cover	Macroalgae (M)	Coral (C)
low	any	invade coral	extinct
moderate	high	invade coral	M, C, and T coexist
	low	not invade coral	M, C, and T coexist
high	any	not invade coral	C and T coexist

This table summarizes the TW simulations at high ρ_T. The last column shows the equilibrium state of coral. Extinction corresponds to zero coral equilibrium. T represents turf algae.

Since we focus on brooding coral, the assumptions of the nearest neighbour principle and weak dispersal among patches are reasonable. The brooding coral larvae are well developed before being released to the current, so their ability to move is relatively restricted. These two crucial assumptions allow us to solve larvae in terms of adult for the general n patches and derive the weakly-coupled network model and reaction-diffusion equation model.

Chapter 4

Concluding remarks

4.1 Conclusion

This thesis aims to 1) understand how coral, macroalgae, and turf algae occupy available space while competing and give conditions for coral persistence; 2) understand how macroalgae invade coral and turf algae spatially through larval or propagules dispersal and give conditions under which coral will retreat or expand; 3) generate some insights into the role of turf algae in the coral-algae ecosystem.

In this thesis, we develop a one-patch model (2.6) that emphasizes the difference in the ability to occupy available space for different functional groups. Using persistence theorems, we show coral persist under high grazing pressure. We understand the coral-algae interaction within the patch concerning the various levels of grazing effect through numerical bifurcation analysis. We split our investigation into two main scenarios, slow turf algae and fast turf algae, based on the rate that turf algae take available space. In both scenarios, algae are dominant at low grazing effect, and coral are dominant at very high grazing effect; when the grazing effect is within a moderate range, algae and coral can coexist. We show reasonable fishing helps maintain the herbivorous fish population, and a healthier herbivorous fish population can support a higher level of coral cover. We find coral are more resistant to the decline of larval recruitment due to the negative environmental impact in the fast turf algae case.

We derive a weakly-coupled network of multiple-patches model (3.31) and

reaction-diffusion equation model (3.38) for brooding coral based on the one-patch model (2.6). Using numerical travelling wave analysis, we understand how macroalgae invade coral spatially through travelling waves and how coral-dominant phase shifts into algae-dominant phase in both fast and slow turf algae scenarios. Macroalgae invade coral and drive coral to extinction at low grazing effect. Macroalgae fail to invade coral at a very high grazing effect. For moderate grazing level, the invasion depends on the initial coral cover; high initial coral cover induces invasion by macroalgae, and low initial coral cover prevents the invasion. Algae and coral can coexist after the invasion at a moderate grazing level.

4.2 Limitations and future work

Our one-patch ODE model (2.6) does not show bistability behaviour at high grazing pressure as in the original MCT model proposed by Mumby et al. (2007). This difference is primarily due to the structure of the grazing term. The original MCT model proposed by Mumby et al. (2007) used Holling Type II response for the grazing term, and our models use linear grazing term to make the mathematical analysis easier. Since Mumby et al. (2007) assumed that available space became turf algae immediately, $T = 1 - M - C$, the resulting model is a two dimensional ODE system and mathematical analysis is relatively easier than our three dimensional ODE system (2.6). The original MCT model proposed by Mumby et al. (2007) showed macroalgae dominance at low grazing pressure and bistability behaviour at high grazing pressure. Mathematically, the macroalgae-only equilibrium was the only global stable equilibrium at low grazing pressure; the macroalgae-only equilibrium and coral-only equilibrium were both locally stable at high grazing pressure. In the bistability behaviour, coral dominated if the initial coral cover was high and macroalgae dominated if the initial coral cover was low. Mathematically, the coral-only equilibrium attracted all solutions with high initial coral cover, and the macroalgae-only equilibrium attracted all solutions with low initial coral cover. Although our one-patch ODE model (2.6) does not show bistabil-

ity behaviour, our findings are compliant with the MCT model proposed by Mumby et al. (2007) that coral-algae system is sensitive to the grazing effect and macroalgae dominate at low grazing pressure. The explicit discussion of available space allows us to investigate two important scenarios: slow and fast turf algae. The coral-algae dynamics are quite different in those two scenarios. The separation of turf algae from available space allows us to study the effect of turf algae on the invasion of coral by macroalgae. The reaction-diffusion model gives us the tool to study the spatial invasion of coral by macroalgae through travelling waves, which is rarely discussed in the literature.

In the future, we can test different grazing forms. Suppose we use the Holling Type II response for the grazing. In that case, our model may exhibit bistability behaviour in addition to the existing spatial dynamics, though it will be mathematically challenging. We mainly focus on the grazing effect in this thesis; however, we can also investigate the impact of other parameters, such as the rates of taking available space and diffusion coefficients on dynamics. We derive a network of weakly-coupled multiple-patches model, but we lack the mathematical tools to do rigorous analysis. We can run simulations for different patches to understand how the patches are connected in the discrete space case. We assume every patch is the same for simplicity. However, it is promising to consider some spatial heterogeneity in the grazing effect. Herbivorous fish are often observed in groups, travelling between patches and even reefs searching for food. They will move from low algae density patches to high algae density patches. Fishing effort is also not uniform across all locations in reality. We can consider the grazing effect as a function of space $g(x)$ to account for the spatial heterogeneity. We simulate travelling waves numerically without proving their existence. We can find rigorous conditions for the existence and non-existence of travelling waves mathematically in the future.

References

C. J. Bampfylde and M. A. Lewis. Biological control through intraguild predation: Case studies in pest control, invasive species and range expansion. *Bulletin of Mathematical Biology 2007 69:3*, 69:1031–1066, 2 2007. ISSN 1522-9602. doi: 10.1007/S11538-006-9158-9.

K. Barott, G. Williams, M. Vermeij, J. Harris, J. Smith, F. Rohwer, and S. Sandin. Natural history of coral-algae competition across a gradient of human activity in the line islands. *Marine Ecology Progress Series*, 460, 07 2012. doi: 10.3354/meps09874.

D. Bellwood, T. Hughes, C. Folke, and M. Nyström. Confronting the coral reef crisis. *Nature*, 429:827–33, 07 2004. doi: 10.1038/nature02691.

J. Blackwood, A. Hastings, and P. Mumby. The effect of fishing on hysteresis in caribbean coral reefs. *Theoretical Ecology*, 5:105–114, 02 2010. doi: 10.1007/s12080-010-0102-0.

S. Box and P. Mumby. Effect of macroalgal competition on growth and survival of juvenile caribbean corals. *Marine Ecology Progress Series*, 342:139–149, 07 2007. doi: 10.3354/meps342139.

C. Briggs, T. Adam, S. Holbrook, and R. Schmitt. Macroalgae size refuge from herbivory promotes alternative stable states on coral reefs. *PLOS ONE*, 13: e0202273, 09 2018. doi: 10.1371/journal.pone.0202273.

K. Brown, D. Bender-Champ, A. Kubicek, R. van der Zande, M. Achlatis, O. Hoegh-Guldberg, and S. Dove. The dynamics of coral-algal interactions in space and time on the southern great barrier reef. *Frontiers in Marine Science*, 5, 05 2018. doi: 10.3389/fmars.2018.00181.

K. Cameron and P. Harrison. Density of coral larvae can influence settlement, post-settlement colony abundance and coral cover in larval restoration. *Scientific Reports*, 10, 03 2020. doi: 10.1038/s41598-020-62366-4.

S. Connell, M. Foster, and L. Airoldi. What are algal turfs? towards a better description of turfs. *Marine Ecology Progress Series*, 495:299–307, 01 2014. doi: 10.3354/meps10513.

G. Diaz-Pulido and L. McCook. *Environmental Status: Macroalgae (seaweeds)*. Great Barrier Reef Marine Park Authority, 2008.

H. Fattahpour, H. Zangeneh, and H. Wang. Dynamics of coral reef models in the presence of parrotfish. *Natural Resource Modeling*, 32, 12 2018. doi: 10.1111/nrm.12202.

N. Foster, S. Box, and P. Mumby. Competitive effects of macroalgae on fecundity of the reef-building coral montastraea annularis. *Marine Ecology Progress Series*, 367:143–152, 09 2008. doi: 10.3354/meps07594.

T. Fung, R. Seymour, and C. Johnson. Alternative stable states and phase shifts in coral reefs under anthropogenic stress. *Ecology*, 92:967–82, 04 2011. doi: 10.2307/41151219.

T. Fung, R. Seymour, and C. Johnson. Warning signals of regime shifts as intrinsic properties of endogenous dynamics. *The American naturalist*, 182: 208–22, 08 2013. doi: 10.1086/670930.

V. Harriott. Mortality rates of scleractinian corals before and during a mass bleaching event. *Marine Ecology-progress Series - MAR ECOL-PROGR SER*, 21:81–88, 01 1985. doi: 10.3354/meps021081.

A. Hartmann, K. Marhaver, and M. Vermeij. Corals in healthy populations produce more larvae per unit cover: Higher fecundity in healthy coral populations. *Conservation Letters*, 10 2017. doi: 10.1111/conl.12410.

T. Hughes. Catastrophes, phase shifts, and large-scale degradation of a caribbean coral reef. *Science (New York, N.Y.)*, 265:1547–51, 10 1994. doi: 10.1126/science.265.5178.1547.

T. Hughes, M. Rodrigues, D. Bellwood, D. Ceccarelli, O. Hoegh-Guldberg, L. McCook, N. Moltschaniwskyj, M. Pratchett, R. Steneck, and B. Willis. Phase shifts, herbivory, and the resilience of coral reefs to climate change. *Current biology : CB*, 17:360–5, 03 2007. doi: 10.1016/j.cub.2006.12.049.

T. Hughes, N. Graham, J. Jackson, P. Mumby, and R. Steneck. Rising to the challenge of sustaining coral reef resilience. *Trends in ecology & evolution*, 25:633–42, 11 2010. doi: 10.1016/j.tree.2010.07.011.

K. C. James Gilmour, Luke Smith and S. Pincock. *Discovering Scott Reef : 20 years of exploration and research*. Australian Institute of Marine Science, 2013. ISBN 9780642322654.

J. Jompa and L. McCook. Coral-algal competition: Macroalgae with different properties have different effects on corals. *Marine Ecology-progress Series - MAR ECOL-PROGR SER*, 258:87–95, 08 2003. doi: 10.3354/meps258087.

M. Kot. *Elements of Mathematical Ecology*. Cambridge University Press, 2001. doi: 10.1017/CBO9780511608520.

X. Li, H. Wang, Z. Zhang, and A. Hastings. Mathematical analysis of coral reef models. *Journal of Mathematical Analysis and Applications*, 416:352–373, 08 2014. doi: 10.1016/j.jmaa.2014.02.053.

D. Lirman. Competition between macroalgae and corals: Effects of herbivore exclusion and increased algal biomass on coral survivorship and growth. *Coral Reefs*, 19:392–399, 05 2001. doi: 10.1007/s003380000125.

J. McManus and J. Polsenberg. Coral-algal phase shifts on coral reefs: Ecological and environmental aspects [review article]. *Progress In Oceanography*, 60:263–279, 02 2004. doi: 10.1016/j.pocean.2004.02.014.

P. Mumby, A. Hastings, and H. Edwards. Thresholds and the resilience of caribbean coral reefs. *Nature*, 450:98–101, 12 2007. doi: 10.1038/nature06252.

G. Polis. The ecology and evolution of intraguild predation: Potential competitors that eat each other. *Annual Review of Ecology and Systematics*, 20: 297–330, 01 1989. doi: 10.1146/annurev.ecolsys.20.1.297.

R. Richmond and C. Hunter. Reproduction and recruitment of corals: Comparisons among the caribbean, the tropical pacific, and the red sea. *Marine Ecology-progress Series - MAR ECOL-PROGR SER*, 60:185–203, 02 1990. doi: 10.3354/meps060185.

H. Smith and H. Thieme. *Dynamical Systems and Population Persistence*. Graduate studies in mathematics. American Mathematical Society, 2011. ISBN 9780821849453. URL `https://books.google.ca/books?id=ZYyDAwAAQBAJ`.

T. Swierts and M. Vermeij. Competitive interactions between corals and turf algae depend on coral colony form. *PeerJ*, 4:e1984, 05 2016. doi: 10.7717/peerj.1984.

E. Tekwa, L. McManus, A. Greiner, M. Colton, M. Webster, and M. Pinsky. Geometric analysis of regime shifts in coral reef communities. *Ecosphere*, 12, 01 2021. doi: 10.1002/ecs2.3319.

M. Vermeij, R. Heijden, J. Olthuis, K. Marhaver, J. Smith, and P. Visser. Survival and dispersal of turf algae and macroalgae consumed by herbivorous coral reef fishes. *Oecologia*, 171, 09 2012. doi: 10.1007/s00442-012-2436-3.

Appendix A

Tables for one-patch model in chapter 2

Table A.1 Description of original variables

Original	Description	Units
M	surface area occupied by macroalgae	$meter^2$
C	surface area occupied by coral	$meter^2$
T	surface area occupied by turf algae	$meter^2$
S	available space	$meter^2$
l_R	density of larvae or propagules	$\frac{1}{meter^3}$
t	time	$year$

This table explains the dependent and independent variables in the dimensional one-patch model (2.1). $R = M$, C, or T represents three functional groups. Adult macroalgae, coral, and turf algae are measured as surface area in meter square; propagules of macroalgae and turf algae are measured as density in number per meter cubic; time is measured in year.

Table A.2 Description of original parameters

Original	Description	Units	Value
α	rate macroalgae overgrow coral	$\frac{1}{meter^2 * year}$	$\frac{0.1}{N}$
β	rate macroalgae overgrow turf algae	$\frac{1}{meter^2 * year}$	$\frac{0.8}{N}$
γ	rate coral overgrow turf algae	$\frac{1}{meter^2 * year}$	$\frac{1}{N}$
ρ_M	rate of macroalgae taking available space	$\frac{1}{meter^2 * year}$	$\ll \rho_T$
ρ_C	rate of coral taking available space	$\frac{1}{meter^2 * year}$	$\ll \rho_T$
ρ_T	rate of turf algae taking available space	$\frac{1}{meter^2 * year}$	$\left[\frac{2}{N}, \frac{40}{N}\right]$
g	grazing effect of fish	$\frac{1}{year}$	-
ϕ_C	volume of water column per coral polyp	$meter^3$	$\left[3.95 \times 10^{-5}, 8.85 \times 10^{-3}\right]$
ϕ_M, ϕ_T	volume of water column per algae	$meter^3$	-
A_C	cross-sectional area of coral polyp	$meter^2$	$\left[0.79 \times 10^{-6}, 1.77 \times 10^{-4}\right]$
A_M, A_T	cross-sectional area of algae	$meter^2$	-
κ_C	coral larvae settling rate	$\frac{1}{year}$	29.66
κ_M, κ_T	algae propagules settling rate	$\frac{1}{year}$	-
δ_M	mortality rate of macroalgae if not grazed	$\frac{1}{year}$	$< g$
δ_C	mortality rate of coral	$\frac{1}{year}$	0.44
δ_T	mortality rate of turf algae if not grazed	$\frac{1}{year}$	$< g$
N	total surface area of the reef as one patch	$meter^2$	-
L	average depth of water column	$meter$	≤ 50
ψ_C	number of coral adults per unit area	$\frac{1}{meter^2}$	$\left[2.82, 6.33 \times 10^2\right]$
ψ_M, ψ_T	number of algae adult per unit area	$\frac{1}{meter^2}$	-
b_C	birth rate of coral larvae	$\frac{1}{year}$	$\left[2.31 \times 10^2, 5.18 \times 10^5\right]$
b_M, b_T	birth rate of algae propagules	$\frac{1}{year}$	-
μ_C	death rate of coral larvae	$\frac{1}{year}$	168.09
μ_M, μ_T	death rate of algae propagules	$\frac{1}{year}$	-

This table explains the parameters in the dimensional one-patch model (2.1). $R =$ M, C, or T represents three functional groups. $\phi_R = A_R L$ can be decomposed as the cross-sectional area of a single individual polyp multiplies the height of the water column. $b_R \psi_R$ the number of larvae or propagules produced per polyp per unit time represents the fecundity. NL is the volume of the water column above the whole patch. $\frac{b_R \psi_R I}{NL}$ is the density of larvae or propagules produced by functional group R per unit time.

Values for α, β, γ, and δ_C are adapted from Blackwood et al. (2010). We assume turf algae are the fastest colonizer, and occupying empty space is

much easier than overgrowing other functional groups, so $\rho_T \gg \rho_M > \alpha$, $\rho_T \gg \rho_M > \beta$, and $\rho_T \gg \rho_C > \gamma$. ρ_T ranges from $\frac{2}{N}$ to $\frac{40}{N}$, adapted from Fung et al. (2011). In literature, the grazing effect from herbivorous fish is considered the main death factor for algae, so we assume δ_M and δ_T are less than the grazing effect g. We only consider coral reefs in the tropical area, and hermatypic coral live in the photic zone, so $L < 50$ meters. We assume the age of death for coral larvae follows an exponential distribution with mean $\frac{1}{\mu_C}$. The survival rate of coral larvae in the early stage is extremely low, only about ten percent (Harriott, 1985). The probability of coral larvae settling before dying during the five days settlement period is around 0.15 (Cameron and Harrison, 2020). We solve for $\mu_C = 168.09$ and $\kappa_C = 29.66$ from $e^{-\mu_C \frac{5}{365}} = 0.1$ and $\frac{\kappa_C}{\kappa_C + \mu_C} = 0.15$. We further assume κ_M, κ_T and μ_M, μ_T are of the same scale as κ_C and μ_C. The fecundity has vast variations. $\psi_C b_C$ approximately ranges from 1.46×10^5 to 1.46×10^6 based on different coral species and healthy conditions. The range for $\psi_C b_C$ is adapted from figure $2(B)$ in Hartmann et al. (2017). The diameter of an individual coral polyp is usually 1 to 15 millimetres, so the cross-sectional area of a single individual ranges from 0.79×10^{-6} to 1.77×10^{-4} $meter^2$, which implies $\phi_C \in \left[3.95 \times 10^{-5}, 8.85 \times 10^{-3}\right]$. ψ_C can be calculated as the coral cover rate divided by the cross-sectional area of a single individual polyp. Coral cover rate is measured as the area of coral cover per unit area and is estimated to be 5 centimetres square per meter square from figure $2(A)$ in Hartmann et al. (2017), which implies $\psi_C \in \left[\frac{5 \times 10^{-4}}{1.77 \times 10^{-4}}, \frac{5 \times 10^{-4}}{0.79 \times 10^{-6}}\right] = \left[2.82, 6.33 \times 10^2\right]$. The birth rate of coral larvae $b_C \in \left[\frac{1.46 \times 10^5}{632.91}, \frac{1.46 \times 10^6}{2.82}\right] = \left[2.31 \times 10^2, 5.18 \times 10^5\right]$.

Table A.3 Non-dimensionalization and Non-dimensionalized parameters

Non-dimensionalized	non-dimensionalization	Value
$\tilde{M}$	$\tilde{M} = \frac{M}{N}$	-
$\tilde{C}$	$\tilde{C} = \frac{C}{N}$	-
$\tilde{T}$	$\tilde{T} = \frac{T}{N}$	-
$\tilde{S}$	$\tilde{S} = \frac{S}{N}$	-
$\tilde{l}_R$	$\tilde{l}_R = \phi_R l_R$	-
$\tilde{t}$	$\tilde{t} = \delta_C t$	-
ϵ_C	$\epsilon_C = \frac{\delta_C}{\mu_C}$	0.0026
ϵ_M, ϵ_T	$\epsilon_R = \frac{\delta_C}{\mu_R}$	-
θ_C	$\theta_C = \frac{\tilde{\kappa}_C}{\tilde{\kappa}_C+1}$	0.15
θ_M, θ_T	$\theta_R = \frac{\tilde{\kappa}_R}{\tilde{\kappa}_R+1}$	-
Θ_M	$\Theta_M = \theta_M \tilde{\psi}_M \tilde{b}_M$	-
Θ_C	$\Theta_C = \theta_C \tilde{\psi}_C \tilde{b}_C$	$\left[1.03 \times 10^{-4}, 2.31 \times 10^{-1}\right]$
Θ_T	$\Theta_T = \theta_T \tilde{\psi}_T \tilde{b}_T$	-
$\tilde{\alpha}$	$\tilde{\alpha} = \frac{\alpha N}{\delta_C}$	0.23
$\tilde{\beta}$	$\tilde{\beta} = \frac{\beta N}{\delta_C}$	1.82
$\tilde{\gamma}$	$\tilde{\gamma} = \frac{\gamma N}{\delta_C}$	2.27
$\tilde{\rho}_M$	$\tilde{\rho}_M = \frac{\rho_M N}{\delta_C}$	$\ll \tilde{\rho}_T$
$\tilde{\rho}_C$	$\tilde{\rho}_C = \frac{\rho_C N}{\delta_C}$	$\ll \tilde{\rho}_T$
$\tilde{\rho}_T$	$\tilde{\rho}_T = \frac{\rho_T N}{\delta_C}$	$[4.55, 90.91]$
$\tilde{g}$	$\tilde{g} = \frac{g}{\delta_C}$	-
$\tilde{\delta_M}$	$\tilde{\delta_M} = \frac{\delta_M}{\delta_C}$	$< \tilde{g}$
$\tilde{\delta_T}$	$\tilde{\delta_T} = \frac{\delta_T}{\delta_C}$	$< \tilde{g}$
$\tilde{\kappa}_C$	$\tilde{\kappa}_C = \frac{\kappa_C}{\mu_C}$	0.18
$\tilde{\kappa}_M, \tilde{\kappa}_T$	$\tilde{\kappa}_R = \frac{\kappa_R}{\mu_R}$	-
$\tilde{\psi}_C$	$\tilde{\psi}_C = \frac{\phi_C \psi_C}{L}$	5×10^{-4}
$\tilde{\psi}_M, \tilde{\psi}_T$	$\tilde{\psi}_R = \frac{\phi_R \psi_R}{L}$	-
$\tilde{b}_C$	$\tilde{b}_C = \frac{b_C}{\mu_C}$	$\left[1.37, 3.08 \times 10^3\right]$
$\tilde{b}_M, \tilde{b}_T$	$\tilde{b}_R = \frac{b_R}{\mu_R}$	-

This table explains the variables and parameters in the non-dimensional one-patch model (2.2). $R = M$, C, or T represents three functional groups. $\tilde{R}$ represents the proportion of surface area occupied by functional group R. θ_R is the probability of settling before dying. Θ_R counts the total contribution from larvae or propagules settling to adult abundance. ϵ_R is the ratio of adult mortality rate and larvae or propagules mortality rate for functional group R.

The probability of settling before dying θ_C equals 0.15 (Cameron and Harrison, 2020). ϵ_C is very close to zero since the larvae mortality rate is much higher than adult coral. $\tilde{\psi}_C$ is the same as the coral over, equals to 5×10^{-4}:

$$\tilde{\psi}_C = \frac{\phi_C \psi_C}{L} = \frac{A_C L}{L} \frac{\text{coral cover rate}}{A_C} = \text{coral cover rate}.$$

The total contribution from larvae or propagules settling into adult abundance Θ_R depends on the probability of settling before dying, the cross-sectional area of polyp, fecundity, and mortality:

$$\Theta_C = \theta_C \tilde{\psi}_C \tilde{b}_C = \theta_C \frac{\phi_C \psi_C}{L} \frac{b_C}{\mu_C} = \theta_C \frac{\phi_C}{L} \frac{\psi_C b_C}{\mu_C} = \theta_C \frac{A_C L}{L} \frac{\psi_C b_C}{\mu_C} = \frac{\theta_C A_C \psi_C b_C}{\mu_C}.$$

Θ_R is independent of water depth L, so our models are independent of water depth L after non-dimensionalization. The range of Θ_C is estimated to be:

$$\begin{aligned} \Theta_C &\in \left[\frac{0.15 \times 0.79 \times 10^{-6} \times 1.46 \times 10^5}{168.09}, \frac{0.15 \times 1.77 \times 10^{-4} \times 1.46 \times 10^6}{168.09} \right] \\ &= \left[1.03 \times 10^{-4}, 2.31 \times 10^{-1} \right]. \end{aligned}$$

Appendix B

Tables for multiple-patches model and reaction-diffusion model in chapter 3

Table B.1 Description of original variables in weakly-coupled network model

Original	Description	Units
M_i	surface area occupied by macroalgae in patch i	$meter^2$
C_i	surface area occupied by coral in patch i	$meter^2$
T_i	surface area occupied by turf algae in patch i	$meter^2$
S_i	available space in patch i	$meter^2$
l_{Ri}	density of larvae or propagules in patch i	$\frac{1}{meter^3}$
t	time	$year$

This table explains the dependent and independent variables in the dimensional multiple-patches model (3.2). $R = M$, C, or T represents three functional groups. Adult macroalgae, coral, and turf algae are measured as surface area in meter square; propagules of macroalgae and turf algae are measured as density in number per meter cubic; time is measured in year.

Table B.2 Description of original parameters in weakly-coupled network model

Original	Description	Units	Value
α	rate macroalgae overgrow coral	$\frac{1}{meter^2 * year}$	$\frac{0.1}{N}$
β	rate macroalgae overgrow turf algae	$\frac{1}{meter^2 * year}$	$\frac{0.8}{N}$
γ	rate coral overgrow turf algae	$\frac{1}{meter^2 * year}$	$\frac{1}{N}$
ρ_M	rate of macroalgae taking available space	$\frac{1}{meter^2 * year}$	$\ll \rho_T$
ρ_C	rate of coral taking available space	$\frac{1}{meter^2 * year}$	$\ll \rho_T$
ρ_T	rate of turf algae taking available space	$\frac{1}{meter^2 * year}$	$\left[\frac{2}{N}, \frac{40}{N}\right]$
g	grazing effect of fish	$\frac{1}{year}$	-
ϕ_C	volume of water column per coral polyp	$meter^3$	$\left[3.95 \times 10^{-5}, 8.85 \times 10^{-3}\right]$
ϕ_M, ϕ_T	volume of water column per algae	$meter^3$	-
A_C	cross-sectional area of coral polyp	$meter^2$	$\left[0.79 \times 10^{-6}, 1.77 \times 10^{-4}\right]$
A_M, A_T	cross-sectional area of algae	$meter^2$	-
κ_C	coral larvae settling rate	$\frac{1}{year}$	29.66
κ_M, κ_T	algae propagules settling rate	$\frac{1}{year}$	-
δ_M	mortality rate of macroalgae if not grazed	$\frac{1}{year}$	$< g$
δ_C	mortality rate of coral	$\frac{1}{year}$	0.44
δ_T	mortality rate of turf algae if not grazed	$\frac{1}{year}$	$< g$
N	total surface area of one patch	$meter^2$	-
L	average depth of water column	$meter$	≤ 50
ψ_C	number of coral adults per unit area	$\frac{1}{meter^2}$	$\left[2.82, 6.33 \times 10^2\right]$
ψ_M, ψ_T	number of algae adult per unit area	$\frac{1}{meter^2}$	-
b_C	birth rate of coral larvae	$\frac{1}{year}$	$\left[2.31 \times 10^2, 5.18 \times 10^5\right]$
b_M, b_T	birth rate of algae propagules	$\frac{1}{year}$	-
μ_C	death rate of coral larvae	$\frac{1}{year}$	168.09
μ_M, μ_T	death rate of algae propagules	$\frac{1}{year}$	-
$d_{Ri,j}$	immigration or emigration rate	$\frac{1}{year}$	-
e_R	uniform immigration or emigration rate	$\frac{1}{year}$	-

This table explains the parameters in the dimensional multiple-patches model (3.2). $R = M$, C, or T represents three functional groups. $d_{Ri,j}$ is the immigration or emigration rate from patch j to patch i. We assume all patches are the same, so the parameter values are the same for every patch; thus, the subscript $_i$ is neglected, except for immigration or emigration rate.

Table B.3 Non-dimensionalization and non-dimensionalized parameters in weakly-coupled network model and reaction-diffusion model

Non-dimensionalized	Non-dimensionalization	Value
$\tilde{M}_i$	$\tilde{M}_i = \frac{M_i}{N}$	-
$\tilde{C}_i$	$\tilde{C}_i = \frac{C_i}{N}$	-
$\tilde{T}_i$	$\tilde{T}_i = \frac{T_i}{N}$	-
$\tilde{S}_i$	$\tilde{S}_i = \frac{S_i}{N}$	-
$\tilde{l}_{Ri}$	$\tilde{l}_{Ri} = \phi_R l_{Ri}$	-
$\tilde{t}$	$\tilde{t} = \delta_C t$	-
ϵ_C	$\epsilon_C = \frac{\delta_C}{\mu_C}$	0.0026
ϵ_M, ϵ_T	$\epsilon_R = \frac{\delta_C}{\mu_R}$	-
θ_C	$\theta_C = \frac{\tilde{\kappa}_C}{\tilde{\kappa}_C+1}$	0.15
θ_M, θ_T	$\theta_R = \frac{\tilde{\kappa}_R}{\tilde{\kappa}_R+1}$	-
Θ_M	$\Theta_M = \theta_M \tilde{\psi}_M \tilde{b}_M$	-
Θ_C	$\Theta_C = \theta_C \tilde{\psi}_C \tilde{b}_C$	$\left[1.03 \times 10^{-4}, 2.31 \times 10^{-1}\right]$
Θ_T	$\Theta_T = \theta_T \tilde{\psi}_T \tilde{b}_T$	-
$\tilde{\alpha}$	$\tilde{\alpha} = \frac{\alpha N}{\delta_C}$	0.23
$\tilde{\beta}$	$\tilde{\beta} = \frac{\beta N}{\delta_C}$	1.82
$\tilde{\gamma}$	$\tilde{\gamma} = \frac{\gamma N}{\delta_C}$	2.27
$\tilde{\rho}_M$	$\tilde{\rho}_M = \frac{\rho_M N}{\delta_C}$	$\ll \tilde{\rho}_T$
$\tilde{\rho}_C$	$\tilde{\rho}_C = \frac{\rho_C N}{\delta_C}$	$\ll \tilde{\rho}_T$
$\tilde{\rho}_T$	$\tilde{\rho}_T = \frac{\rho_T N}{\delta_C}$	$[4.55, 90.91]$
$\tilde{g}$	$\tilde{g} = \frac{g}{\delta_C}$	-
$\tilde{\delta_M}$	$\tilde{\delta_M} = \frac{\delta_M}{\delta_C}$	$< \tilde{g}$
$\tilde{\delta_T}$	$\tilde{\delta_T} = \frac{\delta_T}{\delta_C}$	$< \tilde{g}$
$\tilde{\kappa}_C$	$\tilde{\kappa}_C = \frac{\kappa_C}{\mu_C}$	0.18
$\tilde{\kappa}_M, \tilde{\kappa}_T$	$\tilde{\kappa}_R = \frac{\kappa_R}{\mu_R}$	-
$\tilde{\psi}_C$	$\tilde{\psi}_C = \frac{\phi_C \psi_C}{L}$	5×10^{-4}
$\tilde{\psi}_M, \tilde{\psi}_T$	$\tilde{\psi}_R = \frac{\phi_R \psi_R}{L}$	-
$\tilde{b}_C$	$\tilde{b}_C = \frac{b_C}{\mu_C}$	$\left[1.37, 3.08 \times 10^3\right]$
$\tilde{b}_M, \tilde{b}_T$	$\tilde{b}_R = \frac{b_R}{\mu_R}$	-
$\tilde{d}_{Ri,j}$	$\tilde{d}_{Ri,j} = \frac{d_{Ri,j}}{\mu_R}$	0.0001
$\tilde{e}_R$	$\tilde{e}_R = \frac{e_R}{\mu_R}$	-

This table explains the variables and parameters in the non-dimensional multiple-patches model (3.5) and the parameters in the reaction-diffusion equation model (3.38).

Table B.4 Description of variables and partially non-dimensionalized parameters in reaction-diffusion model

Variables	Description	Units
$\hat{M}(x,t)$	proportion of macroalgae at time t and location x	-
$\hat{C}(x,t)$	proportion of coral at time t and location x	-
$\hat{T}(x,t)$	proportion of turf algae at time t and location x	-
$\hat{S}(x,t)$	proportion of available space at time t and location x	-
x	one-dimensional space	$meter$
t	non-dimensionalized time	-
d_R	partially non-dimensionalized diffusion coefficient	$meter^2$

This table explains the dependent and independent variables in the reaction-diffusion equation model (3.38). $R = M$, C, or T represents three functional groups. $\hat{R}(x,t)$ is non-dimensional and represents the proportion of surface area occupied by functional group R at time t and location x. Time and diffusion coefficient are non-dimensionalized by multiplying the same parameter δ_C.